THE PRODUCTION OF ACETYLENE IN A HIGH-INTENSITY ELECTRIC ARC

A thesis presented for the Degree of

Doctor of Philosophy in Chemical Engineering

in the

University of Canterbury

Christchurch, New Zealand

by

R. A. WARD

1974

CONTENTS

ACKNOWLEDGMENTS

The author wishes to thank Dr J.B. Stott, who supervised the work, for his active interest and support, and Dr J. Abrahamson for his assistance with theoretical aspects of the work.

Thanks are also accorded to Mr L. Heath, Mr C. Campbell and the rest of the technical staff of the Department of Chemical Engineering for technical assistance in the construction of apparatus; to the staff of the Engineering Library for obtaining many difficult references; to the Chemistry Division of the D.S.I.R. and, in particular, Miss J. Ross for chromatogram gas analyses; and to all the other people who have helped in innumerable ways with all aspects of the work.

The work was made possible by personal and research grants from the Mineral Resources Subcommittee of the University Grants Committee and a research grant from the Golden Kiwi Scientific Research Distribution Committee and these are gratefully acknowledged.

Finally, the author wishes to acknowledge the patience and understanding of his wife, Irene, to whom this work is dedicated.

ABSTRACT

The aim of this work was to develop further a process for producing acetylene in a high-intensity arc first suggested by Abrahamson (1). This process consisted of ablating a graphite anode into an atmosphere of hydrogen and then rapidly quenching the resultant hot gas mixture so as to preserve the acetylene which is the major hydrocarbon species in the carbon/hydrogen system at high temperatures.

The reactor designed by Abrahamson had a throughput of up to 70 gm hr^{-1} and an energy consumption of up to 3 kW. This reactor was scaled up in the present work to have a throughput of up to 500 gm hr^{-1} and an energy consumption of up to 30 kW.

The reactor design was modified from the original to improve its operating capability and this also simplified the design of the reactor surrounds. The number of cathodes used was reduced from three to one, the cathode material changed from tungsten to carbon, and the design modified so that carbon did not deposit on the cathode tip during operation, a factor which had severely limited the length of operation possible in the small-scale plant.

Abrahamson noted consistent deficits in the carbon balance over his reactor and hypothesised that this was due to the splitting off of graphite particles from the anode during ablation which were sufficiently small to escape collection in filters and hence in the carbon balance. This hypothesis was investigated at length in this work by accurate mass flow measurement and product gas analysis. No deficiencies were found in the carbon balances in this work. However, significant quantities of carbon compounds other than acetylene were found, most notably carbon monoxide and methane, and it is considered that the failure to monitor these by Abrahamson gave rise to the deficiency in his carbon balance which he explained by what is considered in the light of this work to be both a doubtful and unnecessary hypothesis. Further evidence against the prolonged existence of small carbon

particles is given by calculations that showed that the majority of such particles would be evaporated within about 3 mm of the anode face.

The results from this work are compared with those obtained by Abrahamson and with those predicted by his theory of "supercooled" equilibrium which hypothesised the attainment of gas phase only equilibrium prior to quenching and the supercooling of the gas stream with respect to solid carbon during quenching. It was found at first sight that the current results did not appear to agree with "supercooled" equilibrium. This disagreement is explained in terms of the quench rate obtained in the water-cooled tube used to quench the product and, in fact, although no positive support is given, the results in this work may not be at variance with Abrahamson's theory and this was adopted for subsequent calculations.

Using the "supercooled" equilibrium theory, the optimum pre-quench conditions for operation of the reactor were found to be a mass carbon to hydrogen ratio of 2.5 and a specific enthalpy of 3.5 kcal gm^{-1}. Using these conditions, the best results obtained in this work (conversion of carbon to acetylene of 90%, an acetylene yield of 11.8 mol % and an energy consumption of 45 kWh kg^{-1} acetylene) and the best results obtained by Abrahamson (conversion 55%, yield 8 mol % and energy consumption 130 kWh kg^{-1} acetylene), a procedure has been developed by which the performance of larger reactors can be predicted. It is predicted that although increasing the scale of the reactor will reduce the energy requirement per unit of acetylene this cannot be reduced to an economic level without some means of recovering waste heat. The optimum pre-quench enthalpy of 3.5 kcal gm^{-1} can be obtained with the heat imparted to the carbon on ablation of the anode (less than 40% of the total heat input) so that for optimum conditions to prevail large amounts of the input energy to the arc are wasted. The presentation of the reactor heat flows in block diagram form enabled the energetic feasibility of this process and similar ones to be studied simply, but precisely and as a result it is shown that this low efficiency of energy usage given above may be able to be

overcome by using a secondary reagent feed of methane following the arc. Under these conditions, the energy requirement is shown to be potentially as low as 7 kWh kg^{-1}, a figure which is economical when compared with other processes (see page 79 for a table summarising these) and is especially important in the light of the discovery of major natural gas deposits in New Zealand during the process of this work. It is concluded that further development in this direction would be worthwhile.

CHAPTER 1

INTRODUCTION

This work resulted from a preliminary investigation into the possibility of producing acetylene from coal in a high-intensity arc undertaken by Abrahamson (1).

New Zealand is well placed in terms of coal reserves, proved at 162,500,000 tons and probably as high as 1,032,600,000 tons (108), to make use of a process which utilizes coal to produce acetylene as the first step in a plastics industry and with the possibility of cheap electrical energy the use of an electric arc process could be most attractive. Discovery of natural gas at Kapuni (total proved plus inferred reserves of 1,270,000 million cu ft (109,110)) and the Maui field off the coast of Taranaki (total proved plus inferred reserves 8,428,000 million cu ft (110)) has added to this by virtue of its possibility as an alternative or complementary feedstock. At present, New Zealand is spending ten million dollars a year (2) on polyvinylchloride imports and is exporting significant quantities of coal to Japan. With increasing pressure on world oil reserves, more importance will be placed on coal as a raw material and it is important that it is begun to be seen in this light rather than as a fuel which has essentially been its lot in the past. Development of a PVC industry based on coal and natural gas would, therefore, be of benefit to New Zealand both as a means of conserving overseas monetary reserves and as a more far-sighted use of a valuable raw material.

The potential advantage of an electric arc process is the high rate of heat transfer to the reactants which is possible compared with conventional heat transfer equipment and, to a lesser extent, plasmatrons. This efficiency of heat transfer enables smaller devices, with smaller capital costs, to be built which potentially outweighs the disadvantage of having to use electrical energy as against cheaper fossil fuels in conventional plant. The additional possibility of supplementing the electrical energy by using fossil fuels to preheat the reactants also exists. If a consumable electrode is used,

as in this work, an added advantage is obtained in that the solid reagent is "ground" by ablation to a degree impossible mechanically, thus allowing a greater degree of reaction within the hot reaction zone.

Out of this background, Abrahamson designed and constructed a small-scale high-intensity arc reactor with a throughput of up to 70 gm hr^{-1} in which a 3.3 mm diameter graphite anode was ablated into an atmosphere of hydrogen. Graphite was used as a substitute for coal because of its ease of fabrication into anodes. The major development of the design over existing arc processes was the maintenance of high wall temperatures in the reaction chamber which enabled better energy utilisation by reducing losses from the arc by radiation.

Simultaneously, work has been carried out on the formation of anodes from coal (85,86,87,88) and, at the time of writing, these have been developed to the point where they appear promising as a substitute for graphite in future work. Although anode carbons are available, e.g. for use in electrochemical processes such as aluminium smelting, the requirements in this case are somewhat different. As much of the volatile material present in the coal as possible must be preserved and the production costs of anodes must be small. What was required and ultimately obtained was a carbon shell with a largely unmodified coal interior.

Using his reactor, Abrahamson was able to convert up to 55% of the feed carbon to acetylene, producing a product stream containing 8% by volume of acetylene for an energy consumption of 130 kWh kg^{-1} acetylene.

The work reported here was concerned with continuing development of this basic process, in particular by constructing a larger reactor and investigating the effect of scale, reactant carbon to hydrogen ratio, power input and quench rate on the conversion of carbon and energy consumption per unit of acetylene. Associated with this were the development of a positive carbon feed, improved visual study of the arc processes and an investigation of the hydrogen flow patterns, the latter in an attempt to overcome the major operating problem of

carbon deposition within the reaction chamber which had limited the length of run obtainable by Abrahamson. Abrahamson observed large deficits in the carbon balance over the reactor and hypothesised that this was the result of very small diameter (less than 0.5 micron) particles of carbon which were split off the anode during ablation and which were small enough to bypass all product filters and hence avoid inclusion in the mass balance. To test the validity of this hypothesis, the mechanisms of carbon heat and mass transfer in the arc had to be studied and the accuracy of the reaction stoichiometry greatly improved.

Analysis of past work showed a low efficiency of utilisation of energy, i.e. the portion of the input energy transferred to the reagents was low. This is shown for a typical plasmatron device in fig. XXVII. As the energy requirement per unit of product is ultimately dependent on the efficiency of energy transfer to the reagents, it was desirable to look into ways of improving this, e.g. high reaction chamber wall temperatures. Whilst this work was proceeding, a major natural gas field (Maui) was discovered in New Zealand and it became important to consider the above problem in relation to this potential new feedstock, particularly with respect to the possibility of replacing the hydrogen atmosphere with methane. This is discussed in detail in chapter 7.

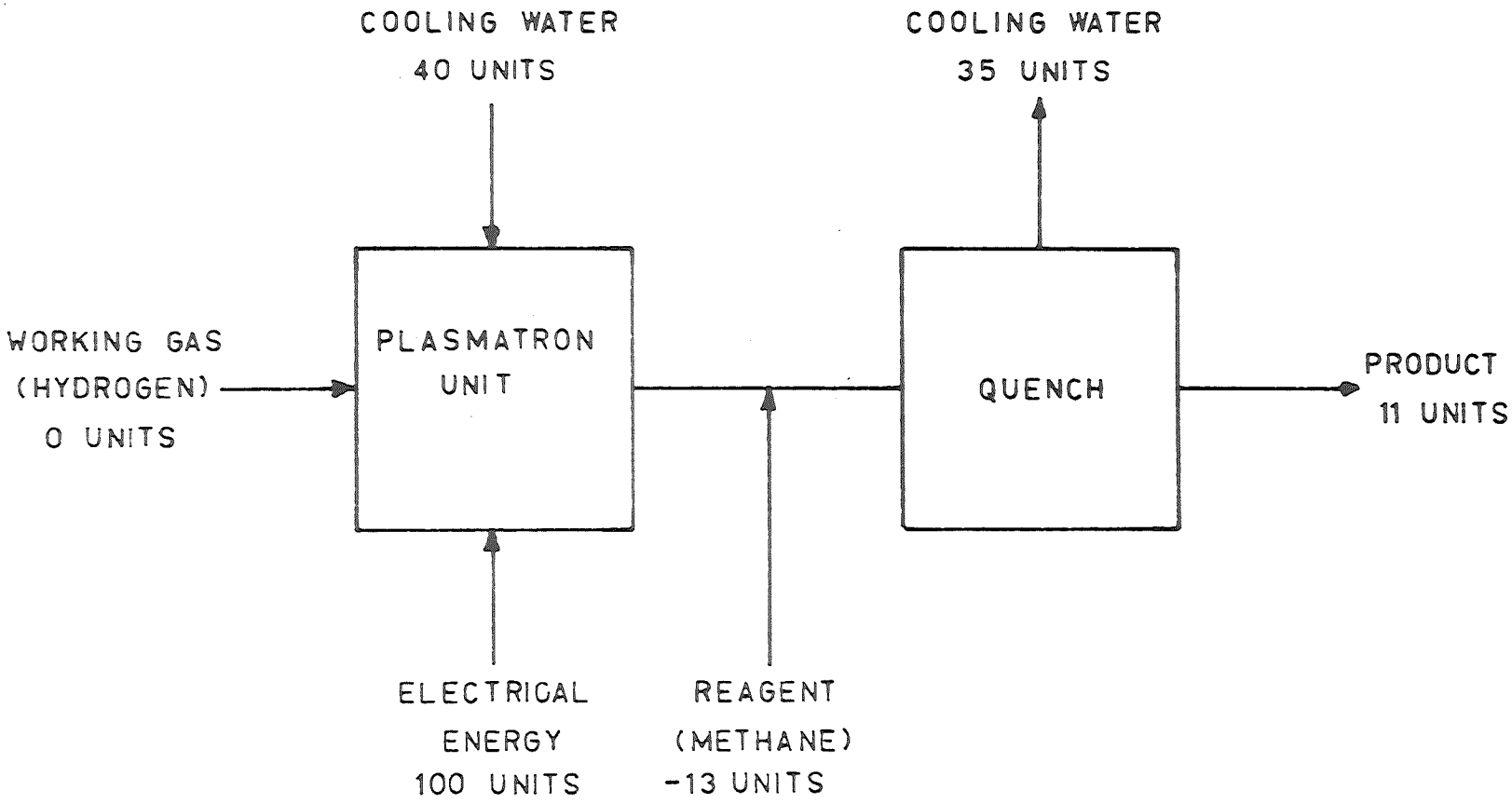

FIG XXVII

TYPICAL ENERGY FLOW FOR PLASMATRON

CHAPTER 2

BACKGROUND AND LITERATURE SURVEY

Acetylene was first produced in industrial quantities about 1896 using the carbide process. This continued to be the sole industrial method of production until 1939 when Chemische Werke Huls began operation of an electric arc process producing acetylene from gaseous hydrocarbons, e.g. natural gas and coke oven gas, at an initial rate of 60,000 t yr^{-1} (3). After World War II, there was an upsurge in interest in the development of new processes for the production of acetylene from hydrocarbons and these developed, alongside the carbide process which still remains the principal source of acetylene, in three main categories:

(i) regenerative pyrolysis,

(ii) partial combustion,

(iii) electrical processes.

All three types of process are based on raising a hydrocarbon feedstock to high temperatures to break down the hydrocarbons into their elements and simple radicals before rapidly quenching the hot gas mixture to preserve the acetylene formed.

(i) Regenerative pyrolysis:

In this method, the hydrocarbon feed is heated to temperatures in the range 1100 - 1300 K for a fraction of a second by a hot solid, e.g. refractory tiles, before being rapidly quenched. The solids are heated in a separate operation. The best example of this method is the Wulff process (4).

(ii) Partial combustion:

This method uses a flame to provide a high temperature environment in which the hydrocarbon feed is partially combusted. Oxygen is commonly used to provide the flame which heats the products of the incomplete combustion to about 1800 K before quenching. Examples are the BASF process (3) and the SBA-Kellogg process (5,6).

(iii) Electrical processes:

This group of processes uses electrical energy in the form of a spark or arc discharge to heat the hydrocarbon feedstock to around 2000 K, followed by rapid quenching of the product. Although this method was one of the first found to make acetylene on a laboratory scale, very few electrical processes have become economic propositions. The only real exception to this is the Chemische Werke Huls process (7), although several other processes have reached pilot-plant scale.

Good surveys of the first two types of process are available (3) and because of their limited relevance to this work they will not be discussed any further.

LITERATURE SURVEY OF ELECTRICAL METHODS

Types of Reactor

The types of reactor utilising electrical energy to promote chemical reactions are many and varied, ranging from glow, radio frequency and microwave discharge to high-intensity arcs and plasmatrons. Only the latter two types of reactor will be discussed here as the others, which are well described in the literature (8,9,10), are outside the scope of this work.

The plasmatron, sometimes referred to as a plasma jet, is the most common type of plasma reactor. The term "plasmatron" will be used exclusively hereafter to describe any reactor in which one or more reagents are reacted in a stre of highly ionized gas, known as a plasma, which is produced in a region separate from the reaction chamber. The gas forming the plasma may take part in the reaction, e.g. hydrogen, or be inert, e.g. argon. As jets of plasma occur in many types of arc, the term "plasma jet" is too general to be applied to specific electrode geometries and will not be used in this work. A typical plasmatron is shown in fig. I. The working gas is introduced into the arc

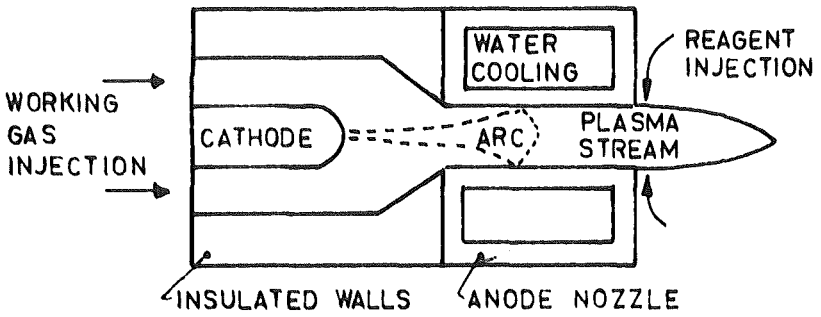

FIG I
TYPICAL PLASMATRON WITH
GAS LAYER STABILISATION

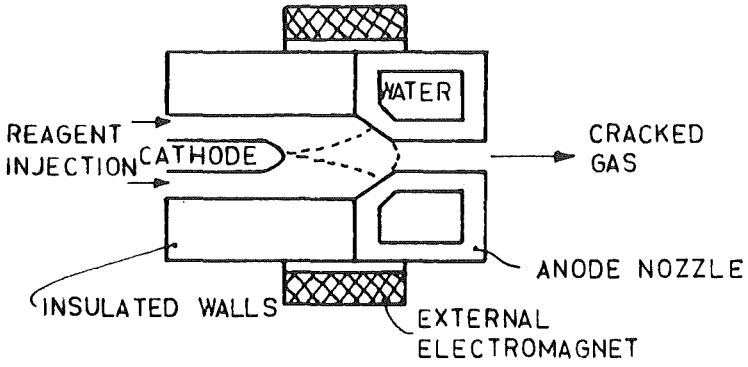

FIG II
TYPICAL TRANSFERRED ARC
WITH MAGNETIC STABILISATION

formed between the cathode and anode, typically tungsten and water-cooled copper respectively. The resulting hot ionized gas streams through an orifice in the anode to form a stable cone of plasma into which the reagents, solid, liquid or gas, are introduced. The arc is stabilised in one of a number of ways (11), the three most commonly used being:

(i) Gas layer stabilisation: The working gas, introduced from behind the cathode, prevents the arc from contacting the chamber walls by forming a cold gas sheath around it.

(ii) Vortex stabilisation: The working gas is fed tangentially into the arc chamber, producing an intense vortex off the tip of the cathode. The arc is contained within this vortex.

(iii) Magnetic Stabilisation: The arc, struck between an inner and outer electrode, is rotated at high speed with an external magnetic field. The working gas is fed axially through the inter electrode annulus.

The transferred arc and the high-intensity arc (fig. II) differ from the plasmatron in that there is no working gas, the reactants being introduced directly into the arc. If a solid reagent is used, it is generally fed as a consumable anode, e.g. a graphite rod or a fluidised coal bed. If all the reagents are gaseous, the anode is non-consumable, e.g. water-cooled copper. In the majority of cases, the cathode is tungsten, used because of its low work function and high melting point, and the arc is stabilised as for the plasmatron. The thermal efficiency of an arc reactor is defined as the percentage of the input energy transferred to the working gas, in the case of a plasmatron, or the reagents for a transferred or high-intensity arc.

Quenching of the hot product stream from the reactor can be effected in a number of ways, e.g. water-cooled tube (13,12), fluidised bed (12,14), cold gas mixing (12) and liquid sprays (12). All of these methods give quench rates of the order of 10^4 K sec^{-1} and the method employed is often dictated by the reagents used.

Review of Processes

For the purposes of this review, it is convenient to divide the processes which utilise electrical energy for the production of acetylene into two classes, those with gaseous reagents and those which include one or more solid reagents.

(i) Gaseous Reagents

By far the majority of the work carried out on electrical processes has been done on those systems using gaseous reagents, in particular natural gas. In addition to the following descriptions, a summary of the main features of the major processes is given in Tables I and II.

A. Plasmatron processes:

Knapsack Griesheim WLP Process

The basis of this hydrogen plasma process is contained in a patent granted in 1957 (15). Hydrogen, preheated to 1000 C, is used to form a vortex stabilised plasma into which the reactant, also preheated to 1000 C, is introduced. The electrodes are constructed of carbon or tungsten. With propane as a feedstock, 85% of carbon from the propane was converted to acetylene and 8% to ethylene. No soot formation was observed and the energy requirement per unit of acetylene was about 6.5 kWh kg^{-1}. The process has subsequently been developed to the stage of a 4000 kW pilot plant (16). A range of hydrocarbon feedstocks has been used with conversions of carbon to acetylene ranging from 36% (propane) to 64% (methane). Typical results for a light gasoline feed are given in table I. This process was the subject of a further patent in 1970 (17).

Chemische Werke Huls and Farbwerke Hoechst Processes

In 1971, Chemische Werke Huls and Farbwerke Hoechst announced the development of new processes for the production of acetylene and ethylene (18). Both processes, which have been developed to the pilot-plant scale, are based on hydrogen plasmatrons. The Huls process (19,20) is based on a 8500 kW dc

plasmatron with a thermal efficiency of 85-88%. The feedstock, mainly liquid hydrocarbons, is injected tangentially into the reaction zone in excess to prevent carbon deposits forming on the walls. Presumably this is effected by creating an outer layer of relatively cold reagent which condenses any carbon vapour diffusing to the walls and sweeps it away in the gas stream. From 20 to 30% of the feed is reacted, the remainder being recycled following quenching of the product stream by high boiling point hydrocarbons.

The Hoechst process (19) is based on a 10,000 kW three-phase ac system with a thermal efficiency of 90 to 92%. Vaporised or liquid naphtha, which is used as the reactant, is converted to acetylene by from 50 to 70%. Carbon deposits on the graphite walls of the reaction chamber are minimised by washing the walls with liquid hydrocarbons. Crude oil is used as the quench medium.

Vortex stabilisation is used in both reactors. Typical operating figures for both processes are shown in table I. It is stated (19) that the economic viability of both processes will depend on the cost of electrical energy.

Plasmatron Processes in the USSR

A prodigious quantity of work on the production of acetylene in plasmas has been done in the USSR, chiefly by a group of workers at the "Institute for the Synthesis of Petrochemicals of the Academy of Sciences of the USSR". As reviews of this work are available (21,22), only a brief outline of the principal results will be given here.

Because of the large deposits of natural gas which have been discovered in the USSR, there has been considerable emphasis on the pyrolysis of natural gas and methane in plasmatrons. Various working gases have been considered, including argon, hydrogen and methane.

Gulyaev et al (23) cracked methane in a 15 kW, gas-layer stabilised, argon plasma, gaining methane conversions of up to 80% and energy consumptions as low as 12.9 kWh kg^{-1} acetylene. Minc, Szymanski and Warycka claim (24)

that these values were obtained by sampling the plasma stream along its axis and are, therefore, unlikely to be representative of the bulk flow. They used a similar system to investigate the effect on yield of acetylene of both the position of injection of methane into the plasma and the ratio of argon to methane in the reaction chamber. They found a minimum energy requirement of 16.8 kWh kg^{-1} acetylene when the argon to methane ratio was 1.96 and the methane was injected through four ports in the anode nozzle wall. Valibekov and Bolotov (25,26) introduced methane into a 3-5 kW argon plasma through the anode wall and quenched the cracked gas mixture with a cold stream of argon. Conversions of methane to acetylene of up to 80% with energy requirements down to 8 kWh kg^{-1} were claimed. However, the latter figure is based on useful power input to the plasma and if the plasmatron inefficiencies are taken into account the energy requirement becomes 18 kWh kg^{-1} acetylene. Conversion of methane to acetylene is reported to decrease with increasing methane to argon ratio, a trend also shown by the results of Minc, Szymanski and Warycka (24).

Kozlov et al (27) reacted methane in a 14-33 kW hydrogen plasmatron and investigated the effect of stabilising the arc by both the vortex and gas layer methods. They concluded that vortex stabilisation is preferable as it gives better mixing between the reactant and plasma streams and results in a higher thermal efficiency than the gas layer method. They report a minimum power consumption of 14.7 kWh kg^{-1} acetylene at a methane conversion of 63%. A more detailed summary of their results is shown in table I.

Similar results were obtained by Kobzev, Kozlov and Khudyakov (28).

Kobzev, Kozlov and Khudyakov (29) also used a 30 kW methane plasmatron to pyrolyse natural gas. For a working gas methane feed of 50 l min^{-1} and a reactant methane feed of 60 l min^{-1}, they obtained a product gas containing 19.4 vol % acetylene, compared with 13-14% for a hydrogen plasma (27) and 8-10% for an argon plasma (23), with an energy consumption of 8.6 kWh kg^{-1} acetylene (a figure most likely based on effective power input to the reactor).

The other area in which the Russians are actively engaged is that of gasoline pyrolysis in plasmatrons. Polak et al (30) pyrolysed gasoline (61.6% C_5 and 21.06% C_6 paraffins) in a hydrogen plasma and quenched the products with a water spray. For a range of power inputs from 3.9 to 10.2 kW the mean reactor temperature was varied from 1200 to 1750 K. The energy consumption varied from 4.1 to 6.0 kWh kg^{-1} acetylene (based on useful power input). Above 1750 K, the production of carbon black fouled the reactor. Similar results were obtained by Volodin et al (31) who obtained conversions of gasoline to acetylene and ethylene of 75-92% with energy consumptions of 4.0 to 5.3 kWh kg^{-1} acetylene and olefins (based on useful power input) as the reaction temperature was increased from 1370 to 1640 K. I'lin and Eremin (57) used a water vapour plasma to pyrolyse gasoline. They claim that practically no carbon black was formed for an energy consumption, based on useful power input, of about 6 kWh kg^{-1} acetylene and its homologs.

Although a considerable quantity of laboratory-scale work has been done in the USSR, very little appears to have reached pilot-plant scale or greater. Valibekov and Bolotov (25) reported the proposed establishment of a plasma-based industry to manufacture acetylene using cheap electrical power from the Nurekskii hydro-electric plant and local resources of natural gas, but no further confirmation of this is available. In 1969, Khudyakov, Kobzev and Kozlov were granted a patent (32) for a plasmatron process to pyrolyse methane which is used as both working gas and reactant. No data on scale is given, but a conversion of methane to acetylene of 71.3% with an energy consumption of 7.15 kWh kg^{-1} acetylene is claimed. Sidorov, I'lin and Polak (33) describe a 250 kW pilot plant also using a natural gas plasma at a pressure of 2.5 atm. They claim conversions of methane to acetylene of 50%, with an energy consumption of 8.7 kWh kg^{-1} acetylene.

Other Plasmatron Devices

In 1964 it was reported (34) that Magnetohydrodynamics Inc. had developed a plasmatron process for the production of acetylene from various feedstocks ranging from methane to naphtha to powdered coal. A 9.1×10^5 kg yr^{-1} pilot

TABLE I Typical Operating Conditions for Plasmatrons

Process	Electrodes	Power Consumption kW	Working Gas	Reactant Gas	Product Concentration Vol % C_2H_2	Product Concentration Vol % C_2H_4	Conversion of Feed Carbon % C_2H_2	Conversion of Feed Carbon % C_2H_4	Energy Requirement kWh kg^{-1} C_2H_2	Energy Requirement kWh kg^{-1} $C_2H_2 + C_2H_4$	Quench Process	Ref.
Knapsack Griesheim	Tungsten or Carbon	1930 DC	Hydrogen 484 m^3 hr^{-1}	Gasoline 765 kg hr^{-1}	13.84	10.8	30	24	8.3	4.57		38
Huls	Iron	8500 DC	Hydrogen	Crude Oil	14.8	6.51	27	13	9.8[1]	6.6	High BPt Hydrocarbons	44
Hoechst	Graphite	10000 AC	Hydrogen	Naphtha	13.7	6.4	52	26	9.3	6.2	Crude Oil Residues	26
Gulyaev et al	Copper Tungsten	10 DC	Argon 63 l min^{-1}	Methane 27 l min^{-1}	8.71	.25	71.3	-	14.4	-	Water Cooled Probe	48
Minc et al	Copper Tungsten	9.o DC	Argon 2602 l min^{-1}	Methane 1328 l min^{-1}	9.0	<1.0	69.2	-	16.8	-	-	49
Kozlov et al	-	26.5 DC	Hydrogen 46 l min^{-1}	Methane 55 l min^{-1}	13.5	.32	74.1	-	12.4[2]	-	Water Spray	52
			50 l min^{-1}	60 l min^{-1}	13.0	.78	72.1	-	12.3[3]	-		
Kobzev et al	-	30 DC	Methane 50 l min^{-1}	Methane 60 l min^{-1}	19.4	-	76.0	-	8.6[4]	-	-	54
Diamond Alkali Co	-	425 DC	Hydrogen	Methane	-	-	65	-	9.35	-	Water Spray	40

1 Including Power Consumed in Product Separation
2 With Vortex Stabilisation
3 With Gas Layer Stabilisation
4 Based on Effecrive Power Input

plant had been built which would, it was claimed, produce acetylene at less than 5c per pound.

In 1968, the Diamond Alkali Co. was granted a patent (35) for a process for producing acetylene from methane in a hydrogen plasmatron. Conversion of carbon in the methane to acetylene was claimed to be 65%, with an energy consumption of 9.35 kWh kg^{-1} acetylene.

The Linde Co. was reported (36) to have developed a plasmatron device for the synthesis of acetylene. Good results were claimed, but these claims were not supported by data.

Anderson and Case (37) cracked methane in a hydrogen plasma and compared their experimental results with analytical predictions. A good fit between the two is claimed and they found an optimum experimental value for carbon conversion to acetylene of 76% and an optimum energy consumption of 9.2 kWh kg^{-1} acetylene. From the thermodynamic and kinetic data, the most critical parameter was found to be the speed of mixing of the methane with the plasma.

Leutner and Stokes (38) cracked methane in an argon plasma to obtain very high acetylene yields (80.1%) but with a very high energy consumption of 145 kWh kg^{-1} acetylene. Operation was limited to less than three minutes by severe chamber erosion.

B. High-intensity and Transferred Arc Processes:

The Chemische Werke Huls "Flaming Arc" Process

This is the largest and the oldest of the various processes to have reached commercial operation, having been in operation with only minor design modifications since 1940. The installation consists of nineteen pairs of vortex stabilised arcs, each arc operating at 8000 kW (7000 V and 1150 A), and has an annual output of 1.32×10^8 kg of acetylene and 6.1×10^7 kg of ethylene (7). Several hydrocarbon feedstocks are used, including refinery gas, liquified petroleum gas ($C_3 + C_1$), naphtha and natural gas. Initially, the hot reactant gases were quenched by a water spray, but this has been

replaced by a hydrocarbon spray which is itself cracked in the quenching process. The unreacted hydrocarbons in the product are separated and recycled as additional feedstock. Detailed descriptions of the reactor are available in the literature (7,39).

Conversion of hydrocarbon to acetylene is 36%, with a further 17% converted to ethylene; the other principal products are hydrogen and carbon black. Early figures (3) gave the energy requirements per unit of acetylene as 13.2 kWh kg^{-1} (including 2.9 kWh required for separation processes), but more recent figures (7) claim a reduction in this to 9.8 kWh kg^{-1}.

The Du Pont Process

In 1963, Du Pont began operation of a commercial installation at Montague, Michigan, for the production of 23 x 10^6 kg yr^{-1} acetylene from refinery hydrocarbons (40). The hydrocarbon is pyrolysed in a 3,100 A, 3,500 V arc (41), magnetically rotated sufficiently fast to approach a continuous plasma. The reactor is operated at .525 bar and sufficient hydrogen is recycled from the product to give an overall ratio of hydrogen to carbon atoms of 4:1. Carbon deposit on the electrodes is prevented by using a consumable graphite cathode and by continuous mechanical scraping of the anode. The best yield, 75%, is obtained with butane and decreases with increase in chain length to 65% for a hydrocarbon, averaging ten atoms in length. The energy requirements are 6.6 kWh kg^{-1} acetylene including the generation of the magnetic field but excluding product separation costs (42).

This plant was shut down in 1968 (43) due to a reduction in the price of calcium carbide, making the latter route to acetylene more economic. This highlights the dependence of these processes on the cost of electric power as Huls, with a unit cost of 6.9 kWh kg^{-1} acetylene (excluding separation costs) but who own their own power generating plant, still remain economic.

Roumanian Process

In 1960, an arc process to produce acetylene and ethylene from liquid hydrocarbons reached full-scale development at Borzesti in Roumania (44). The process (45) consists of two stages. In the first stage, liquid hydrocarbons, e.g. gasoline and gas oils, are cracked in a thermal cracking furnace. The hot, partially cracked gases then pass to the second stage which consists of an ac or dc electric arc, and are further cracked to a product consisting predominantly of acetylene and ethylene, the ratio of these being from 3:2 to 2:1. It is claimed that the conversion of feedstock to acetylene and ethylene is between 40 and 56% and that the energy requirement of the arc is between 4.5 and 5.5 kWh kg^{-1} acetylene plus ethylene. The advantage of this process over the more usual single-stage one is that part of the electrical energy is replaced by cheaper thermal energy.

Czechoslovakian Process

This process, brought into the stage of a 30 kW pilot plant in 1960 (46,47), uses an ac arc to produce acetylene and ethylene from natural gas and naphtha. Natural gas is cracked in an ac arc before being quenched, firstly by naphtha, which is itself cracked in the quenching process, and secondly by a water spray, the total quench time being from 10-100 msec. The use of ac and a two-stage quench is reported to give a reduction in the capital cost of the power circuitry of 66%, compared with the equivalent dc process, and to give an 18-20% reduction in the unit cost of acetylene. The energy consumption for acetylene is 10 kWh kg^{-1} and that for acetylene plus ethylene 7.25 kWh kg^{-1} (48).

Westinghouse Process

In this process, methane is pyrolysed in a magnetically rotated arc (49) which because of a very narrow arc gap, .95 cm at 100 kW, can operate on either ac or dc. It is claimed (50) that methane conversions (on a carbon basis) of up to 80% can be obtained when the methane is well mixed with the arc, and a minimum energy consumption of 5.8 kWh kg^{-1} acetylene is also reported.

TABLE II Typical Operating Conditions for Transferred Arcs

Process	Arc Type	Power kW	Reactant	Production Rate	Product Conc. Vol %		% Conversion of Feed Carbon		Energy Consumption kWh kg^{-1}		Quench Method	Ref.
					C_2H_2	C_2H_4	C_2H_2	C_2H_4	C_2H_2	C_2H_2 + C_2H_4		
Huls	Long Arc ~1000 cm	8000 DC	Refinery, Natural & Petroleum Gases	1.32×10^8 kg yr^{-1} C_2H_2 6.1×10^7 kg yr^{-1} C_2H_4	15.9	7.1	48	15	9.8[1]	7.7	Liquid Hydrocarbon Spray	17,23
Du Pont	Short Arc Magnetic Rotation 8000 RPM	10,850 DC	Refinery Hydrocarbons	23×10^6 kg yr^{-1} C_2H_2	15.2		65-75		6.6		Water Spray	24
Roumanian		20 AC or DC	Petroleum fractions		16.7	8.1	50	25	8.4-9.3[2]	5.6	Water Spray	29
Czech.		30 AC	Natural Gas	3 kg hr^{-1} C_2H_2	12.7	4.8	30	12	10.0	7.25	Naphtha & Water Spray	34
Westinghouse Short Arc Gap ~5 cm		3000 AC or DC	Methane		9.5	0.88	50		14.9		Water Cooled Probe	36

1. Including product separation power

2. Feed preheated to 500 - 700 C

However, considerable doubt is expressed over this latter figure as the enthalpy requirement for the reaction is 5.3 kWh kg^{-1} and, in addition, sensible heat must be provided. A more representative set of results gives a methane conversion of 46.7% for a power consumption of 14.9 kWh kg^{-1} acetylene.

Hirayama, Fey and Camp (51) used a 3000 kW ac arc to pyrolyse methane and investigated the effect of reaction chamber pressure on the yield of acetylene. They found that the conversion of carbon to acetylene decreased from 40% at 1.0 bar to less than 10% at 7.0 bar and that the energy consumption per unit of acetylene rose from 8.8 kWh kg^{-1} to 22 kWh kg^{-1} over the same range.

They discussed their results in terms of the decomposition of acetylene to carbon which they claim is the final step (suppressed by rapid quenching) in the chain of reactions resulting in the pyrolysis of methane. The rate of decomposition increases as the square of the pressure (52) and hence one would expect the observed fall-off in conversion with increasing pressure.

(ii) Solid Reagents

The use of solid reagents for the production of acetylene in electric arc processes can be divided into two principal categories, the injection of powdered coal into argon and argon/hydrogen plasmas and the use of graphite as a consumable electrode in high-intensity arcs using hydrogen or methane as the source of hydrogen. The only exception to this classification comes in a description of the work of the AVCO Corp. and their work will be discussed in a separate section.

A. Coal Pyrolysis in Plasmatrons:

At 298 K, the minimum energy requirement for the conversion of methane to acetylene by equation 1 is 3.96 kWh kg^{-1} acetylene. Because of the necessity of raising the methane to 1500-2000 K to obtain favourable thermodynamic and kinetic conditions, the actual minimum energy requirement

will also include an amount of sensible heat.

$$2CH_4 \longrightarrow C_2H_2 + 3H_2 \qquad H(298) = 90 \text{ kcal} \qquad (1)$$

For high volatile bituminous coals, however, the minimum energy requirement, again excluding sensible heat, for the reaction shown in equation 2 is only 2.20 kWh kg^{-1} acetylene.

$$(C + H)_{coal} \longrightarrow C_2H_2 \qquad H(298) = 2 \text{ kcal/gm } C_2H_2 \qquad (2)$$

These figures, in addition to its low cost compared with most hydrocarbons, show why coal has been considered such an attractive reactant for the production of acetylene in spite of disadvantages such as the presence of impurities, e.g. ash, oxygen, nitrogen and sulphur, and the difficulties in transferring sufficient energy to the coal to vaporise it completely within the reaction chamber. This latter point is discussed in chapter 7.

In 1963, Bond et al (54) reported a preliminary investigation of the reactions of coal in an argon/hydrogen plasma. They claimed conversions of carbon to acetylene of up to 45% for an argon to hydrogen ratio of 9:1 and suggested that higher values could be obtained if all the coal feed could be raised to the arc temperature. Bond, Ladner and McConnel (55,56) injected powdered coal, suspended in a stream of argon, into an argon plasma for power inputs of 4.5 - 8.6 kW. The hot gas mixture was quenched in a water-cooled chamber. The effect on yield of acetylene (on a carbon basis) of coal particle size, rank and residence time and the plasmatron working gas were investigated. As expected, the yield of acetylene was strongly dependent on the particle size of the coal; particles over 200 microns scarcely reacted at all, whilst carbon conversions of up to 20% were obtained for particle sizes of 50 micron and smaller. The carbon conversion was found to be directly proportional to the percentage of volatile matter (rank) in the coal over a range of volatile concentrations from 10 to 60%. This gives support to the argument that the majority of the acetylene is formed by the reaction of the volatiles rather than by complete evaporation of the coal. Further support

for this argument is given by the fact that very low yields were obtained when the feed was very low volatile content carbon black. Bond et al postulated that an increase in the residence time of coal in the plasma would result in increased vaporisation of the coal particles and hence higher acetylene yields. However, such a dependence was not observed; this was put down to less efficient quenching causing acetylene decomposition. When argon was replaced by argon/hydrogen mixtures as the working gas, an increase in carbon conversion from 14 to 37% was obtained for an increase in working gas hydrogen of 0 to 8% at a power input of 4 kW and using 53-74 micron particles. Above 8% hydrogen, the carbon conversion fell gradually to 18% at 100% hydrogen. This was probably due to a contraction of the plasma lowering the residence time of the coal particles. Argon/methane mixtures were also tried as a working gas, but the results showed that the conversion of carbon was not significantly enhanced by using methane. Soot deposited in the reactor was submicron in size and appeared spherical in shape. It is suggested that, for the most part, this was formed by shattering of coal particles by the rapid evolution of gas during the rapid heating as low volatil coals passed through the plasma virtually unchanged in size. The best results obtained gave carbon conversions of about 35% for energy requirements of about 800 kWh kg^{-1} acetylene using a working gas of 85% argon and 15% hydrogen and a power input of 4.2 kW.

Kawana and various co-workers have also investigated the reactions of coal in argon, argon/hydrogen and hydrogen plasmas. Kawana, Makino and Kimura (58) used a 20 kW plasmatron to react powdered coal, entrained in a stream of argon, in an argon plasma, the products being quenched in a water-cooled chamber. The effect of coal feed rate, electrical power input and argon flow rate on the yield of acetylene were investigated. For a power input of 7.02 to 7.56 kW and a working gas flow of 25 l min^{-1}, the coal feed was varied from 0.4 to 2.86 gm min^{-1}. The conversion of carbon to acetylene decreased from 52 to 24% and the energy requirement from 834 to 250 kWh kg^{-1} acetylene over the

range of coal feeds. When the arc power was varied from 3.8 to 7.5 kW, the yield of acetylene remained unchanged at about 20% and, as a result, the energy consumption rose from 156 to 250 kWh kg^{-1} acetylene. Quantities of unreacted coal found in the reaction chamber suggested that not all the coal was entering the plasma and it was suggested that this may be a partial cause of the unexpected constant yield for varying power input. The efficiency of the coal entry into the plasma was investigated by increasing the argon flow rate, and hence the plasma volume, from 20 to 30 l min^{-1} for an arc power of 3.6 kW. The yield of acetylene increased from 6 to 24%, suggesting that the lower the argon flow the less the amount of coal entering the plasma. The best experimental conditions found by Kawana et al were an argon flow of 30 l min^{-1}, an arc power of 3.8 kW and a coal feed of 2.74 gm min^{-1}; under these conditions the energy consumption was 135 kWh kg^{-1} acetylene.

Kawana and Makino (59) used the same apparatus to react coal in plasmas of argon/hydrogen and hydrogen. They found that the hydrogen plasma gave more favourable results than the argon/hydrogen plasma. The best experimental conditions found were a hydrogen flow rate of 60 l min^{-1} and an arc power of 11 kW. Under these conditions, the conversion of coal to acetylene was 65%, with an energy consumption of 66.5 kWh kg^{-1} acetylene. In agreement with Bond et al, they found that the yield increased with increase in the volatile content of the coal. The maximum acetylene concentration in the product gas was 3.8%.

This work has been summarised and compared with the pyrolysis of gaseous feedstocks by Kawana (60).

Graves, Kawa and Kiteshue (61,62) used a conventional plasmatron rated at 28 kW to study the reactions of coal in argon and argon/hydrogen plasmas. However, their data on the conversion of carbon to acetylene are of limited value because the product gases were bubbled through water before sampling and no account has been taken of acetylene dissolution in the water. This is underlined by the fact that their carbon balances for the system

consistently show deficits of 3-8%. If the loss of acetylene to the bubbler water is assumed a constant factor, some trends can be observed. In all runs, considerable amounts of solid residue remained after reaction of the coal. The volatile content of this residue was the same as the initial coal feed, suggesting that at the feed rates used, 1.41 and 0.5 kg hr^{-1} coal, coal-plasma contact was poor. The effect of a number of variables on coal-plasma contact (as indicated by the amount of unreacted residue) and acetylene yield was investigated. Decreasing the particle size had a very marked effect, the percentage of coal unreacted falling from 84% for 70x100 mesh to 63% for -325 mesh; this was accompanied by a substantial rise in acetylene yield. An increase in plasmatron power input and coal feed rate caused increases and decreases respectively in acetylene yield, but these were slight compared with the effect of change in particle size. A decrease in acetylene yield with coal rank was also noted. Addition of 12% hydrogen to the plasmatron working gas also increased the acetylene yield.

Similar results were obtained by McDonald (63), Anderson et al (64) and Newman et al (65). All their results supported the theory that the majority of acetylene is formed by the rapid pyrolysis of the volatile matter released during the progressive carbonisation of the coal particles. Anderson et al noted that substitution of a water spray for the usual water-cooled chamber had little effect on acetylene yield.

A summary of results from the above works is shown in table III.

B. High-intensity Arcs

Apart from the work carried out for the AVCO Corp., all the remaining work carried out on the production of acetylene in high-intensity arcs using consumable carbon electrodes has been consequent on an initial study by Baddour and Iwasyk (66). The latter developed a reactor in which ablation of a graphite anode was effected by a high-intensity arc struck between the anode and a cylindrical graphite cathode. Although subsequent variations

TABLE III Summary of Results for Plasmatron Pyrolysis of Coal

	Power Input kW	Volatile Content of Coal daf %	Coal Feed gm min^{-1}	Coal Particle Size μ	Gaseous Reagent	Gas Feed l min^{-1}	Vol Conc Acetylene %	Conversion of Carbon to Acetylene %	Energy Requirement kWh kg^{-1}	Ref.
Bond et al	4.2	36.4	.08	53-74	99.7% Argon 0.3% Hydrogen	9.51	-	18	5365	71
	4.2	36.4	.05	53-74	91.7% Argon 8.3% Hydrogen	9.51	-	37	4177	71
	-	36.4	.06 + .18 gm min^{-1} CH_4	53-74	Argon	9.51	.77	48	-	71
Kawana et al	7.02-7.56	45.6	1.6	147	Argon	29.3	1.0	29	400	72
	7.6	"	2.61-2.86	"	"	"	-	25	250	"
	3.8	"	"	"	"	"	-	20	156	"
	3.4-3.8	"	2.63-2.79	"	"	34.3	-	24	137	"
Graves et al	10.2	38	5.6	50	Argon	40.5	-	18.3	181.6	76
Newman et al	22.0	37.8	55.1	246	Hydrogen	178	-	20	28.1	79
Anderson et al	6.0	49.3	2.14	74	Argon	15	.78	6.8	818.5	77
	"	50.0	1.23	"	87.7% Argon 12.3% Hydrogen	17.1	.15	2.86	3559	78

in the diameters of the two electrodes occurred, the radial inter-electrode spacing has remained unchanged at .318 cm. The gaseous reagent was introduced into the reaction chamber either through three ports around the anode or, if it was hollow, through the anode itself. Samples of the hot product gas were taken through water-cooled probes, the diameter and position of which were variable, which also quenched the hot gas. Initially, power levels were limited to 10 kW, but this was later increased by other workers to 50 kW. Apart from the initial study by Baddour and Iwasyk, the arc was magnetically rotated. A summary of the various investigations is given in table IV.

All workers determined that the major parameters affecting the yield of acetylene were the ratio of carbon to hydrogen in the reacting gases and the temperature of reaction. The effect of these parameters on the acetylene yield was investigated by variation of the power input, gas flow rate and addition of dilutant.

The importance of the quench process in arc reactions was shown by dependence of the acetylene yield on both the diameter and the position of the sample probes. A maximum in the plot of acetylene yield vs probe distance from the cathode was found by Blanchet and Parent (68) for both ethane and propane. This distance corresponded to a residence time in the reactor before quenching of about 30 msec and was in contrast with Baddour and Iwasyk (66) who found that the acetylene yield increased as the residence time decreased to 10 msec. However, the power input in the latter case was about 7 kW compared with 25 kW in the former for identical gas flows and it is suggested that the apparent discrepancy is due to the existence of an optimum quench temperature, the position of which will depend on the power input. Similarly, the probe diameter affected the yield, presumably because of a variation in quench rate with probe diameter. The product gas analyses obtained in these studies show consistently higher concentrations of acetylene than those obtained for other arc processes, reaching up to 50% for a methane reactant (67) compared with a maximum of about 15% for gaseous reagent

TABLE IV Summary of High-intensity Arc Studies

	Gaseous Reagent	Dilutant	Anode Diam. cm	Reference
Baddour & Iwasyk	hydrogen	helium	.635	2
Baddour & Blanchet	hydrogen, methane	-	.635, .935	3
Blanchet & Parent	ethane, propane	-	.935, 1.27, 1.59	62
Cholette, Courtois, Parent	propane	argon	1.59	80
Lafond, Meubus, Kaliaguine, Parent	methane	argon helium	1.59	81

plasmatrons (table I). A possible reason for this is the quench method which allows very rapid local quenching but, because it is limited to a laboratory scale, gives artificially high concentrations when compared with pilot-scale and larger plants. In all cases, the yield of acetylene increased with increasing carbon to hydrogen ratio and increasing power input (i.e. increasing reaction temperature). Cholette et al (69) and Baddour and Iwasyk (66) found that an increase in inert dilutant in the gas feed caused an increase in yield and this is probably attributable to higher reaction temperatures obtained with the use of dilutants. However, this was accompanied by a drop in carbon conversion (69). Neither the vaporisation rate of carbon nor its conversion to acetylene appeared to vary significantly with the gaseous reagent used (68). The maximum conversion of carbon obtained was about 35% and one of the major problems with this reactor system is the deposit of both hard carbon and soot on the inner walls of the cathode.

Lack of data on the coefficient of volume expansion for the product stream made evaluation of energy requirements difficult. The only figures available give minimum energy requirements of about 22 kWh kg^{-1} acetylene for propane (68), 66 kWh kg^{-1} acetylene for methane/argon mixtures (70) and 110 kWh kg^{-1} acetylene for hydrogen (67). Details of the operating conditions for these results are shown in table V.

C. AVCO Research

One of the most concerted efforts to find a viable process for making acetylene from coal has come from the AVCO Space Research Centre who have been sponsored in this by the U.S. Department of the Interior Office of Coal Research since 1964. Since then, various workers at AVCO have investigated three basic reactor designs. The first design was based on a consumable coal anode; this was superseded by a rotating arc device with powdered coal fed into the arc gap and this in turn was superseded by the pyrolysis of coal in a hydrogen plasmatron.

TABLE V Summary of Best Operating Conditions for High-intensity Arcs

Gaseous Reagent	Dilutant	Process input kW	Gas feed $l\ min^{-1}$	(C/H_2) mole in feed	Vol. conc. C_2H_2 vol %	Conversion of carbon	Energy requirement $kWh\ kg\ m^{-1}$	Reference
Propane	-	30	20.0	~1	14	32	22	62
Methane	Argon	~15	12.0	~1	12	24	66	81
Hydrogen	-		16.0		12	27	110	3

The initial approach to the problem was outlined by Ammann et al (71) who carried out a static experiment in which a coal anode (88% high-volatile bituminous coal, 11% pitch) was vaporised by a 24 kW arc into a chamber, initially under vacuum but allowed to come to 1 bar during the run. The resulting gas was sampled with a water-cooled probe and analysed for hydrocarbons. The principal products were hydrogen (72.42%), methane (9.41%), carbon monoxide (8.35%) and acetylene (5.04%) and it was claimed that by improving the design of the reaction chamber to lower the residence time of the gases in the arc, the acetylene yield would be improved. Having established the technical feasibility of such a process, an economic evaluation of a 10,000 t coal per day plant was carried out to determine the economic feasibility.

This basis was built upon by Krukonis and Schoenberg (53) who fed coal through a 2.54 cm diameter copper tube into an arc struck between the coal face and a 1.59 cm diameter graphite cathode for power inputs of 20-40 kW. The products were quenched by cold gas injection, sampled and analysed by gas chromatograph. Using argon as the quench gas, the yield of acetylene, based on carbon in coal, increased from 3% at 20 kW to 6% at 40 kW. The energy requirement remained approximately constant at 88 kWh kg^{-1} acetylene over the power range. When no quench gas was used, the yield remained substantially unchanged and this was taken to imply that argon was not an efficient medium and hence that higher acetylene yields and lower energy requirements should be attainable with a change in quench gas. When a hydrogen quench was used, the yield of acetylene rose to 6% at 24 kW and 14% at 40 kW and the energy requirements fell to 33 kWh kg^{-1} acetylene. Krukonis and Schoenberg give three possible reasons for the improvement in performance. They claim that the hydrogen forms additional acetylene, both by reacting with the carbon in the coal and by combining with radical species such as C_2H in line with the mechanism proposed by Plooster and Reed (72). In addition, they claim that hydrogen is a better "preserver" of acetylene than argon. The possibility

of reaction between the quench hydrogen and coal was investigated by using char (.12% hydrogen compared with 5.64% for coal) instead of coal in the arc. The yield of acetylene at 25 kW was 5.5%, showing that such a reaction does enhance the acetylene yield. The effect of hydrogen as a preserver was shown by passing mixtures of acetylene and argon and acetylene and hydrogen through an arc. The decomposition of acetylene was 60% for the former mixture compared with only 10% for the latter. No theoretical explanation of these phenomena was attempted.

This work was also described by Krukonis, Gannon and Schoenberg (73) as a prelude to describing the second reactor type used by AVCO, the high-intensity rotating arc. The reasons for changing the reactor geometry were twofold: it was necessary to increase arc-coal contact as as much as one-third of the coal from the anode was passing through the arc unreacted. It was also desirable to decrease the residence time of acetylene in the arc. With the consumable anode, the reaction zone at the anode was from .64 to 1.27 cm in depth and any acetylene formed below the anode surface would be in contact with incandescent char in this region and hence would be liable to decomposition. The rotating arc reactor was similar to that developed by Du Pont (42), powdered coal, entrained in a stream of hydrogen axial to the graphite cathode, passed through a magnetically rotated arc struck between the cathode and an annular anode 3.82 cm in diameter. The power consumed by the magnet was 1.6 kW which was negligible compared with the 20-70 kW reactor power. The arc was operated at 0.2 bar as well as at atmospheric pressure. The yield of acetylene ranged from 6-14% for power inputs of 20-45 kW at 0.2 bar compared with 3.5-5% for 35-65 kW for 1.0 bar. The corresponding energy requirements were 9 kWh kg^{-1} acetylene and 26-38 kWh kg^{-1} respectively. This shows a marked improvement in performance at lower pressures. A decrease in the amount of soot in the reaction chamber led to the conclusion that a reduction in pressure had its most pronounced effect on decomposition of acetylene. Subsequent runs were carried out using a

cold hydrogen quench; under these conditions the yield ranged from 7-18% for ar energy requirement of 11-6.5 kWh kg^{-1} acetylene and a power input of 80-100 kW. A feasibility study was carried out in 1969 for AVCO by Stone and Webster Engineering Corp. (74) who considered the economics of 682 x 10^6 and 136 x 10^6 kg yr^{-1} plants. They found that for the process to be viable at these production levels, the energy requirements would need to be reduced to 7.7-8.8 kWh kg^{-1} acetylene. It was claimed that using a laboratory-scale plant of the type outlined above of 75-100 kW with a production rate of 4.1-5.5 kg hr^{-1} acetylene, the energy requirements had reached a level of 12.2 kWh kg^{-1} acetylene and conversions of up to 25% had been obtained.

The third reactor type investigated by AVCO was a plasmatron where powdered coal was fed into a plasma of hydrogen (75,76), the resulting hot gas mixture being quenched in a water-cooled chamber. A hydrogen plasma was generated by a 30 kW plasmatron with a thermal efficiency of 75%; coal was injected into this as a powder entrained in a secondary hydrogen stream through a circular manifold. The yield, energy requirement and product concentration of acetylene were investigated as a function of hydrogen enthalpy and coal feed rate. It was found that the conversion was enhanced by running the reactor at reduced pressures and pressures of .2 bar and .5 bar were used. For a constant coal feed, the yield and concentration increased with increasing hydrogen enthalpy and the energy requirement went through a minimum over the same range. At the hydrogen enthalpy for which the minimum energy requirement occurred, the yield fell markedly with an increase in coal feed rate, e.g. doubling the coal feed rate halved the yield. Over the same range, there was a slight increase in concentration and a slight decrease in energy requirement, but these rapidly reached constant values of 8.5% and 15.4 kWh kg^{-1} acetylene respectively. Gannon, Krukonis and Schoenberg (75) outline projected future developments including improving coal-plasma contact by feeding coal through a hollow cathode or countercurrent to the plasma flow. They also raise the possibility of injecting coal into both the arc and the resulting hydrocarbon plasma.

SUMMARY OF LITERATURE SURVEY

Two of the most important criteria in determining the economic viability of the processes described here are the degree of conversion of feedstock carbon to acetylene and the energy consumption per unit of acetylene produced. The best results obtained for the principal processes reviewed are shown in the light of these two criteria in fig. III. However, this graph can only give an indication of the relative merits of the various processes as in the final analysis it is the cost of electrical energy which determines whether or not a process is economically viable. For example, fig. III suggests that the Du Pont process is as much an economic proposition as the Huls "flaming arc" process, yet the former was closed down in favour of a more economic carbide plant whereas the latter has steadily expanded since 1940. This shows the ultimate dependence of economic viability on local conditions and policies.

The energy consumption figures shown in fig. III are for acetylene alone. Some of the processes, e.g. the Knapsack Griesheim and Hoechst plasmatron processes, produce considerable quantities of ethylene and if this is taken into account the energy consumption per unit of useful olefins falls significantly, e.g. from 8.3 to 4.57 kWh kg^{-1} for the Knapsack Griesheim process. The other main point which must be considered when evaluating these processes is that of the costs of product separation which, with the exception of the Huls process, are over and above the quoted energy consumptions. An indication of the energy consumed in separating a product stream containing 10-20% acetylene is given by the Huls figure of 2.9 kWh kg^{-1} acetylene (39).

All the works reviewed here show the dependence of yield and energy consumption on five basic parameters: the carbon to hydrogen ratio, degree of mixing, pre-quench temperature and rate of quenching of the hot reacting gas mixture and the pressure of the reaction chamber. Variation of the other parameters associated with arc, e.g. power input and reagent feed rate,

FIG III
CONVERSION OF CARBON AND ENERGY CONSUMPTION FOR VARIOUS PROCESSES

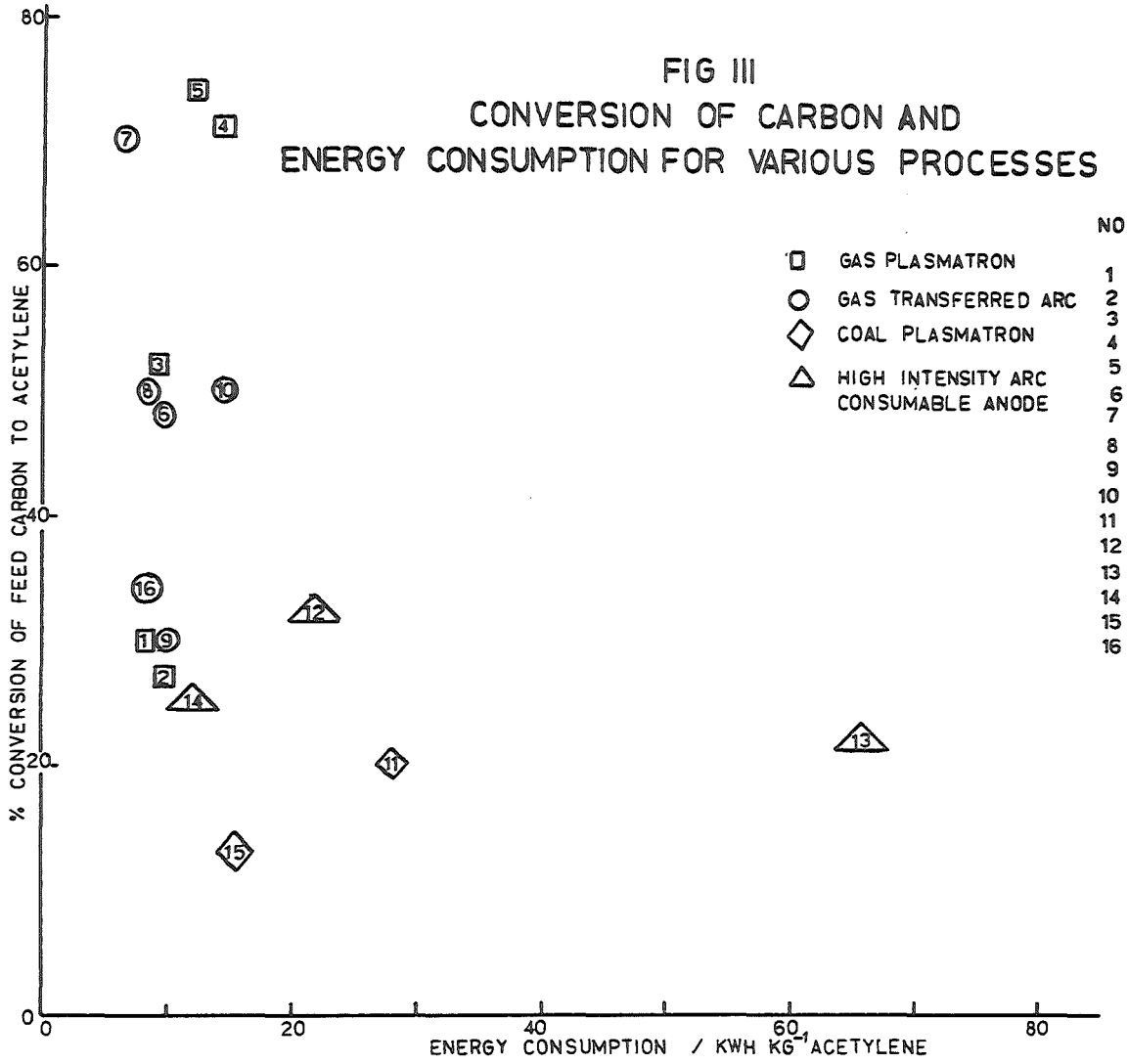

NO	PROCESS	POWER /KW	REF.
1	KNAPSACK GRIESHEIM	1930	38
2	HÜLS	8500	44
3	HOECHST	10000	26
4	GULYAEV ET AL	10	48
5	KOZLOV ET AL	265	52
6	HÜLS	8000	17, 23
7	DU PONT	10000	24
8	ROUMANIA	20	29
9	CZECHOSLOVAKIA	30	34
10	WESTINGHOUSE	3000	36
11	NEWMAN ETAL	22	79
12	BLANCHET & PARENT	30	62
13	LAFOND ET AL	15	81
14	AVCO	85	65
15	AVCO	6-3	67
16	HIRAYAMA ET AL	1440	60

only has the effect of altering one or more of these basic parameters.

The equilibrium diagram for the carbon-hydrogen system, fig. XXII (for greater detail of minor species see refs 111,112), shows clearly the dependence of the yield of acetylene on both the carbon to hydrogen ratio and the system temperature (67).

Almost all workers have used a variety of methods to vary these two parameters in an attempt to optimize their operating conditions. These include varying the power input and reactant flow rates and the use of dilutants. Several workers have found optimum values for these parameters, e.g. Valibekov and Bolotov (25) found that a maximum yield of acetylene was obtained for a pre-quench temperature of 1750 K, whilst Kozlov et al (27) found an optimum molar carbon to hydrogen ratio of .38.

The degree of mixing in the reacting system is of the utmost importance. Different methods of ensuring good mixing have been employed for different arc geometries. In plasmatron process, the method of injecting the reagent into the plasma plays an important part in determining how well the reacting gases are mixed. Minc et al (24) investigated the effect of varying the position at which methane was injected into an argon plasma and found that the best mixing was obtained when the methane was injected through several ports in the anode annulus. This method has subsequently been used by the majority of workers using plasmatrons. More recently, Mosse et al (77) found that injecting the reagents countercurrent to the plasma stream further improved mixing and resulted in higher yields. The problem of obtaining adequate mixing to ensure all the reagents reach the desired pre-quench temperature explains why solid reagent processes are lagging so far behind gaseous reagent processes in economic viability (see fig. III). Because of the size of the coal particles, only a small amount of each particle vaporises before it passes through the plasma zone and this results in a poor conversion of carbon and a high energy consumption. The importance of this effect has been shown by Bond et al (56) who improved the degree of conversion

FIG XXII

EQUILIBRIUM DIAGRAM FOR C/H SYSTEM

PRESSURE 1.0 BAR, C/H MASS 1.2

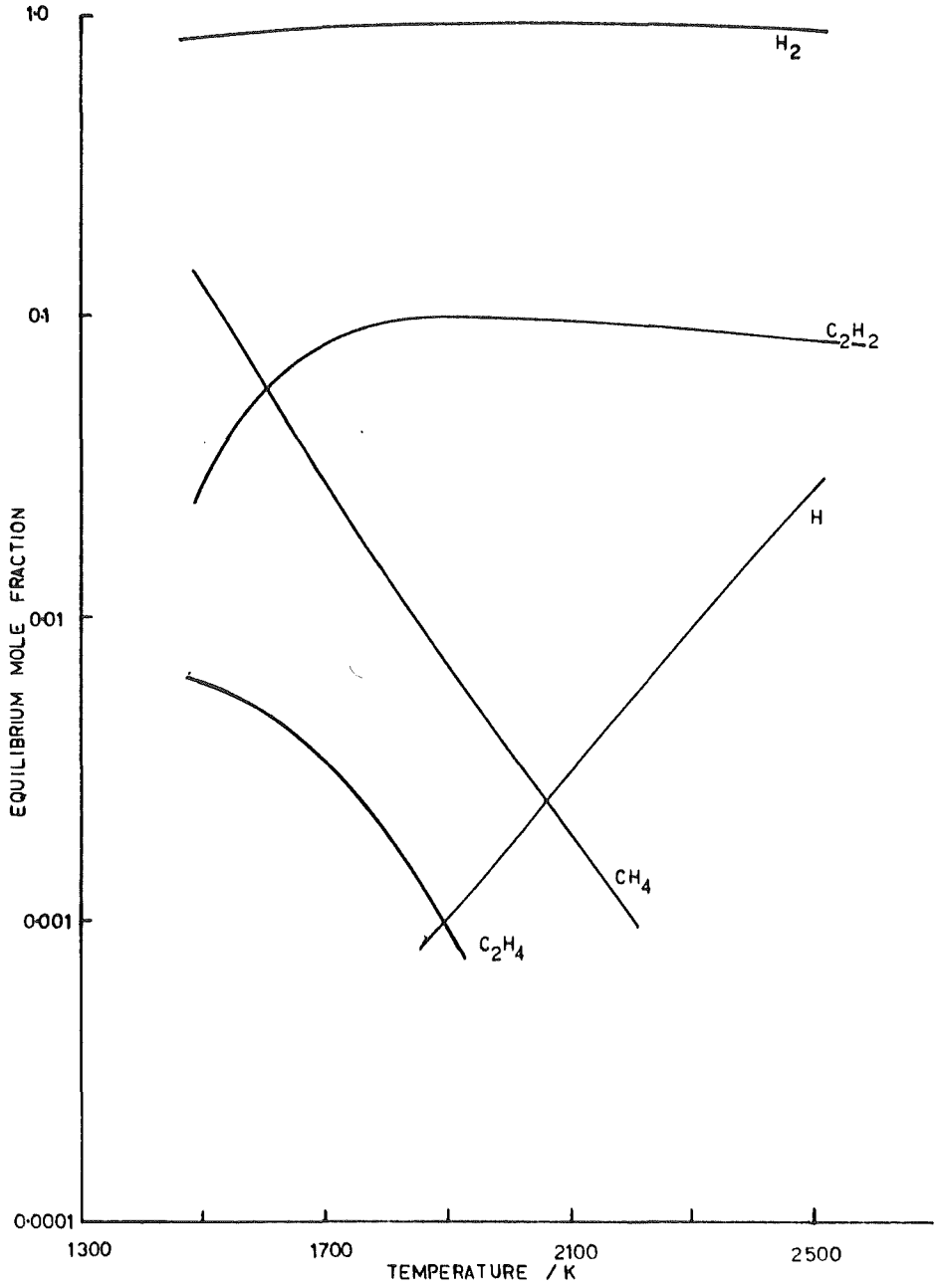

from 0 to 20% by decreasing the particle size from 200 to 50 micron. This is by far the most important problem to be overcome with coal-fed plasmatrons and since large residence time increases are not possible because of acetylene decomposition it may be that this type of process will never become competitive in an economic sense. In processes where gaseous reagents are fed directly into the arc, e.g. Du Pont and Westinghouse, good mixing is essential to stop carbon deposits forming in localised cold spots and to ensure uniform heating of the gas, and this has been achieved with marked success by magnetic rotation of the arc.

The Du Pont and AVCO processes have been operated at a pressure of 0.2 bar to maximise energy consumption. The increase in performance which accrues from operation at low pressures is probably due to a reduction in the decomposition of acetylene to carbon black in line with the mechanism proposed by Hougen and Watson (52). The effect of increasing pressure has been investigated by Kozlov et al (27) and Hirayama et al (51) who both found a fall-off in yield and an increase in energy consumption as the pressure was increased to 7.0 bar. They also noted increasing yields of carbon black, giving support to the theory that changes in performance with pressure are due to changes in the rate of decomposition with pressure.

The final parameter which affects the efficiency of processes for the high-temperature synthesis of acetylene is that of the rate, and hence the method, of quenching. Those processes which have been developed to pilot-plant scale and beyond have all employed a liquid or gas spray quench, the advantage in this lying in the fact that a hydrocarbon can be used which is, itself, cracked in the quench process. This improves the thermal efficiency of the process, e.g. Cagas et al (48) claimed a reduction in energy consumption from 11.1 to 9.7 kWh kg^{-1} acetylene by replacing a water spray quench by naphtha. On a laboratory scale, by far the best yields have been obtained by using water-cooled probes to sample the hot gas. These probes give very fast quench rates but are not at all suited to large-scale plants and the results obtained with them are not necessarily representative of the

bulk gas and therefore must be treated with a degree of scepticism. The worst quench method, used by the majority of coal researchers, is probably that of cooling in a large water-cooled chamber. The low quench rates obtained here may be another reason for the poor results obtained by these workers.

CHAPTER 3

DESIGN AND OPERATION OF APPARATUS

DESIGN OF A SOLID-GAS ARC REACTOR

The experiments to be described in this work were performed in a high-intensity electric arc reactor capable of power inputs of up to 30 kW dc for carbon feed rates of up to 250 gm hr^{-1} and hydrogen feeds of up to 250 gm hr^{-1}.

The basis of the reactor design came from scaling up a small (4 kW) electric arc reactor developed by Abrahamson (1). This design was based on a high-intensity carbon arc which enabled the ablation of a carbon anode into an atmosphere of hydrogen, followed by the rapid quenching of the product stream in a water-cooled tube. The principal development of Abrahamson's design over previous attempts (e.g. 66,67,78) was the maintenance of high surface temperatures within the arc chamber; this feature has a twofold purpose, firstly to minimise energy losses from the arc and secondly to prevent regions of temperature in the range 880-1600 K, in which rapid decomposition of acetylene will occur, before the quench section.

The principal features of the reactor are shown in fig. IV.

Anode:

To operate in the region of a high-intensity arc, current densities of 100 A cm^{-2} and greater are required (5). The power supply used for this reactor was capable of producing currents of up to 300 A so that a .795 cm diameter graphite rod was chosen for the anode which gives a current density of 100 A cm^{-2} for an arc current of 50 A which is suitably low in the range of currents available. At this current, the carbon ablation rate is 30 gm hr^{-1}, whilst for a current of 200 A the current density would be 1270 A cm^{-2} and the carbon ablation rate 250 gm hr^{-1}.

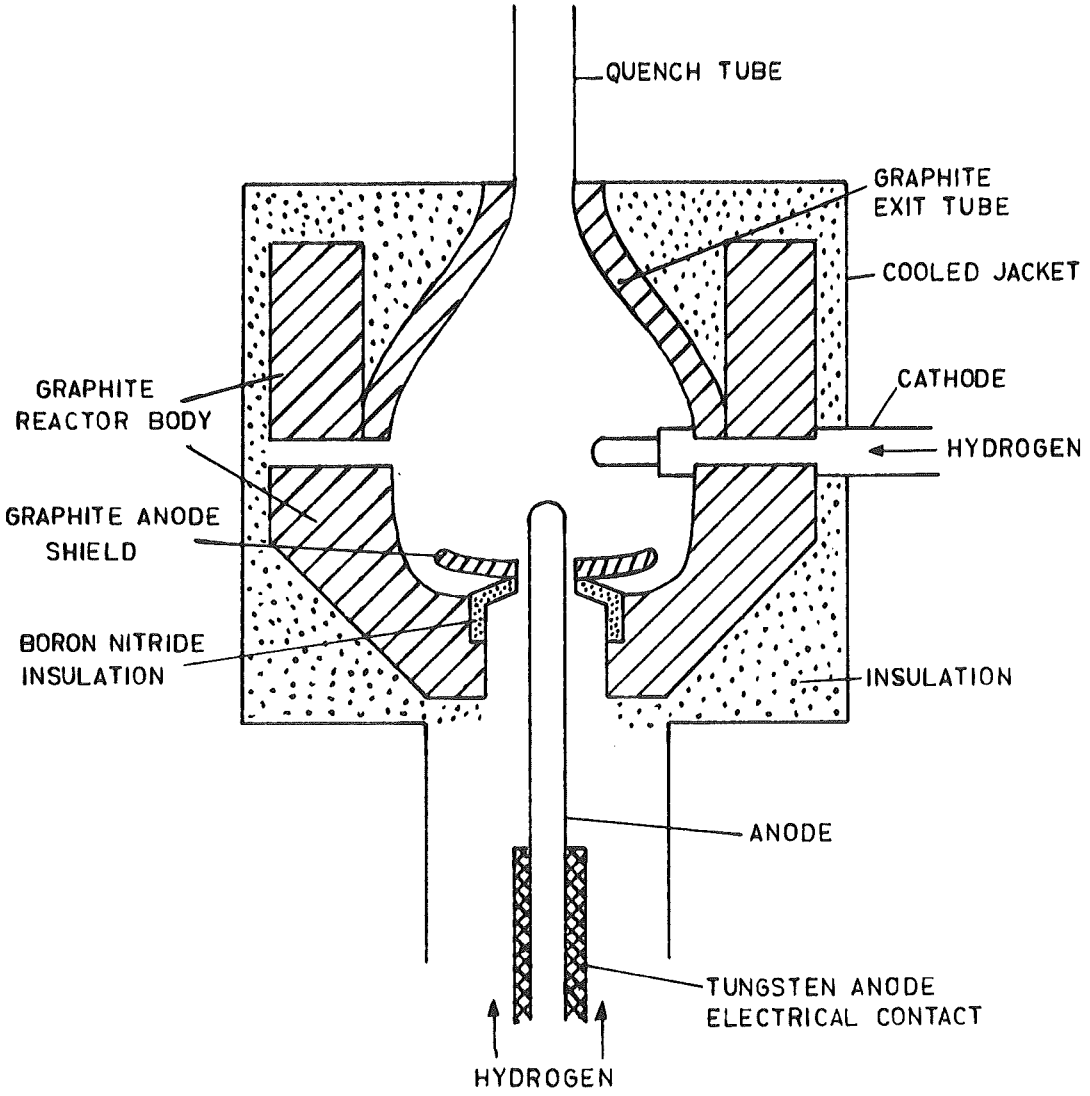

FIG IV
PRINCIPAL FEATURES OF REACTOR

Cathode:

The governing factor in the design of the cathode was that it would permit sufficient thermionic electron emission, determined by the Dushman equation (80), to carry the arc current. This assumes all electron emission is thermionic; in practice, there will be additional contributions from the phenomena of field emission (the Schottky effect) and positive ion bombardment. The Schottky effect can increase the electron emission by up to 20% according to the Schottky equation (81) for the case of a carbon cathode in a hydrogen atmosphere. The latter effect is slight and is likely to be less than 5% (81). This results in diameters for the current-carrying section of the cathode of the following values for a current of 300 A.

Cathode material	Diameter/cm	Cathode tip temperature/K
Tungsten	.70	3500
Carbon	.82	3600

Following the work of Abrahamson (1), it was also desirable to be able to introduce hydrogen through the cathode to irrigate the cathode tip. The reactor was designed to enable up to three cathodes to be used; the number used and their more exact design are discussed in chapter 4 in light of operating experience with the reactor.

Reaction Chamber:

The body of the reactor was constructed from graphite which, besides fulfilling the prerequisites of being able to stand the extreme temperatures and being easy to fabricate, reduced the possibility of introducing other elements into the reacting system. The dimensions of the reaction chamber were determined by scaling up from Abrahamson's design (1), the design criteria being a residence time of 1 msec between the arc and the entrance to the quench section. This gave a length for this dimension of 8.25 cm and the reaction chamber was sized around this dimension.

The thermal design of the reactor body was based on a temperature of 2700 K for the inside walls of the graphite block. This temperature was decided on by considering deposition of carbon on the walls because of too low a wall temperature and the possibility of the walls becoming so hot as to emit sufficient electrons to attract the arc, thus constituting an arc extinction mechanism. The current density at the wall, due to thermionic emission of electrons, was calculated, as a function of temperature, using the Dushman equation and this was compared with the migration of carbon to the walls by diffusion, also as a function of temperature, with the result that 2700 K was decided on as a reasonable compromise.

The physical dimensions of the reactor body were determined, the inner by the criteria above and the outer by the size of graphite available (15.24 cm diameter). The cooling water temperature was arbitrarily fixed at 320 K so as to minimize the risk of boiling in the cooling jacket. The heat flux to the chamber walls was estimated using the result that 72% of the total energy input to the arc was lost to the surroundings as radiation (82). A computer program was written to calculate the heat flows over a grid superimposed on the reactor body by a relaxation technique and a thickness of magnesium oxide insulation, about the carbon block, of 1.25 cm was found necessary to satisfy all the conditions outlined above.

The exit tube, used to channel the reacting gases into the quench tube, was sized so as to minimise eddying in the chamber which could lead to decomposition of the acetylene being produced by retaining it at temperatures in the 800-1600 K range.

The region surrounding the point of entry of the anode was protected by a graphite shield insulated from the rest of the reactor body by a boron nitride insulator. This served to protect the lower sections of the reactor, such as the power contacts, from damage by radiation or falling debris from the arc.

Reactor Casing and Cooling System:

The design of the copper and brass casing and the cooling system is shown in fig. V. Power was transferred to the anode through a tungsten contact, a spring-loaded shoe mechanism ensuring good contact between the graphite and tungsten surfaces. Detailed heat transfer calculations were carried out to determine the amount of heat generated in the contacts and to ensure adequate cooling was available to prevent overheating of any parts.

Provision was made for the introduction of hydrogen around the anode as well as through each of the three cathodes. Cooling of the casing was provided by a water jacket consisting of .635 cm diameter copper tube sound around the copper casing, with water inlets being provided at the anode contact and at the cathode ports. The end plate was cooled by using a spiral tube which led cooling water into the centre and then out again.

Product Gas Quench:

The simplest quench mechanism is that of a water-cooled tube. This system allows quench rates of up to 5×10^4 K sec^{-1} in the range 3000 K to 500 K (12) and was preferred because of its ease of construction and lack of hindrance to gas sampling. The quench tube was sized using the correlation of Skrivan and Jaskowsky (13) to quench a stream of C/H mole ratio of 3:1 with a 50% conversion of carbon and a carbon feed of 250 gm h^{-1}. The quench tube was constructed of copper.

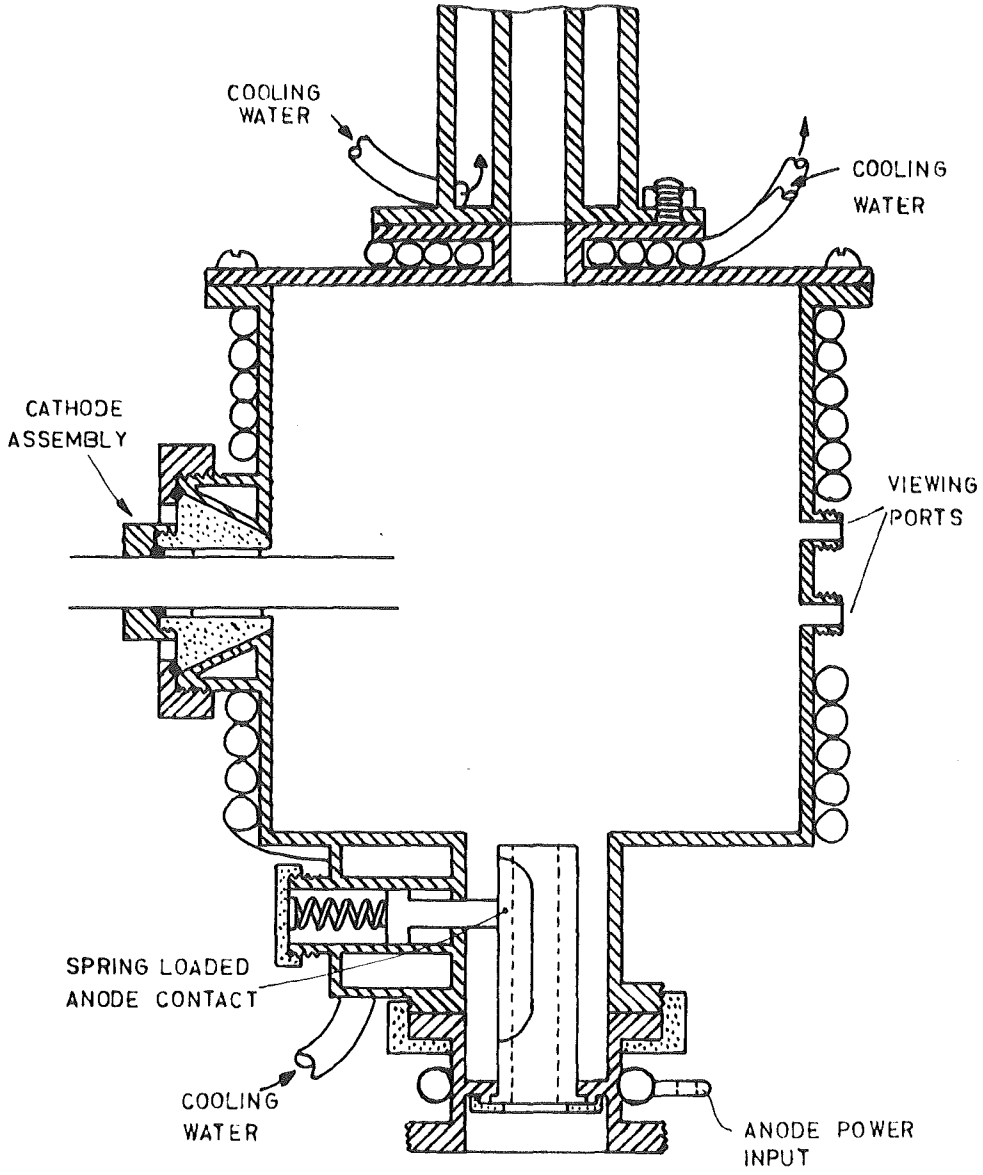

FIG V
DETAILS OF REACTOR CASING

Anode Feed:

The requirements of the anode feed mechanism were that it give a uniform and positive feed of the anode against the resistance of the anode contact and any pressure exerted on the anode by the arc. These requirements were met by feeding the anodes from a hydraulic cylinder fed with oil pumped from a reservoir. The system was capable of feeding 22 gm of carbon to the reactor at rates up to .406 gm s^{-1}. Sections of anode were connected by screwing threaded spigots on one section into tapped holes in the other. The hydraulic system operated at pressures in the range 3.5 to 3.8 bar.

Power Supply:

The power supply was required to deliver up to 300 A dc with an open-circuit voltage of 150 V. This was supplied by constructing a delta-star transformer from three 400 V welding units, the resultant ac was then rectified using a full wave, three-phase bridge of silicon diode rectifiers. The power output was controlled by chokes on the welding units.

EXPERIMENTAL METHOD

Materials:

1. Carbon: Union Carbide graphite, grade AGSR, .795 cm diameter and 30.5 cm long. Maximum ash content .12%.
2. Hydrogen: > 99.7% mol % hydrogen on dry basis
   < 0.01 mol % oxygen
   < 0.01 mol % nitrogen
   < 0.01 mol % carbon dioxide
   < 5×10^{-6} mol fraction carbon monoxide
   < 10^{-5} mol fraction other carbon compounds
   moisture varies .02 to .14 mol %

Apparatus:

An outline of the reactor system is shown in fig. VI. Hydrogen is fed from a pressurised cylinder into the reactor via the anode and the cathodes The flows are controlled by needle valves and metered by variable area flow meters. Graphite is fed to the reactor in rod form by a hydraulic cylinder (see fig. XXVI), the feed rate of graphite being controlled by varying the flow of oil to the cylinder with a needle valve and monitored by metering the oil flow with a variable area flow meter.

The resultant gas stream from the reactor passes through a cyclone, of characteristic diameter 7.5 cm, and then a filter, consisting of a glass tube 3 cm in diameter by 21 cm long filled with cottonwool, to remove any entrained carbon particles before passing through the cell of the infra-red gas analyser. The gas stream is next mixed with compressed air, burnt in a cyclone burner and discharged into the exhaust duct.

Cooling water was supplied to both the reactor and the quench section from high-pressure water mains. The water passed through a filter and a pressure-reducing valve to enter the cooling system at 3.75 bar. The flows were controlled by needle valves and metered by variable area flow meters downstream of the reactor.

Flow Measurements:

The types of flow meter used to meter the various flows are shown in table VI. The hydrogen flow meters were calibrated by measuring liquid displacement rates in a measuring cylinder. Additional calibration points were obtained for the cathode hydrogen flow meters by use of a calorimetric flow meter (fig. VII) suggested by Williamson (83). For a measured heat input to the hydrogen, the temperature rise was measured and the mass flow determined from the following equation:

$$\text{Power input} = \text{Volts} \times \text{Amps} = 4.18 \times (\text{mass flow/gm sec}^{-1}) \times (\text{specific heat/cal gm}^{-1}\ \text{C}^{-1}) \times (\text{temperature rise/C})$$

The gas flow meters were reproducible to ± 2%.

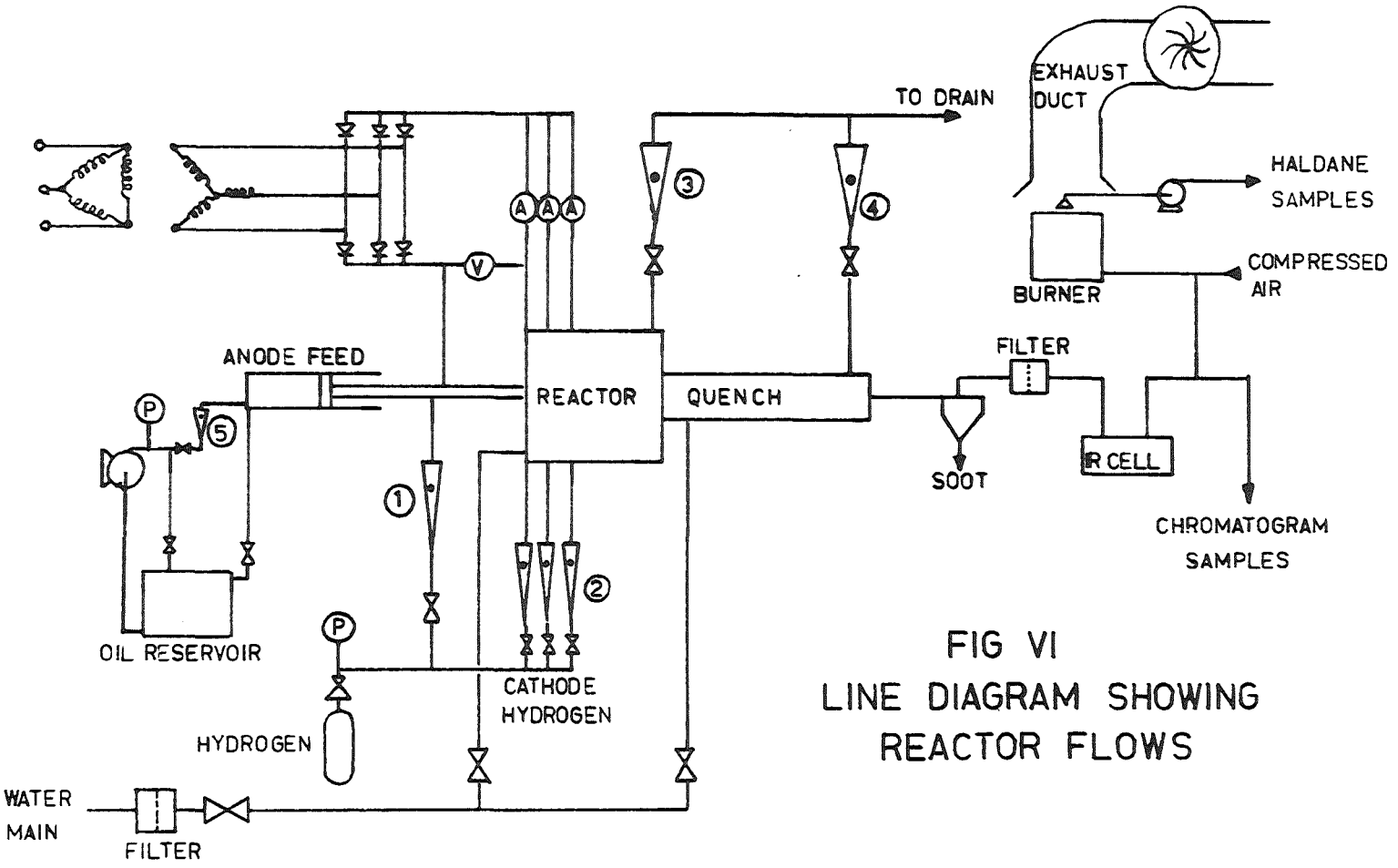

FIG VI
LINE DIAGRAM SHOWING
REACTOR FLOWS

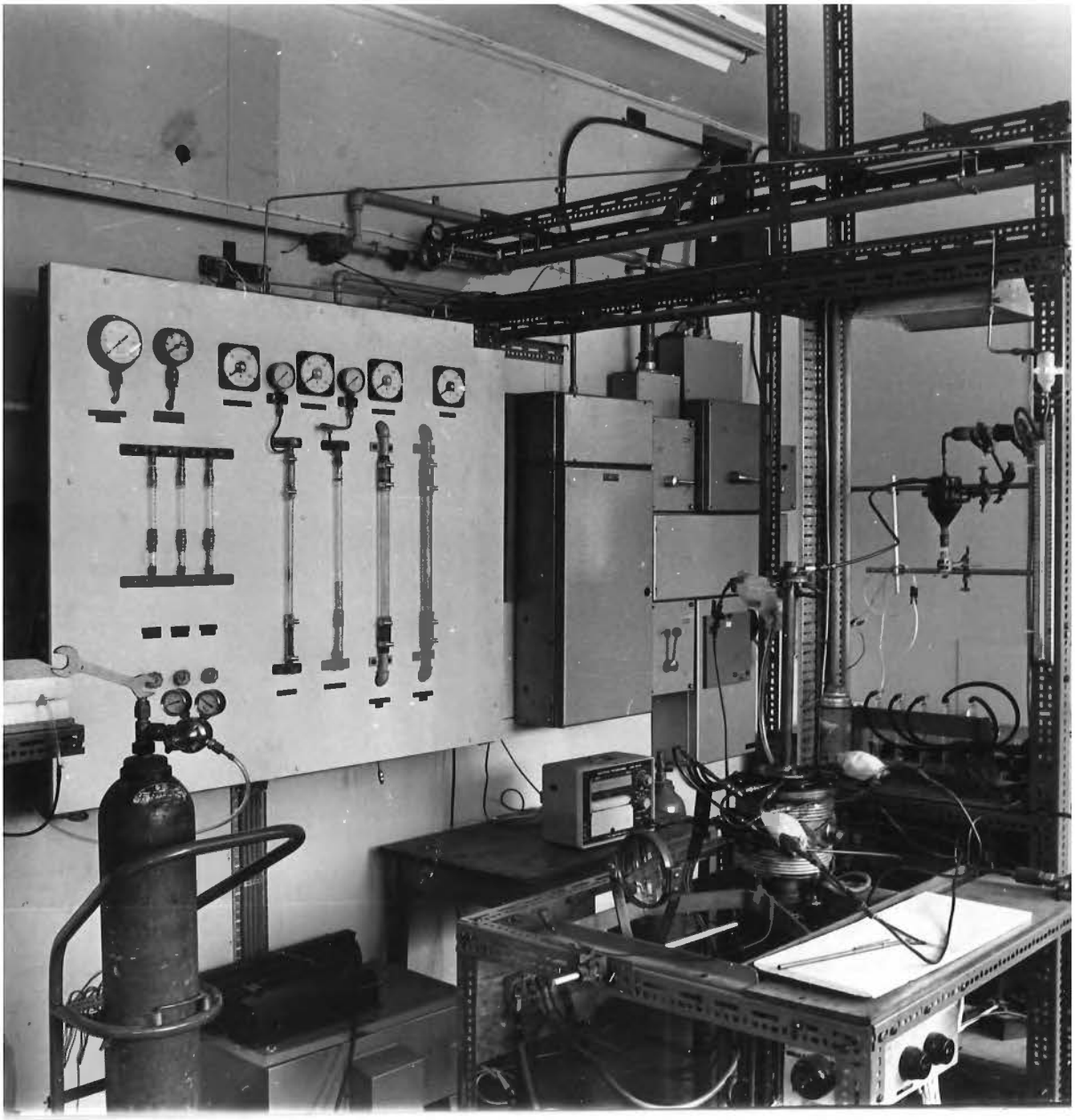

GENERAL VIEW OF APPARATUS

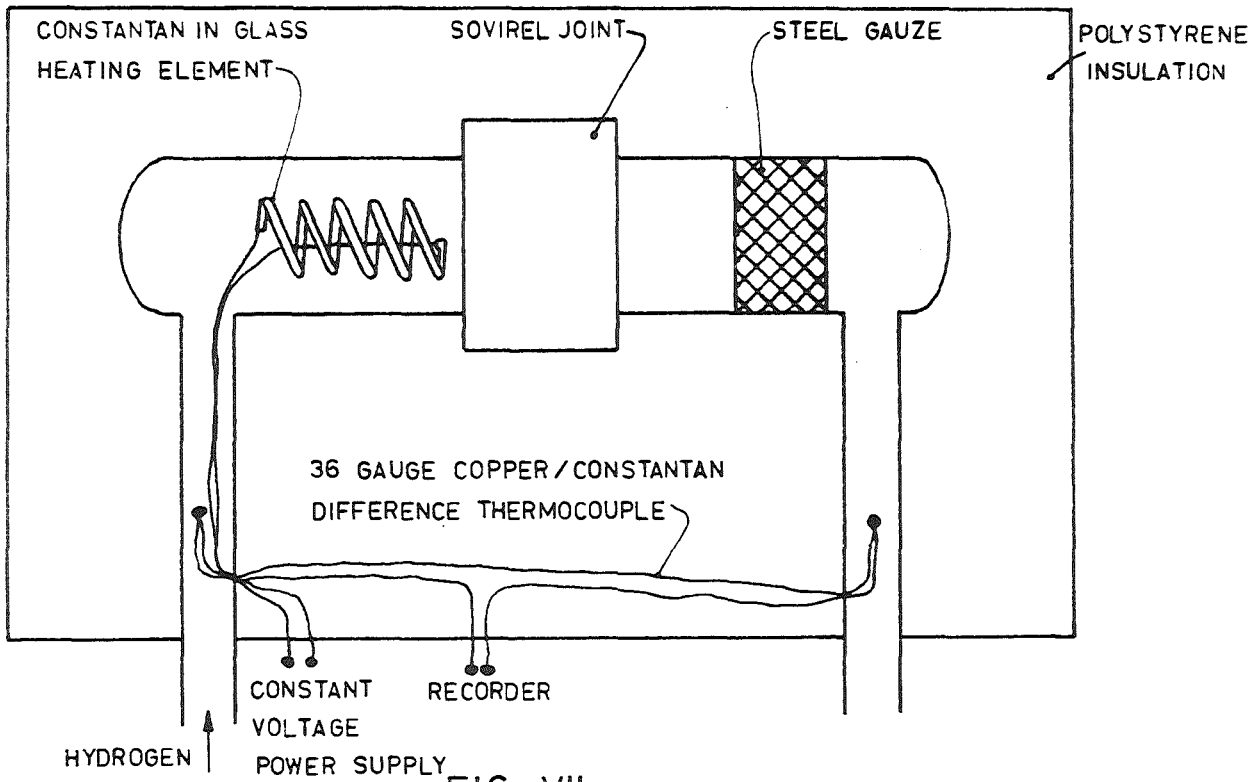

FIG VII

CALORIMETRIC FLOW METER

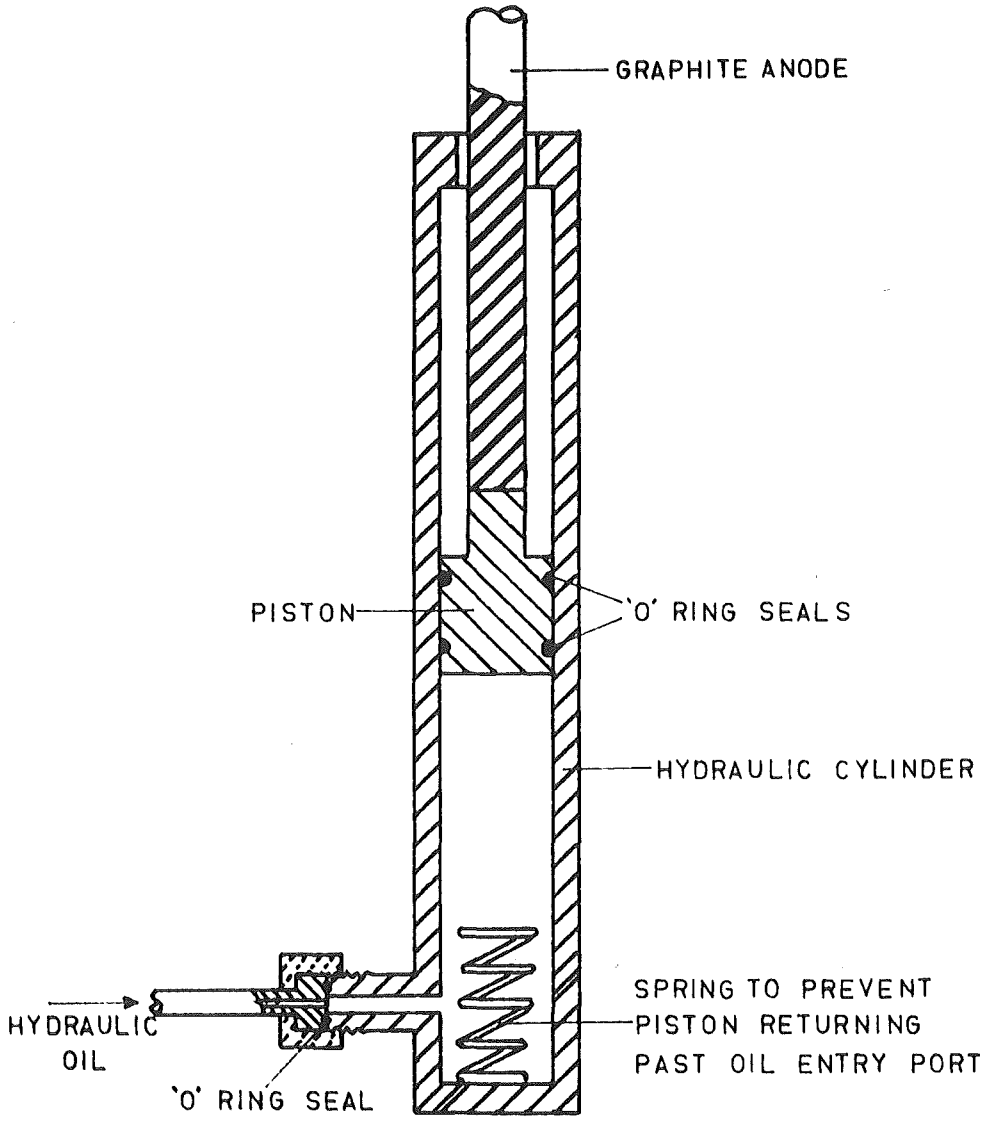

FIG XXVI

ANODE FEED HYDRAULIC CYLINDER

The water flow meters were calibrated by measuring the rate of collection of water in a measuring cylinder. The water flow meters were reproducible to ± 0.5%.

The hydraulic oil flow meter was calibrated directly in linear rate of feed of graphite rod by measuring the linear displacement of graphite rod with time for each flow meter setting. From a measurement of linear density for the graphite rods, the mass flow rate was found. This flow meter gave graphite feed rates reproducible to ± 4.5%.

Item No.	Flow	Make	Tube Type	Float Type
1	Anode Hydrogen	Rotameter	Metric 7	Duralumin
2	Cathode "	Gap Meter	B6	Duralumin
3	Reactor ' Cooling Water	Rotameter	Metric 14	Stainless Steel
4	Quench Cooling Water	"	"	"
5	Hydraulic Oil	"	Series 1100 4-A	"

TABLE VI

Electrical Measurements:

The arc voltage was measured by a Yokogawa Z series type 2102 voltmeter with 150 V full-scale deflection. Similar meters with appropriate shunts were used to measure the currents drawn by the cathodes. These meters have an accuracy of ± 1.5% of full scale.

Temperature Measurements:

In order to find the energy transferred to the cooling water from the reactor and the quench tube, the temperature rise in the cooling water is required in addition to the water flow rates. It was desirable to limit this temperature rise to one of the order of 10 K to keep the copper jacket from getting hot enough to cause structural damage and to prevent any

formation of scale in the cooling tubes. Five copper-constantan thermocouples connected in series were used to measure the temperature rise because of its small size. The hot junction of the thermocouple was placed in the outlet water line and the cold junction in the inlet line so that the temperature rise was measured directly. To prevent any stray electric currents in the reactor casing disturbing the thermocouple signals, the junctions were wrapped with "Teflon" tape before being cemented with "Araldite" into the wall of the water line. To prevent convection losses causing fluctuations in the thermocouple signals, the area around the junctions was lagged with cottonwool and enclosed in a plastic jacket. The thermocouples were calibrated in situ by replacing the reactor with a heat source which enabled known amounts of heat to be transferred to the cooling water, the calculated temperature rise being equated to the generated millivolt signal. The thermocouple outputs were found to be comparable with those given in standard thermocouple calibration tables.

In addition to the cooling water temperatures, intermittent measurements were made of the gas stream temperature at the exit to the quench tube and of the temperature at a point about 1.5 cm from the inside wall of the lower carbon block of the reactor. The product gas temperature was measured with a copper-constantan thermocouple with the reference junction at ice point. The carbon block temperature was measured with a Thermo-Couple Products gas-filled 1000 series tungsten-3% rhenium vs tungsten-25% rhenium thermocouple.

Gas Analysis:

Infra-red spectrophotometer

Continuous analysis of the product gas stream for acetylene was performed by a Perkin-Elmer model 337 Grating Spectrophotometer operating on a fixed wavelength. The gas passed through a gas cell with a path length of 10 cm and the absorption at a wavelength of 3310 cm^{-1} was monitored on an external chart recorder. This wavelength was chosen as being the centre of the broadest absorption band in the IR spectra of acetylene. The spectrophotomet

was calibrated by passing hydrogen-acetylene mixtures of known composition through the cell and measuring the generated millivolt signal so that the external recorder was directly calibrated in vol % acetylene.

Gas chromatography:

Intermittent samples were collected for analysis by gas chromatography. The product gas passed through 125 cm^3 sample bottles which were isolated from the main gas stream when samples were required and these samples later analysed using a Perkin-Elmer model 154 gas chromatograph with a thermal conductivity dectector. The following columns were used:

(i) Separation of Permanent Gases

Glass 1.0 m x .004 m id 13A molecular sieve

(ii) Separation of Lower Hydrocarbons

Stainless Steel 1.0 m x .005 m id Silica Gel

(iii) Separation of Higher Hydrocarbons

Stainless Steel 2.0 m x .005 m id Squalene

Helium was used as the carrier gas at a rate of 50 cm^3 min^{-1} and the columns were held at 20 C.

Haldane Gas Analysis:

Intermittent gas samples were taken for analysis by a method due to Haldane (84). The product gas was burnt with excess air and the resultant gas stream sampled and analysed for carbon dioxide and oxygen. Simple stoichiometric relations (see appendix I) then allow the ratio of carbon to hydrogen in the product gas and, if the hydrogen is known, the carbon flow out of the reactor to be determined. The apparatus (fig. VIII) takes a measured volume of sample and measures the changes in volume after dissolving the carbon dioxide in potassium hydroxide solution and then after dissolving the oxygen in alkaline pyrogallate solution, the remainder is assumed to be nitrogen. 2500 cm^3 of gas was collected which allowed three analyses of each sample and this gave results reproducible to ± 1%.

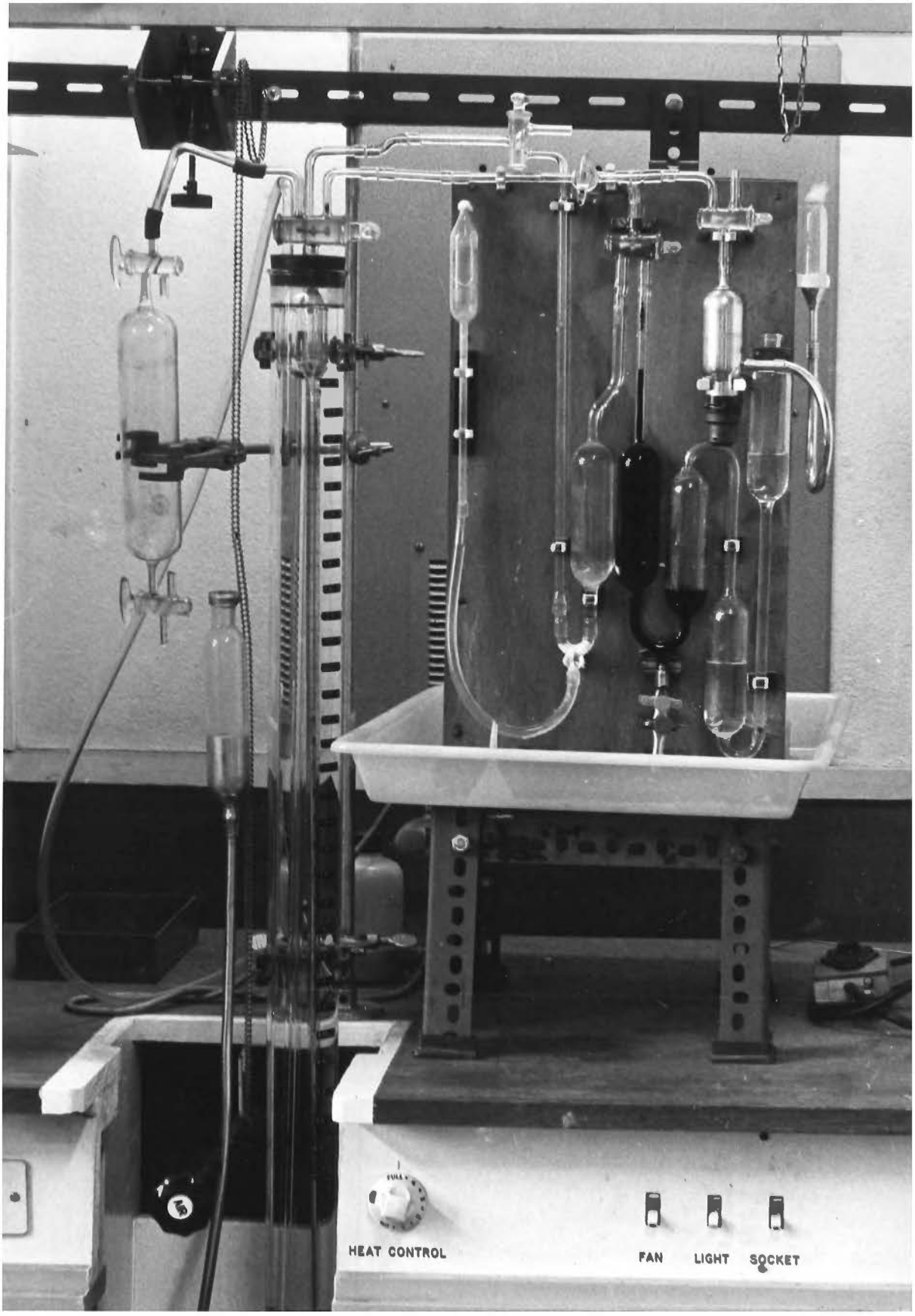

FIG. VIII. APPARATUS FOR HALDANE ANALYSIS

Experimental Procedure:

Pre Run

Prior to each run, the anode was trimmed to fit neatly through the electrical contact and the central rods of the cathodes replaced if necessary. The anode, exit tube, cathode and anode shield were weighed and the reactor assembled with the cathode in the required operating position in relation to the path of the anode. Two hours before the commencement of the run, the hydraulic oil pump was turned on and the oil circulated through a bypass loop in the oil circuit to heat the oil up to a steady running temperature. If this was not done, the temperature of the oil and hence the viscosity of the oil varied during the run and the calibration curves for the graphite feed were invalidated. Thirty minutes before the run, the cooling water was turned on to purge the cooling coils of any air. At the same time, the spectrophotometer was turned on and the balance and drift checked. Ten minutes before the run, the hydrogen flows were turned on to flush out the reactor and the burner and the exhaust fan started.

Run

During the run, all observations and results were taken down verbally on a tape recorder. The spectrophotometer and all thermocouple outputs were recorded on chart recorders. At the start of the run, the bypass in the oil line was closed and the graphite feed set to the required rate, the power was turned on and the arc struck. The arc was controlled by varying the carbon feed rate. If required, samples were taken for analysis by chromatography and the Haldane method. The run was terminated when the anode was fully fed, unless failure occured in some other part of the reactor.

Post Run

Once the reactor had cooled down, it was dismantled as far as the reaction chamber and the state of the reactor components noted. The anode,

exit tube, cathode and anode shields were weighed and all deposited carbon from the chamber collected and weighed. The weight of carbon collected in the filters was determined and analysis of any gas samples carried out.

CHAPTER 4

QUALITATIVE RESULTS AND MODIFICATIONS TO THE REACTOR DESIGN

This chapter deals with modifications made to the design of the reactor to improve its efficiency of operation. These included the number of cathodes used and the development of their design, the reduction in thermal capacity of the surrounds of the reaction chamber and the joining of anode sections. An outline of the appearance of the arc in operation and a qualitative description of the carbon deposited in the reaction chamber during operation is also given.

Appearance of the Arc in Operation

The appearance of the arc remained, with a few minor exceptions, unchanged over all runs. The majority of the gas surrounding the arc ranged from a slightly milky-blue to violet in colour and this was punctuated by spurts of red which issued chiefly from the cathode, although the red areas were noted to extend, on occasions, around the periphery of the central blue zone to the anode, meeting it slightly below the tip, and on the far side of the anode from the cathode. This extension of the red areas was not accompanied by any significant change in any of the operating parameters of the arc other than fluctuations in the voltage and current, but not the power input. It was considered that the path of the arc was changing at all times, corresponding to the fluctuations in voltage and current, and that the extension of the red areas was a consequence of the position and hence observed view of the arc at that time. For short periods of time in some runs, the arc became predominantly green in colour. This was not accompanied by any significant changes in the operating parameters of the arc.

Throughout all runs, the anode-cathode gap remained small, never exceeding a distance of about 5 mm, the length increasing with increasing power input, and this resulted in a variation in the shape of the anode tip with

variation in power input. At low power input levels of 5-7 kW, the arc gap was very short, of the order of 1-2 mm, and the anode had a concave cratered appearance. In this state, pieces of carbon were observed to break away from the thin walls of the anode "crater" and these were later found lying in the bottom of the reaction chamber. As the power input increased to 10 kW and beyond, the arc gap increased and this was accompanied by a change in the anode tip to a convex shape which was a rounded point in the case of two cathodes but which tended to be a plateau with rounded edges in the case of one cathode with its tip level with the far edge of the anode. Under these conditions, no pieces of carbon were observed breaking off the anode.

Occasional pieces of carbon were observed to separate from the cathode and appeared to originate from carbon deposited on the cathode surface by the arc. These small fragments were found in the bottom of the reaction chamber at the end of the run.

Views of the arc under typical operating conditions are shown in the accompanying photographs.

Development of the Cathode Design in the Light of Operating Experience

One of the major problems encountered by Abrahamson and others in the operation of their processes was the formation of carbon deposits in the reaction chamber and particularly on the cathode. As outlined in chapter 2, many methods have been used to prevent these deposits, although the details for most of the industrial scale plants are not available. Techniques used have included vibration of the electrodes (98), mechanical scraping of the electrodes (27,99) and the use of suitable gas flow patterns in the reaction chamber (36). These methods fall into two categories: use of mechanical devices to remove deposits as they form, and design of electrodes and chamber geometry to prevent the formation of deposits. It would seem preferable to prevent deposits of carbon by reactor chamber design rather than to use elaborate mechanical devices to remove them once formed and it

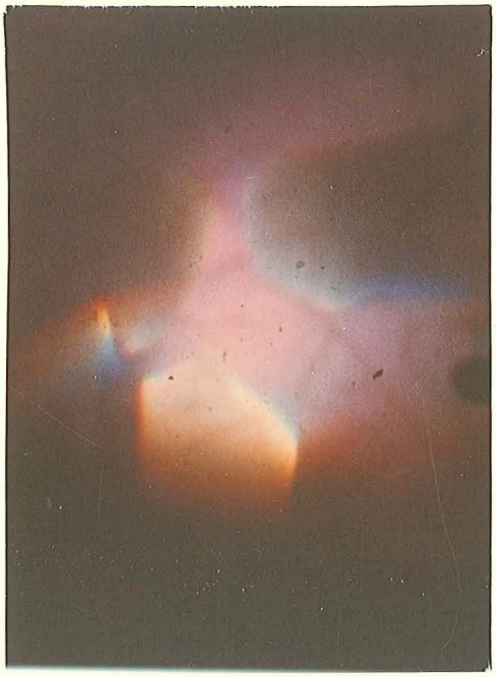

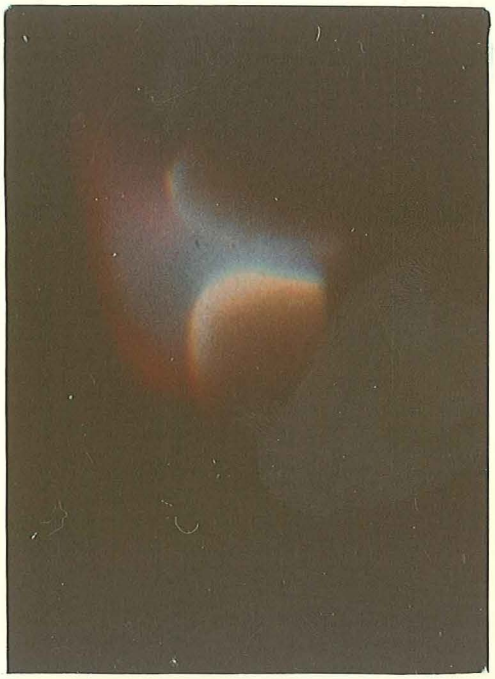

is worth noting that there is no evidence that this latter class of technique has been used in advanced industrial-scale processes. In the light of this, the main design development in this work was the evolution of a design which would eliminate the deposition of carbon on the cathode.

The initial cathode design was adapted from the final design used by Abrahamson (1) and is shown in fig. IX. The cathode tip was fabricated from thoriated tungsten. Hydrogen was introduced through an annulus formed by the central, current-carrying rod and an outer tube, also of tungsten, in an attempt to irrigate the cathode tip and thus prevent carbon deposits forming on it. Abrahamson found that although this cathode design minimised carbon deposition, it was not completely successful in eliminating it altogether so that it was not expected to be immediately successful.

Runs 1-2

Three cathodes were used with a hydrogen flow of 1.0 l min^{-1} through each. Difficulty was experienced in striking an arc. On contacting one cathode with the anode to initiate an arc, there was a noted tendency for the electrodes to fuse together at the point of contact, making withdrawal of the cathode difficult. Once initiated, the arc operated at 70 V and 90-120A. Only a very short arc gap was possible and it was difficult to distribute the current evenly over the three cathodes, with the result that one cathode tended to carry it all. Under these conditions, melting of the cathode tip occurred; condensed tungsten was found on the walls of the exit tube and hard deposits of what was considered to be tungsten carbide were found on the cathode tip. It appeared that at least some of the tungsten carbide resulted from the initial contacting of the electrodes.

Three possible factors contributed to the failure of these cathodes: inadequate cooling of the cathode tip, both by conduction back along the cathode and by convection losses to the cathode hydrogen flows and excessive heating of the cathode tip by radiation from the anode, significant because of the small arc gap of 1-2 mm. Unfortunately, two of these factors were

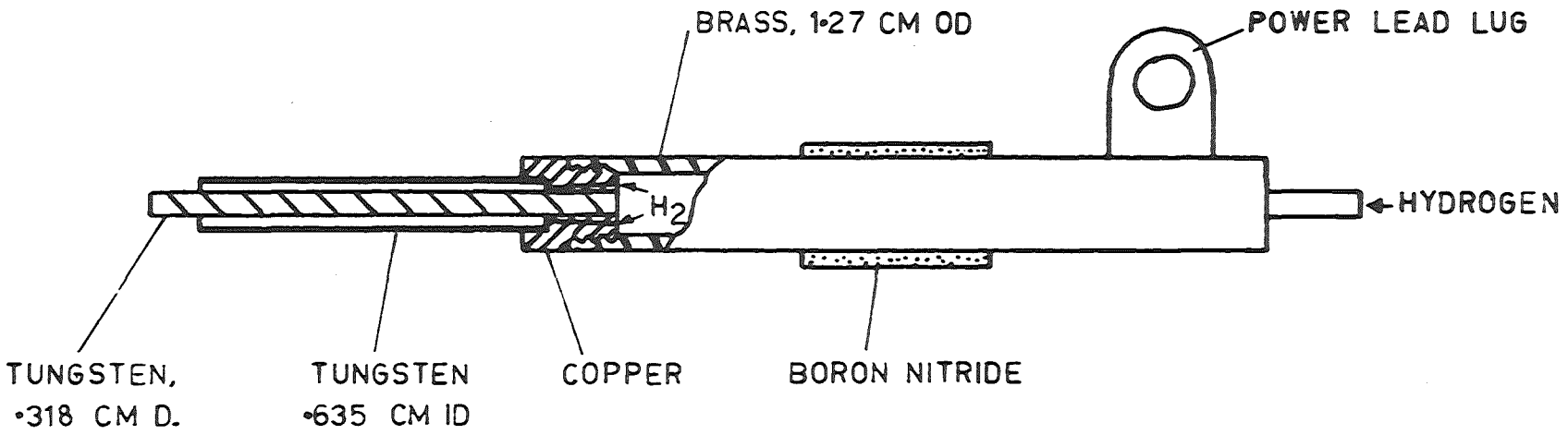

FIG IX

CATHODE DESIGN RUNS 1–2

interdependent; it was considered that one reason for the inability to sustain a longer arc gap was due to the tendency for the cathode hydrogen flows to blow out the arc so that increasing this flow to increase convective cooling would only cause a reduction in the arc gap with an associated increase in radiation problems. It was decided, therefore, to tackle the problem by way of the other heat flow, back conduction by increasing the diameter of the central rod of the cathode from .318 to .476 cm.

Runs 3-5

Three cathodes were used. Initially, the cathode hydrogen flows were set at 2.5 l min^{-1}, but it was found impossible to sustain an arc when the cathode was withdrawn from the anode following arc ignition. This was in line with the mechanism of arc extinction outlined above. The hydrogen flows were lowered to 0.5 l min^{-1} and an arc was able to be sustained. However, the operating problems encountered in runs 1 and 2 persisted, although it was possible to distribute the arc over all three cathodes for short times (up to 30 sec), with currents of 30-50 A and an arc voltage of 50-60 V. By the end of the runs, large bulbous growths had formed on the tips of the cathodes, but there was less melting of the tungsten than in runs 1 and 2. There were smooth areas on these growths where the arc had been attached at the end of the run and it appeared that carbon was being deposited in layers at these points.

Finkelnberg (89) first observed the formation of mushroom-shaped deposits on the cathode of high-current carbon arcs. These growths were found to consist of pure graphite and consisted of about 40% of the carbon evaporated from the anode. Finkelnberg proposed that these deposits were formed from unreacted carbon present in the anode flame. When an electrically neutral body was brought into the arc, about 30% of the carbon deposited on it, showing that a significant percentage of the carbon was positively charged. Similar deposits were observed by Abrahamson (1).

Photographs of the deposits obtained by these workers closely resemble those found in this work, a sample of which is shown in fig. X. This figure shows the face of attachment to the cathode and clearly shows the laminar structure of the deposits. Following the mechanism proposed by Finkelnberg, it appeared that lengthening the arc gap would allow time for diffusion of hydrogen into the anode flame, resulting in a reduction, through reaction with the hydrogen, of the amount of unreacted carbon. However, as has been noted earlier, sustaining the arc for electrode spacings of greater than about 2 mm had proved impossible. One reason for this may have been insufficient ionization of the hydrogen atmosphere, with a resultant shortage of current carriers. An attempt to overcome this was made by using an auxillary high-voltage source to ionize the hydrogen to a greater extent. This appeared to have a two-fold advantage: it would enable a longer arc gap to be used and would also obviate the necessity of initiating an arc by contacting the electrodes. This would, in turn, reduce the likelihood of melting the tungsten cathode with the high heat flows present through the contact area on ignition.

Runs 6-9

Using a resistance to limit the current to less than 2A, one cathode was connected to the phase of a 230 V ac supply and used to initiate an arc in a argon atmosphere. With the ac electrode positioned 2 mm from the anode, a stable ac spark was formed and when the dc electrodes were brought into the system, a stable dc arc formed, with the ac spark seemingly acting as a pilot arc inasmuch as when the dc arc showed a tendency to go out it was reignited by the ac. Following this success with argon, the system was tried in a hydrogen atmosphere. However, under these conditions, no advantage seemed to accrue from the ac spark with maintenance of an arc at anything but a very short arc gap being very difficult.

The greatest disadvantages of tungsten as a cathode material were the difficulty in fabricating complex tip geometries and the tendency for the

FIG. X. TYPICAL CATHODE DEPOSIT SHOWING FACE OF ATTACHMENT TO CATHODE

formation of tungsten carbide to weld the electrodes together when striking an arc. To avoid these problems, the possibility of using graphite as an electrode material was investigated. Two factors were important: sufficient electron emission and a sufficiently low level of ohmic heating. For the cathode design shown in fig. XI, ohmic heating was found to be negligible compared with the arc radiation incident on the cathode. Using the Dushman equation (chapter 3) the electron emission was found to be adequate to carry currents up to 170 A for a tip temperature of 3500 K. Hence the three tungsten cathodes were replaced with carbon ones of the design shown in fig. XI.

Runs 10-11

The hydrogen flow through the cathodes was set at 2.1 l min^{-1}. The ease of initiation of an arc was much improved and steady operation of the arc was easily obtained with currents of 30-50 A and an arc voltage of 50 V, although, once again, only a small arc gap was possible. On termination of the runs, after about 12 minutes, large deposits of carbon were found on the undersides of all cathodes and some of the hydrogen holes were blocked off. No erosion of the cathode had taken place.

These runs showed that graphite was a viable cathode material and that positioning of hydrogen holes to irrigate the cathode face was critical. Two of the three cathodes were altered so that hydrogen was only directed downward towards the arc, whilst the third cathode was left so that hydrogen was directed in all directions as in fig. XI. This made no difference to the deposition of carbon on the cathode face. It was considered that deposits were the result of predominantly positively charged carbon migrating along the arc and depositing on the cathode. This was borne out by the shape of the deposits which showed that they had grown downward from the cathode, i.e. in the observed direction of the arc, and that the arc had been attached to their tips. If this hypothesis was true, then irrigation of the cathode tip with hydrogen to sweep away the carbon before it reached the cathode fall

region was most important, as was the prevention of any stagnant areas about the cathode. The faces of the cathode were altered in an attempt to improve irrigation of the surfaces to which the arc attached, see fig. XII, and in addition the cathode hydrogen flows were increased.

Run 12.

With the cathode hydrogen flows set at 3.8 l min^{-1}, the arc burnt steadily, although the previous problem of balancing the current over the three cathodes remained. In spite of the alterations to the cathode design, there was considerable build-up of carbon on the cathodes after running for 16 minutes. Fig. XIII shows one cathode after this run. From the appearance of the cathodes, it appeared that the arc attached to very small areas, allowing deposits to form on the spaces between the hydrogen holes. This suggested that any cathode design in which the hydrogen flush entered perpendicular to the cathode surface would be unsatisfactory except, possibly, for the use of porous graphite.

An analysis of the system was carried out in an attempt to isolate the dominant driving forces involved in carbon deposition on the cathode (see appendix II). This showed that the main contribution to the growth of the deposits came from the small positively-charged carbon particles, resulting from the vaporisation of the anode, and that the major contribution to their propulsion toward the cathode was the velocity imparted to them by expansion of the carbon stream on ablation of the anode.

This limited solutions to the problem of carbon deposition on the cathode to two, increasing the arc length, and more efficient irrigation of the cathode tip with hydrogen. An increase in arc length would increase the time available for vaporisation and reaction of the carbon particles and would also increase the diffusion path length of the particles, all of which would lower the number of particles arriving at the cathode. Finkelnberg (89) obtained deposits for an electrode gap of 1 cm, so that the arc gap would have to have been longer than this. However, as has been noted, arc lengths greater

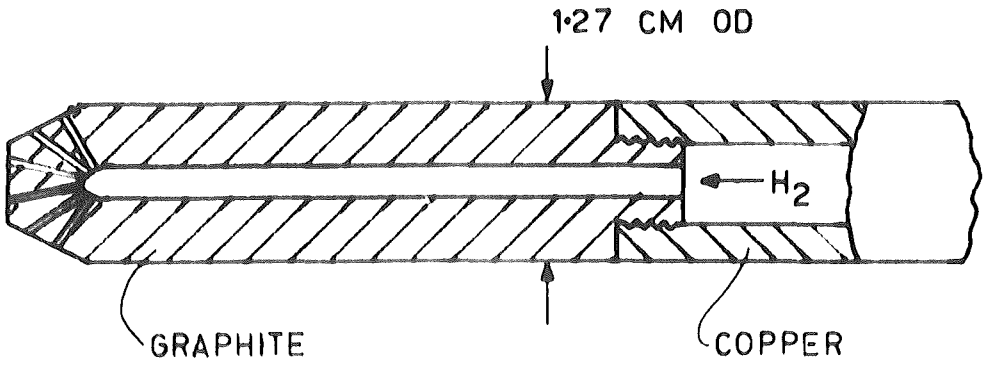

FIG XI
CATHODE DESIGN RUNS 10-11

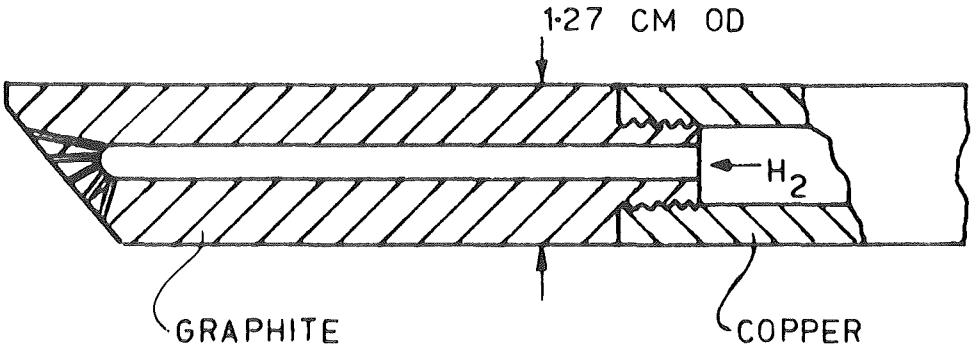

FIG XII
CATHODE DESIGN RUN 12

than 0.5 cm had proved impossible in this work so that this method of reducing the rate of carbon deposit did not appear favourable.

Thus the second method, more efficient sweeping of the cathode tip with hydrogen, was adopted. The principle behind this technique was that sufficient hydrogen would sweep the cathode tip and carry all the carbon particles out into the main vapour stream before they became trapped in the cathode fall region. The cathode design adopted is shown in fig. XIV.

Run 13

No difficulty was experienced in operating the arc, the currents being 35-50 A per cathode and the arc voltage about 50 V. However, only a short arc gap was possible the arc extinguishing if the cathodes were withdrawn beyond about 2 mm. With a cathode hydrogen flow of 3.8 l min^{-1}, large deposits formed on the cathode tips for an overall carbon to hydrogen ratio of 0.98 on a mass basis.

Runs 14-18

To investigate the effect of a higher cathode hydrogen flow, only one cathode was used with the same total cathode hydrogen flow, i.e. 10.8 l min^{-1}. The arc burnt steadily with an arc gap of 1-2 mm, with a current of 80-100 A and an arc voltage of 35-40 V. The formation of carbon deposits was very slight with a mass carbon to hydrogen ratio of 0.28, but was considerable for a mass ratio of 2.52. These results suggested that carbon deposition on the cathode faces could be controlled by irrigation of the cathode tip with hydrogen.

Runs 21-68

During the remaining runs, the cathode design shown in fig. XIV remained unaltered and with the exception of the runs detailed below (28-31) only one cathode was used. In these runs, the hydrogen flows, carbon to hydrogen ratio and power input were varied. The effect of the variations of these parameters on the deposition of carbon on the cathode is shown in fig. XV.

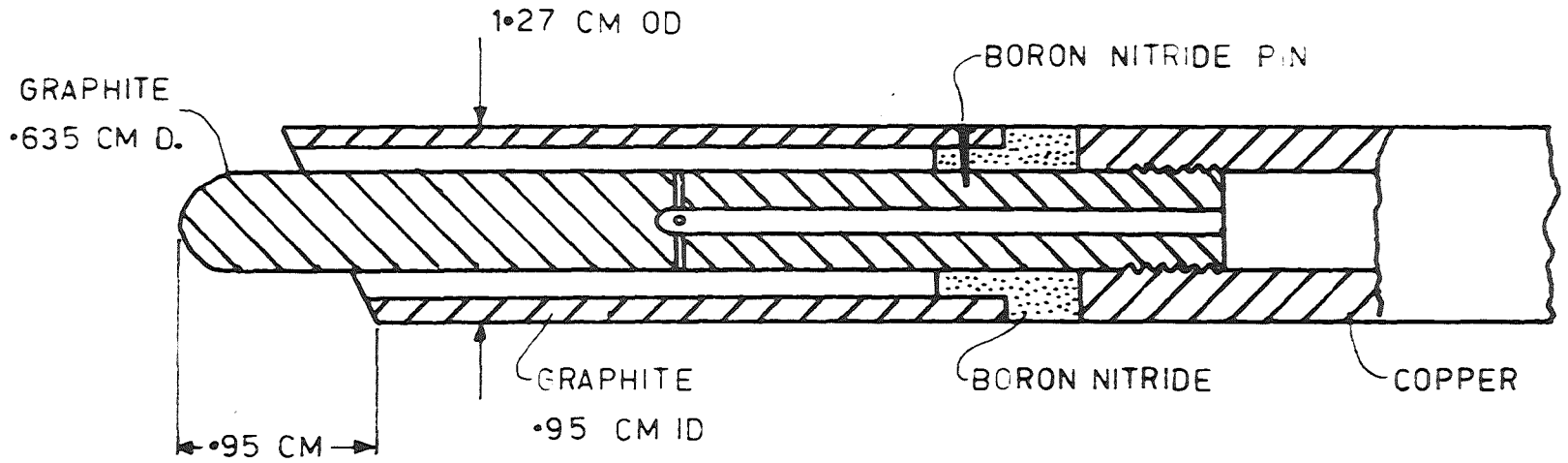

FIG XIV

CATHODE DESIGN RUNS 13 – 68

FIG. XIII. CATHODE SHOWING DEPOSIT AFTER RUN 12

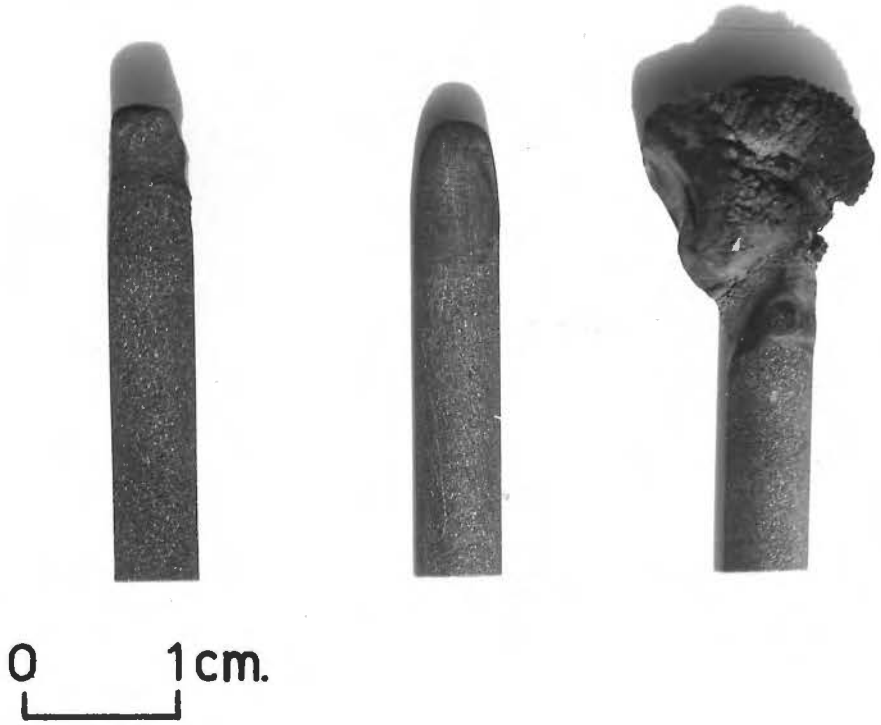

FIG. XVI. TYPICAL CATHODE FROM RUNS 21-68. WITH DEPOSIT, BEFORE RUN AND AFTER EROSION.

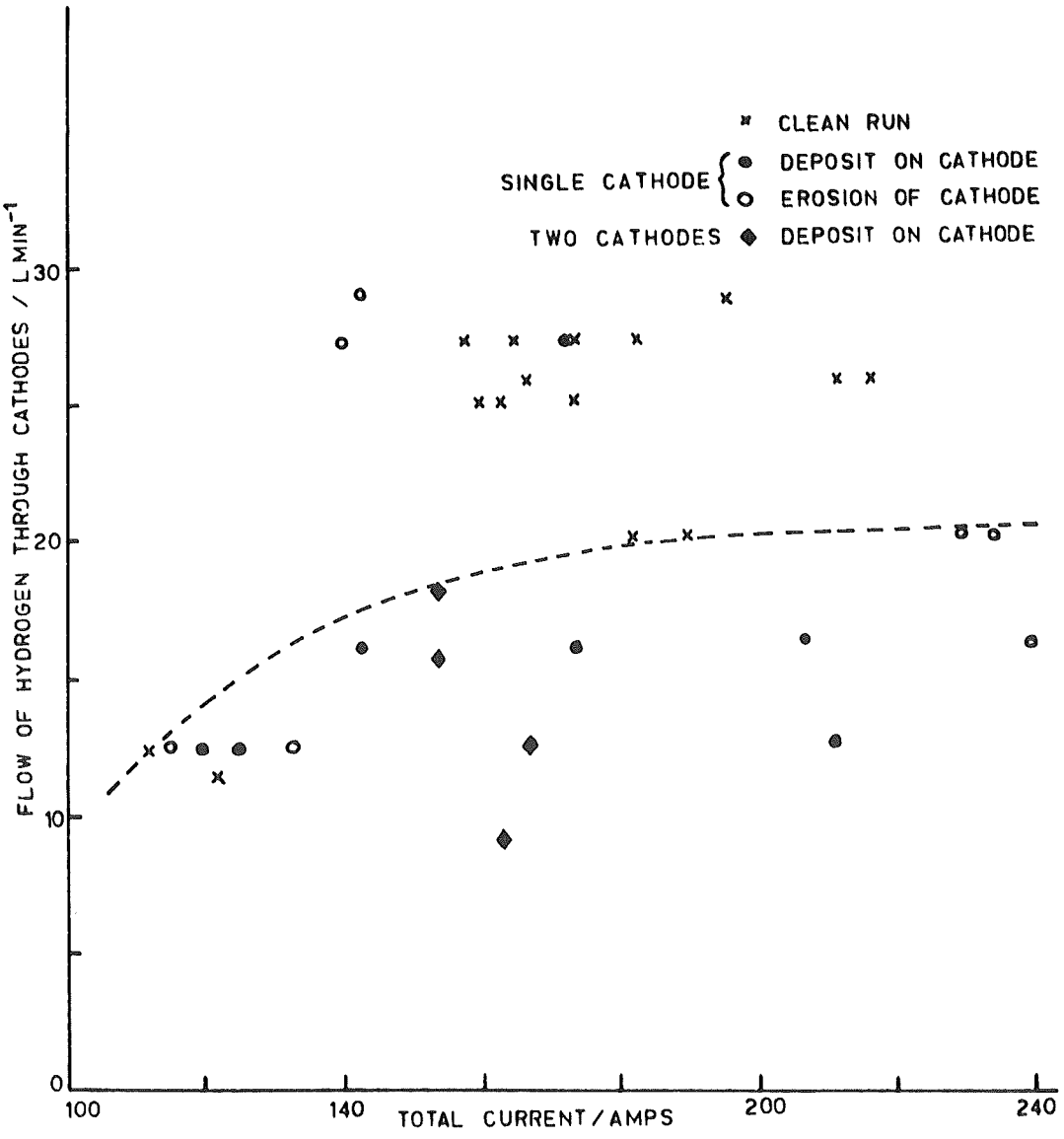

FIG XV

CATHODE HYDROGEN vs ARC CURRENT

For the purposes of this figure, carbon was deemed to have been deposited if, over the period of time considered, a layer of carbon of greater than 2 mm in thickness deposited on the cathode. Erosion was similarly defined.

Fig. XVI shows typical examples of cathodes with deposit, before use and after erosion.

Runs 28-31

One of the critical factors in erosion of the cathode was the amount of current carried by the cathode, in that if too high a current was drawn rapid erosion of the cathode soon resulted. In an attempt to overcome this problem, these runs were performed with two cathodes in order to spread the current load and hence reduce the possibility of cathode erosion. The cathode hydrogen flows were varied from 9 l min^{-1} to 18 l min^{-1} for power inputs of 10-11 kW and mass carbon to hydrogen ratios of from 0.58 to 3.46. In all cases, large deposits of carbon formed on the cathodes. These deposits were far greater in magnitude than the equivalent deposits for a single cathode and were so large as to bridge the inter-cathode gap and block up a large proportion of the reaction chamber. As the deposits became larger, arc instability increased markedly. This was ascribed to cooling of the cathode tip as a result of its increased size with a resultant decrease in electron emission. Because of these problems, a single cathode was reverted to.

Deposit of Carbon on the Reaction Chamber and Exit Tube:

In addition to the carbon deposited on the cathode, deposits also formed in certain parts of the reaction chamber. The structure and position of these deposits appeared to be independent of the design of the cathode used.

Three distinct forms of carbon deposit were observed in the reaction chamber and exit tube.

In all runs, a small amount of fine soot was found evenly distributed over all walls of the reaction chamber and exit tube.

In some runs, a dense layered form of carbon, similar to that deposited on the cathode, occurred. This appeared to be a laminar deposit of pyrolytic graphite, similar to that described by Bokros (100) and was concentrated for the most part on the anode shield and on the reaction chamber walls below the plane of the cathodes, although small amounts were also found on the exit tube. This type of deposit formed almost exclusively opposite the cathode, or cathodes, operating during the run.

The third type of deposit found was a crumbly grey deposit of low density compared with the previous type and may have been the same as the "frothed clinker" described by Abrahamson (1). This deposit also tended to be localised opposite the operating cathodes.

The amount of deposit on the exit tube remained approximately constant for constant power input and carbon to hydrogen ratio, but increased significantly as these two variables increased, e.g. from 5.9 ± 2.5% of total carbon fed at 10 kW and a mass carbon to hydrogen ratio of 0.8-1.2 to 16.5 ± 4.0% at 14 kW and a mass carbon to hydrogen ratio of 3.5 to 5.0.

The amount of deposit in the reaction chamber proper, i.e. on the walls in the plane of and below the cathodes and on the anode shield, did not show any significant trend with change in power input or carbon to hydrogen ratio and varied between 0 and 25% of the total carbon feed. In general, the low percentage deposits corresponded to erosion of the cathode and the high percentage deposits to large deposits on the cathode.

Reduction in the Thermal Capacity of the Reactor

The main factor which made it difficult to obtain good quantitative results from the majority of runs was the time taken for the reactor to reach thermal equilibrium. In some runs of up to 15 minutes duration, the approach to equilibrium, as determined from the rate of increase of the temperature rise in the reactor cooling water, was still not complete. It was considered that this may have been due to the large mass of carbon, surrounding the reaction chamber, which had to be heated. In an attempt to

decrease the time required to reach thermal equilibrium, the masses of exit tube and the upper and lower blocks forming the reaction chamber were reduced by 26%, 54% and 52% respectively. However, no significant improvement was obtained.

This can be explained by considering the specific heats of graphite and the magnesium oxide insulation with which the removed graphite was replaced. These are .34 cal cm^{-3} C^{-1} and .20 to .25 cal cm^{-3} C^{-1} respectively and show the comparatively small decrease in the amount of heat required to bring the reactor surrounds to thermal equilibrium obtained by decreasing the graphite mass in this manner. It would appear desirable in future work to leave large gas-filled spaces in the mass surrounding the reaction chamber to reduce its specific heat and thus the time required to reach thermal equilibrium.

Joining of the Anode Sections

Uninterrupted operation of the reactor was dependent on a smooth change-over from one section of anode to another. The initial method used to join the two sections of anode was that of a spigot and a closely matching hole and although this method worked well on occasions it was unreliable overall. As the join approached the arc, there was a tendency for the upper section of the anode to wobble under the influence of the motion of the arc and this led to faults such as arcing between the two anode sections and arc extinction through the top of the anode falling off. This problem persisted no matter whether the spigot faced up or down.

In an attempt to improve the efficiency of the joint, a paste of graphite powder and grease was placed in the hole before the spigot was pushed in. The idea behind this was that as the joint heated up the paste would act as a binder between the two sections of anode. This method also proved unreliable.

The final technique tried was that of a threaded spigot and a tapped hole so that the two sections of anode screwed together. This method proved to be completely satisfactory and was used in all runs from run 19 onwards.

CHAPTER 5

QUANTITATIVE RESULTS

Once the reactor design had been developed to the stage where continuous operation was possible, the remainder of the runs were concerned with the effect of three parameters on the yield of acetylene. These were the power input, carbon to hydrogen ratio of the reactants and, to a lesser extent, the quench rate of the product stream. The reactor pressure, another possible variable, was kept at ambient pressure throughout all runs.

Carbon Ablation Rate:

The ablation rate of the anode was important in that it determined the carbon to hydrogen ratio of the reacting system. The flow of hydrogen to the reactor was predominantly through the cathodes, this route accounting for from 72 to 92% of the total, and because variations in this flow were restricted by the requirement of no carbon deposit on the cathode, see fig. XV, variation of the carbon to hydrogen ratio was effected principally through manipulation of the carbon feed rate. Fig. XVI shows the variation of carbon ablation rate with current. The high degree of scatter in the points can be attributed to a number of factors; a consideration of ablation rates at constant current showed that there was a broad trend for the ablation rate to decrease with increasing voltage and as the voltages associated with the points in fig. XVI varied from 40-85 V some scatter could be expected. The hydrogen flow rate appeared to have no consistent effect on the carbon ablation rate for constant voltage and current, but as only a few reliable readings were available for comparison it is possible that more data would show some trend. One of the major problems involved in compiling fig. XVI was the difficulty in getting reliable data points. With the arc continually fluctuating, long periods of constant current operation were rare and this will have been a contributing factor to the scatter shown in fig. XVI. A further factor which may have affected the carbon ablation rate was the approach of the reactor to thermal

FIG XVI

CARBON ABLATION RATE vs ARC CURRENT

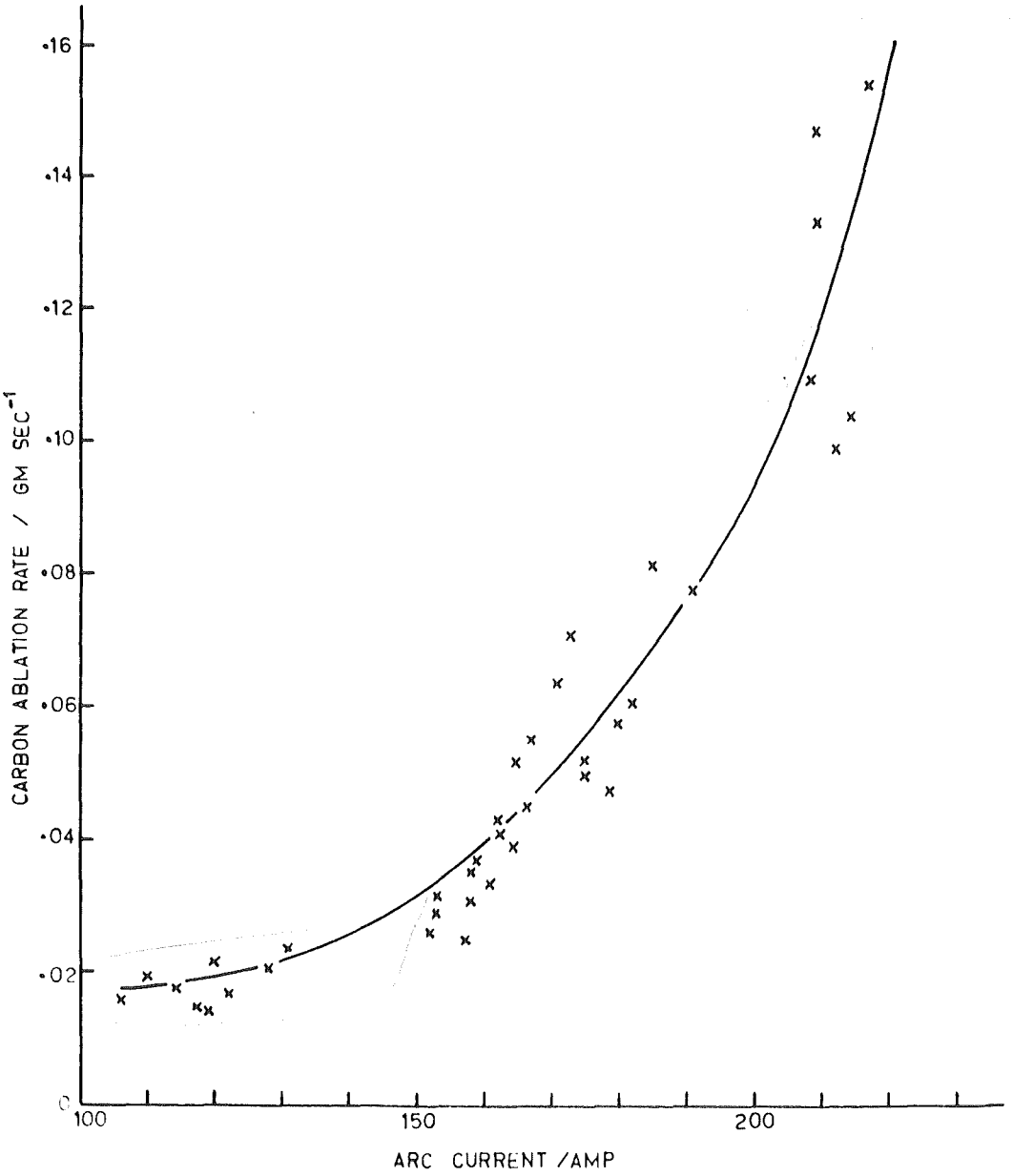

equilibrium; as the arc approached this state less heat would be lost to the arc surrounds as radiation and this would result in an increase in the heat available for ablation, thus increasing the latter. No reliable data was obtained with which to check this possibility.

A similar relationship between current and carbon ablation rate was obtained by Abrahamson (1) for currents of 10-50 A and carbon ablation rates from 0 to 0.015 gm sec^{-1}. Finkelnberg (89) obtained a similar shaped curve to fig. XVI by plotting carbon ablation rate against arc power. However, no such trend was noted in the ablation rates from this work.

Product Gas Analysis:

In all runs from number 26 onwards, the product stream was continuously analysed for acetylene using an IR spectrophotometer, and these results are presented in the following section. In addition, samples were collected for analysis by gas chromatography. Typical examples of these analyses are shown in table VII.

Run No.	43	44	51	58
Power input	10.46	10.40	9.90	9.50
Mass carbon/Hydrogen	0.96	0.90	1.03	1.21
Analysis, mole % Acetylene	4.0	3.7	4.5	6.5
Carbon monoxide	4.0	3.8	1.9	1.2
Ethylene	1.0	1.4	1.8	1.15
Methane	0.6	0.7	1.25	1.00
Ethane	0.02	0.04	0.05	0.02
Carbon dioxide	0.4	0.4	0.5	0.15
Hydrogen (by difference)	89.8	89.6	90.0	89.8

Table VII Gas Chromatograph Analyses

In addition to those compounds shown in table VII, traces of others such as n-butane, n-pentane and n-hexane were retained, but these were less than 0.01 mole percent and have been neglected. Simultaneously taken IR spectra confirmed the concentration figures for acetylene and, although quantitative results were only possible for acetylene, qualitative confirmation of the other species was obtained from the chromatograph analyses.

A third form of analysis was available in the form of carbon to hydrogen ratio determinations using the Haldane gas analyser and the results obtained by this method were used particularly in considering the mass balance over the reactor.

The Presence of Oxygen in the Product Gas

The apparent anomaly presented by the presence of oxygen, largely in the form of carbon monoxide, in the product stream can be explained by reference to the work on high-temperature degassing of carbons. Several workers (113, 114,115,116) have studied the composition and rate of evolution of gases during this process and their results show considerable variation depending on the type of carbon investigated, the temperature to which degasification was carried out and the condition of the sample investigated. The amount of oxygen evolved varied from 2×10^{-5} gm gm^{-1} for nuclear graphites (115) to 45×10^{-5} gm gm^{-1} for an electrode graphite (114) to 3000×10^{-5} gm gm^{-1} for a carbon black (113). Similarly, the amount of oxygen evolved for a nuclear grade graphite increased from 2×10^{-5} gm gm^{-1} at 1800 C (115) to 16×10^{-5} gm gm^{-1} at 2500 C (116). During any run, oxygen will thus be introduced into the reaction system from two main sources, the anode and the cathode. The greater amount can be expected from the former because of the total destruction of the graphite matrix holding the oxygen as well as the greater mass involved.

It is possible to make an accurate estimate of the amount of oxygen which should be present in the product gas because of the lack of data for the carbon being used and because it is not known how the amount of gas evolved will increase as the carbon is heated to its sublimation temperature.

The presence of oxygen due to the leakage of air can be discounted as no nitrogen was found in the product analysis. If any air had been introduced through leaks or other phenomena, significant quantities of nitrogen would have been found, possibly as hydrogen cyanide. The lack of nitrogen in the product is consistent with degasification of carbon being the oxygen source in that workers investigating this phenomena have found that nitrogen is not evolved on heating carbon, presumably because it is not retained in the graphite matrix to anywhere the same extent as oxygen.

Variation of Performance Criteria with Carbon to Hydrogen Ratio

In common with previous workers, the carbon to hydrogen ratio of the reacting gas mixture has been chosen as the parameter to which all others are related. The equilibrium composition of the reacting mixture is dependent on three basic parameters: reactor pressure, carbon to hydrogen ratio and pre-quench enthalpy (or temperature). By relating yield results to one of these parameters, an indication of the approach to equilibrium can be obtained. The reactor pressure was constant throughout all runs and as the pre-quench enthalpy could not be accurately measured for all runs the carbon to hydrogen ratio was chosen as the basic parameter to which to relate all others.

The accuracy with which the carbon to hydrogen ratio could be determined was limited by the accuracy of the calibration of the carbon and hydrogen feeds. No readings were considered unless both flows remained constant for 30 secs either side of the reading. This results in an accuracy of ± 6% for the carbon to hydrogen ratios.

The relationship between the acetylene concentration in the product and the carbon to hydrogen ratio is shown in fig. XVII. These results come from the continuous IR spectrophotometric analysis of the product and correspond to periods where the power input, reagent feeds and acetylene concentration remained constant for greater than 1½ minutes. The majority of readings were taken after the reactor had been running for five minutes. Although there is considerable scatter in the data, there is an evident trend to increase in

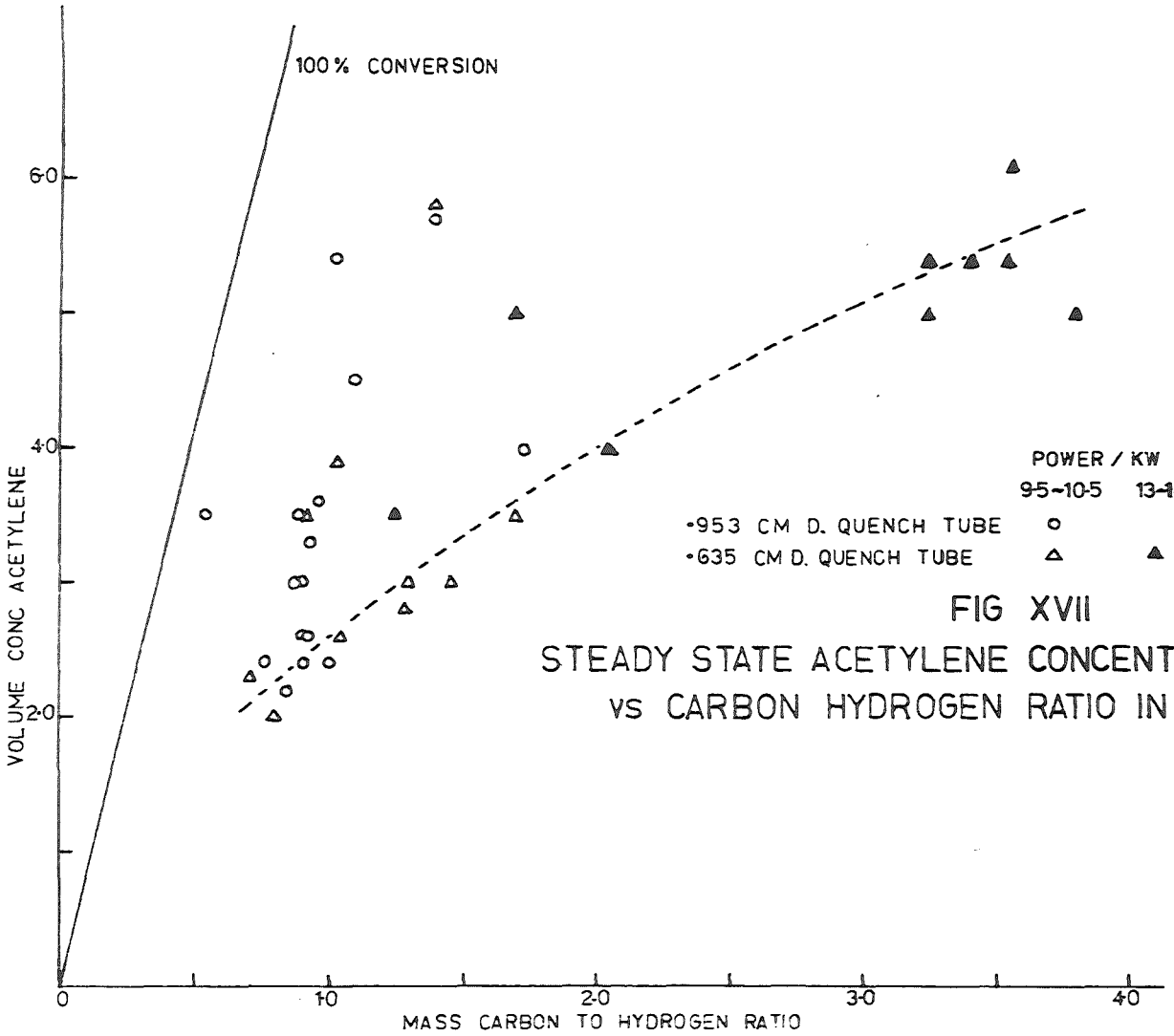

FIG XVII

STEADY STATE ACETYLENE CONCENTRATION IN PRODUCT
VS CARBON HYDROGEN RATIO IN REAGENTS

concentration with carbon to hydrogen ratio, particularly for the case of a .953 cm diameter quench tube, and these data are represented by the dashed curve. The data for the .635 cm diameter quench tube show considerably more scatter and in the absence of data at high carbon to hydrogen ratios it is difficult to be any more specific than noting the trend. Also shown is the line of 100% conversion of carbon feed to acetylene. This shows a decrease in conversion with an increase in carbon to hydrogen ratio and acetylene concentrati

The latter observation is illustrated more vividly in fig. XVIII which presents the conversion of feed carbon to acetylene as a function of carbon to hydrogen ratio. The points shown on this graph were selected by the same criteria applied to those in fig. XVII. The conversion of carbon to acetylene was calculated assuming that the product stream consisted of acetylene and hydrogen. The figures shown in table VII show that this assumption is not strictly true, although acetylene is the main hydrocarbon. Using the values in table VII. the true conversions for the runs given are 22.2, 22.2, 37.7 and 26.3 percent respectively. Using the assumption outlined above, the conversions are 21.5, 21.7, 38.0 and 26.4 percent respectively, showing that use of this assumption does not introduce any appreciable error into the results. The expansion of the hydrogen stream as it passed through the reactor, which was due almost entirely to the formation of carbon monoxide, was calculated by measuring the product stream flow rate with a gas meter which had an accuracy of ± 1.5% for a flow of 56 litres.

The other criteria of performance worthy of consideration is that of energy consumption per unit of acetylene produced. When this was calculated in terms of the total power input to the reactor and plotted against carbon to hydrogen ratio, no pattern was discernable in the points. It was considered that this was the result of variations in the amount of heat lost to the reactor surrounds, both from run to run and with time for any one run, and that a more meaningful figure for energy consumption could be obtained

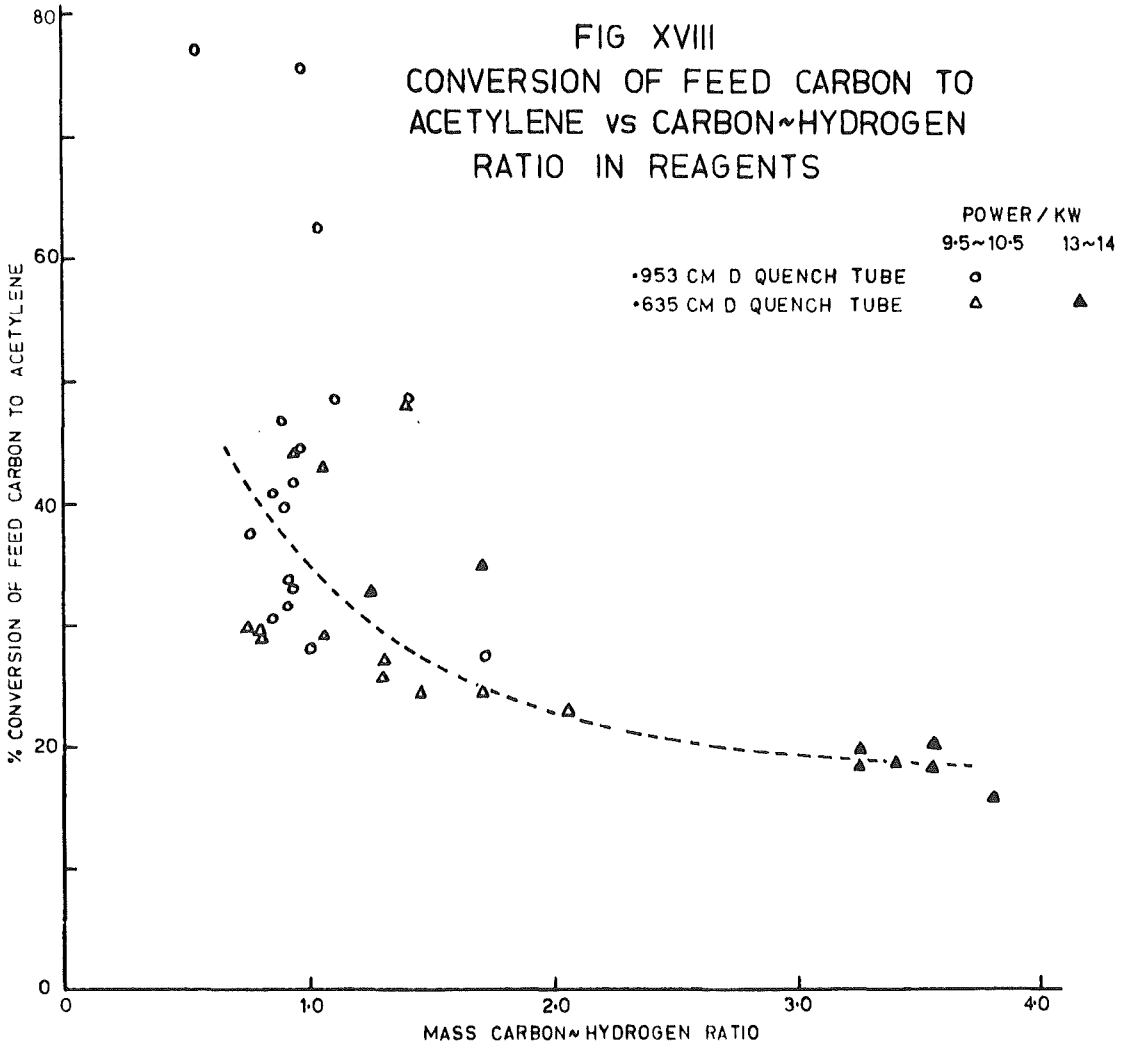
FIG XVIII
CONVERSION OF FEED CARBON TO ACETYLENE vs CARBON~HYDROGEN RATIO IN REAGENTS
POWER / KW
9·5~10·5
13~14
•953 CM D QUENCH TUBE
•635 CM D QUENCH TUBE
% CONVERSION OF FEED CARBON TO ACETYLENE
MASS CARBON~HYDROGEN RATIO
0
20
40
60
80
1·0
2·0
3·0
4·0

by basing it on the amount of heat transferred to the gas stream. This was equated with the pre-quench enthalpy which could be estimated from the heat output through the quench tube. The energy consumptions calculated on this basis are shown in fig. XIX. As in the previous cases, there is considerable scatter in the data, but that for a .635 cm diameter quench tube shows a minimum at a carbon to hydrogen ratio of about 2.5. The data for the .935 cm diameter quench tube is too incomplete to show a minimum, but it appears that such a minimum, if it exists, would be lower than for the previous case. In general, about 15 percent of the energy input was transferred to the reactants so that the minimum for the .953 cm diameter quench tube corresponds to about 100 kWh kgm^{-1} acetylene and the lowest values for the .635 cm diameter quench tube to about 80 kWh kg^{-1} based on total heat input.

Mass Balances

Following the problems encountered by Abrahamson (1) in closing the mass balance over a carbon arc reactor similar to that used here, a concerted effort was made to close the mass balance in this work and to support or offer an alternative to the hypothesis put forward by Abrahamson to account for the observed discrepancy in his work. Abrahamson found deficiencies in the mass output of a carbon arc reactor of between 12 and 44 percent of the carbon fed. To explain this observation, Abrahamson put forward the hypothesis that at sufficiently high-current densities very small, less than 0.5 microns, diameter graphite crystallites were split off the anode and that these particles were entrained in the gas stream and carried out of the reactor, by passing all filtering systems, thus escaping inclusion in the mass balance. Abrahamson supported the existence of these particles by reference to the work of Finkelnberg and others and this has been referred to in the previous chapter and in appendix II.

Overall mass balances were carried out on a number of runs by weighing all components on which carbon deposited, both before and after the run, and by graphically integrating the acetylene concentration vs time curve to determine

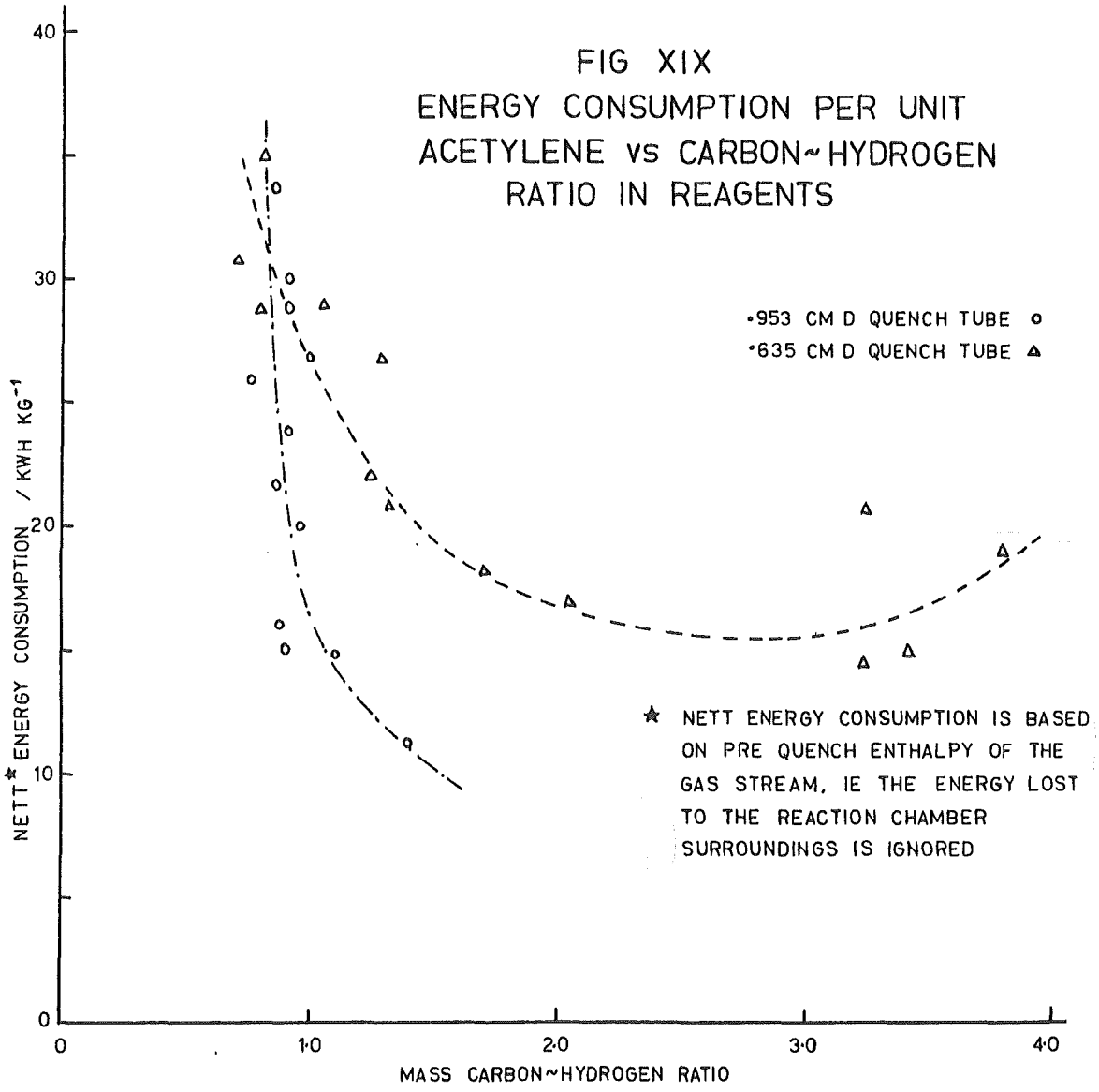
FIG XIX
ENERGY CONSUMPTION PER UNIT ACETYLENE vs CARBON~HYDROGEN RATIO IN REAGENTS
•953 CM D QUENCH TUBE o
•635 CM D QUENCH TUBE Δ
★ NETT ENERGY CONSUMPTION IS BASED ON PRE QUENCH ENTHALPY OF THE GAS STREAM, IE THE ENERGY LOST TO THE REACTION CHAMBER SURROUNDINGS IS IGNORED
NETT★ ENERGY CONSUMPTION / KWH KG⁻¹
MASS CARBON~HYDROGEN RATIO
0
10
20
30
40
1·0
2·0
3·0
4·0

the amount of carbon leaving the system as acetylene. Typical results are shown in table VIII. These figures are based on the assumption that no loss of hydrogen occurred from the system and, as was also assumed by Abrahamson, that the product gas consisted only of hydrogen and acetylene. These results show deficits in the carbon balance of from 23 to 49 percent and over all the runs considered the deficit ranged from 5 to 50 percent. These deficits are of the same magnitude as those noted by Abrahamson and which were explained by the above hypothesis.

Run No.	43	44	51	58
Weight gain in cathode	.0136	.0600	.0770	-.4005
Weight deposit in chamber	1.0127	1.7467	1.7817	5.8286
Weight gain in filters	0.2107	0.0339	0.0660	0.1038
Weight as C_2H_2	7.65	6.68	5.06	8.23
Weight loss in anode	13.7088	15.2545	13.6380	18.0126
Deficit	4.8215	6.7345	6.6533	4.2507
% Deficit	36.0	44.0	48.8	23.6

Table VIII Carbon Balance over Reactor

If this hypothesis is correct and if the carbon deposited within the reaction chamber is taken into account, then the carbon to hydrogen ratio of the product gas, as determined by Haldane analysis, should correspond to the carbon to hydrogen ratio in the feed since all carbon compounds, including any particles, present in the product gas would be combusted to carbon dioxide in the product gas burner. Haldane analyses of a number of runs showed, however, that this was not the case and this can be seen in the figures presented in table IX which shows that the percentage of carbon feed deposited in the reactor comes nowhere near accounting for the difference between the inlet and outlet carbon to hydrogen ratios.

Run No.	30	33	34	43
Mass $(C/H_2)_{in}$	1.170	0.774	0.825	0.921
Mass $(C/H_2)_{out}$	0.595	0.532	0.540	0.519
% Deficiency	49.0	31.4	34.6	43.7
% Feed Deposited	13.5	30.7	9.2	9.0

Table IX Comparison of Carbon to Hydrogen Ratios

The only explanation which would account for these results and still remain consistent with Abrahamson's hypothesis would be the settling out of the entrained carbon particles in the gas lines between the filter and the burner. These lines were blown out with compressed air and any solid matter collected on a pad of filter paper. A negligible quantity of solid was collected compared with the 5 to 7.5 gm which would be required to explain the observed difference in the carbon to hydrogen ratios. In light of these results, Abrahamson's hypothesis was discarded.

The solution to the deficit in the carbon balance lay in the formation of other carbon compounds whose existence was not indicated, and thus not taken into account, in the previous methods. Using the chromatograph analyses given in table VII, the product carbon to hydrogen ratios were calculated for these runs and the results are shown in table X.

Run No.	43	44	51	58
Product Mass (C/H_2)	0.93	0.93	0.98	1.05
Feed Mass (C/H_2)	0.96	0.90	1.03	1.21
% Feed Deposited	9.0	12.1	14.1	30.6

Table X Comparison of Carbon to Hydrogen Ratios

These show that, considering the percentage of feed carbon deposited in the reactor and the errors in the carbon and hydrogen feeds, ± 4.5% and ± 2.0% respectively, the carbon balance can be closed. The percentage of feed carbon deposited is an overall figure as, for obvious reasons, an instantaneous value is unobtainable, and will, no doubt, vary through the run so that a more exact statement of the carbon balance is impossible.

Thus it can be seen that the difficulty in closing carbon balances in this work was a consequence of inadequate gas analyses and that when detailed gas analyses were carried out no problems were encountered. It is suggested that this was also responsible for Abrahamson's difficulties and that his hypothesis of the existence of small carbon particles beyond the reactor and filters is doubtful and unnecessary.

A consideration of heat transfer to the carbon particles in the region immediately in front of the anode provides further evidence against Abrahamson's hypothesis. Appendix II shows that a conservative estimate of heat transfer to the particles is 1.6×10^{-8} cal sec^{-1} and that because of its size the particle is heated uniformly throughout its mass. A 1×10^{-5} cm diameter particle contains 9.6×10^{-17} moles of carbon and from the JANAF tables (107) the enthalpy of vaporisation of carbon at 4000 K is 7.2×10^{4} cal $mole^{-1}$. Thus the energy transfer required to evaporate the particle is 6.9×10^{-12} cal and the time required for this is 4.3×10^{-4} secs. For a particle moving at 500 cm sec^{-1}, the energy transfer will thus be complete within 2.2 mm of the anode face. Although this is a very simplified analysis, for example, it does not consider ratiation losses from the particle to the chamber walls nor the temperature gradient down the anode flame, it is considered adequate to show the very short life which would be enjoyed by even the larger of the particles being split off the anode and tends to argue against Abrahamson's hypothesis that up to 40% of the carbon feed is lost from the reactor in the form of such particles.

Heat Balances:

An accurate statement of the heat balance over the reactor proved a major problem due, in the main, to an inability to attain thermal equilibrium in the reactor within the time span of the run. Fig. XX shows a block diagram indicating typical heat flows as a percentage of power input. This figure shows a deficit, or accumulation within the reactor of about 54% of the total power input. It must be stressed that these figures are only average ones and varied from run to run and with time within a particular run, the latter trend being for the accumulated percentage to decrease with time. The error in measuring heat losses to the cooling water flows was about ± 6% and this is insignificant in comparison with the observed heat deficit. Heat conduction calculations showed that 10-12% of the power input was lost via conduction through the reactor casing to such heat sinks as the power leads and the reactor supports. This leaves a deficit in the heat balance of about 40%. The solution to this deficit was found in the large thermal capacity of the reactor body, in particular the large mass of carbon forming the reaction chamber surrounds. When the temperature of this block was monitored, it was found to steadily increase in temperature with time. Using locally measured rates of increase in temperature and the mass of the block, the heat absorbed in this manner was calculated and found to account for about 35% of the energy input. Several attempts were made to improve on this situation by drastically reducing the mass of the graphite blocks as has already been outlined in chapter 4, but no significant improvement was obtained. It is suggested that, considering the use of a local rate of temperature increase, this is an acceptable degree of closure of the heat balance. It is unfortunate that the length of run possible precluded the proper attainment of thermal equilibrium and this is further commented on in an evaluation of the reactor in chapter 7.

One other aspect of heat flows in the reactor worthy of mention was the seeming inability of the quench system to cope with the heat load of the

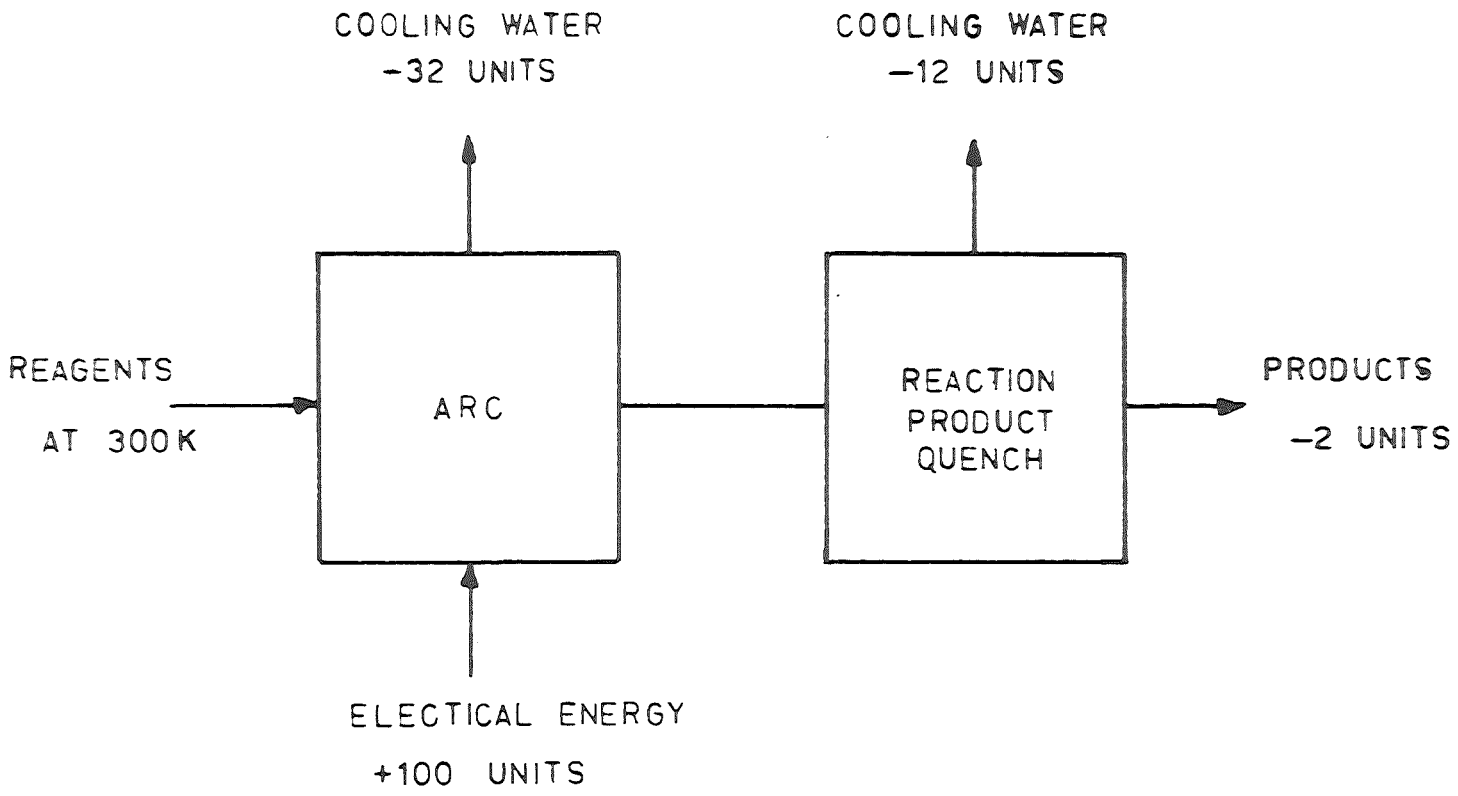

FIG XX

PROCESS HEAT FLOWS

product gas. This manifested itself in a gradual increase in the temperature of the outlet from the quench tube from about 300 K to a steady state value of about 400 K after 7-8 minutes. This was accompanied by a gradual rise in the heat removed from the product gas in the quench and a decrease in the acetylene concentration of the product from an initially high level to a steady-state lower value again after 7-8 minutes.

A typical example of the variation of the various parameters relevant to the heat flows from the reactor is shown in fig. XXI. This shows that although the quench system is very close to achieving equilibrium the principal energy flow, that to the cooling coils about the reaction chamber, is far from an equilibrium condition, inferring that considerable heat is still being accumulated in the mass surrounding the reaction chamber.

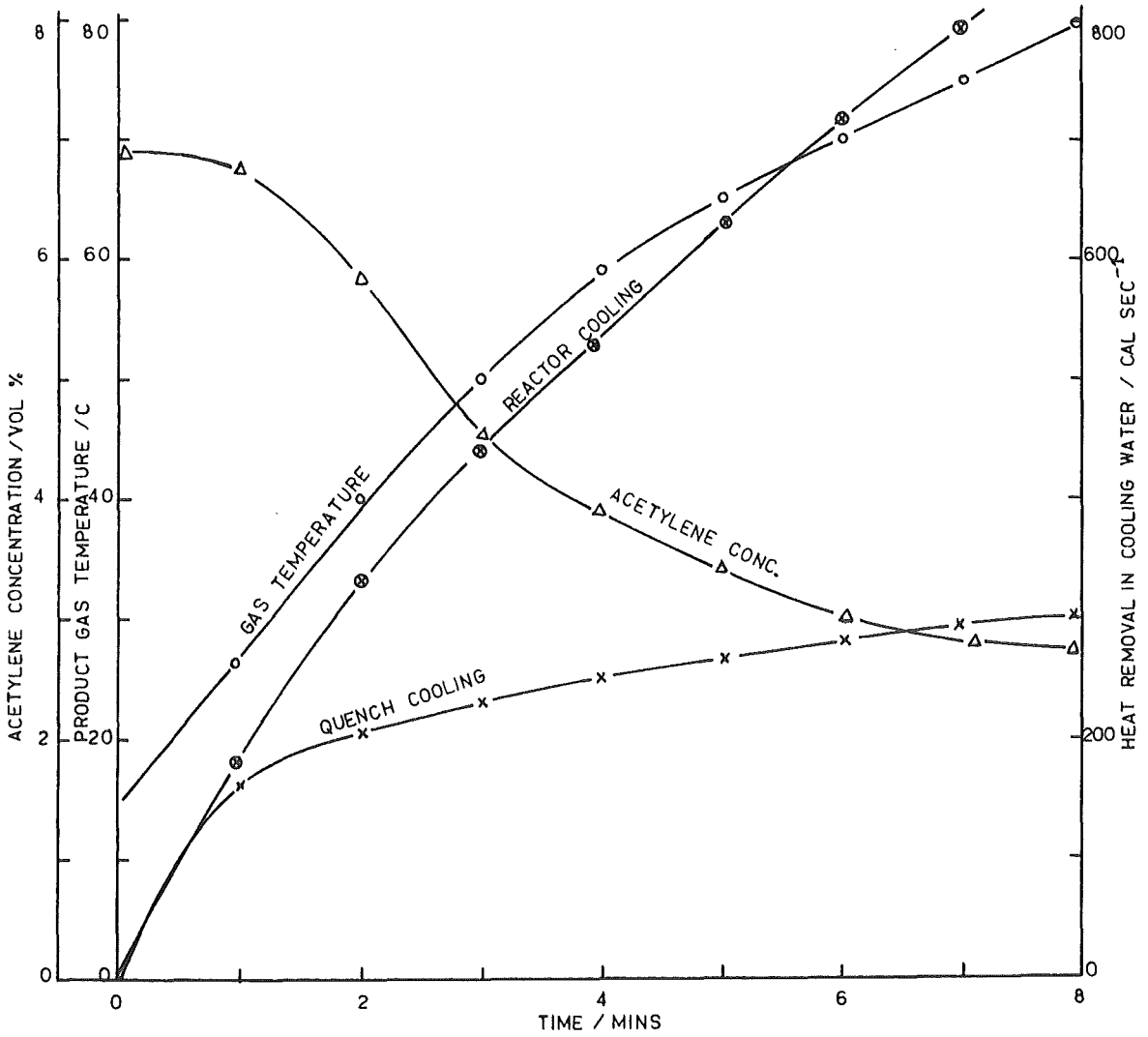

FIG XXI VARIATION IN PRODUCT GAS COMPOSITION AND TEMPERATURE AND HEAT REMOVED IN COOLING WATER WITH TIME FOR A TYPICAL RUN

CHAPTER 6

ACETYLENE FORMATION AND A REACTOR MODEL

Acetylene Formation

Composition - Enthalpy Diagram:

A comparison between the experimental acetylene yields and those predicted by equilibrium considerations of the carbon-hydrogen system can be obtained through use of a composition-enthalpy diagram.

A computer program was written to calculate the equilibrium compositions of the carbon hydrogen system for a variety of carbon to hydrogen ratios over the temperature range 1500 K to 2500 K at a pressure of 1.0 bar. The program was based on the method outlined by Ma and Shipman (117) and was based on minimisation of the free energy of the system. The free energy data of Duff and Bauer (118) were used for the species considered which were CH_2, CH_3, CH_4, C_2H, C_2H_2, C_2H_4, C_3H, C_3H_2, C_3H_3, C_3H_4, C_3H_5, C_4H, C_4H_2, C_4H_3, C_5H_6, C_6H, C_6H_2, C_6H_6, H and H_2, these species being shown, by hand calculation, to be the most important over the temperature range considered. The calculated compositions agreed with those of Duff and Bauer (111) and Lieberman and Mark (112) to within the accuracy to with which their graphs could be read.

Using these results and those obtained by Abrahamson (1) for the temperature range 2500 K to 6000 K, the enthalpy composition diagram shown in fig. XXIII was constructed. The thermodynamic properties of polycrystalline graphite were used to calculate the points for the line showing the saturation temperature for the precipitation of solid graphite. The remainder of the diagram was calculated for the gas phase only.

Experimental Results in relation to the Composition - Enthalpy Diagram:

The enthalpy of the reacting gas mixture can be calculated by two ways: by energy balances over either the reactor or the quench system. In this work, the former method was not suitable because part of the input energy was

accumulated within the reactor during the heating of the reaction chamber surrounds and no accurate measure of this was available; hence the second method, that of a heat balance over the quench tube, was used. The pre-quench enthalpy of the reactants is then given by:

$$h_R = (q_Q + q_p)/m$$

where h_R is the pre-quench enthalpy of the reactants, q_Q is the heat removed in the quench tube, q_p is the enthalpy of the product stream relative to elemental carbon and hydrogen at room temperature, and m is the mass flow of the product stream.

Using specific enthalpies so calculated and carbon to hydrogen ratios based on reagent feed rates, the results from this work were plotted on fig. XXIII, along with the results obtained by Abrahamson (1).

The maximum acetylene concentrations which would occur in the case of full thermodynamic equilibrium can be found by considering the single-phase compositions above the line of saturation temperature for the precipitation of graphite and the two-phase compositions below this line. For an atomic carbon to hydrogen ratio of 1.0, where the graphite saturation temperature is 3520 K, the maximum concentration in the two-phase region is 7% at 3300 K and 5% in the single-phase region at 3520 K. Fig. XXIII shows that the results obtained by Abrahamson were significantly above these maxima and he explained this by formulating a theory of acetylene formation based on "supercooled" equilibrium of the reacting gas mixture. This theory considers that at some time after the carbon and hydrogen streams were mixed, thermodynamic equilibrium was reached in the gas phase independent of any solid carbon, e.g. soot, present. If the gas mixture was then quenched after the time required for this equilibrium to be attained but before significant soot formation could occur, then a product would be obtained by acetylene concentrations the same as for gas only equilibrium. Abrahamson compared this theory with those suggested by Plooster and Reed (72) and Anderson and Case (37) and concluded that the theory outlined above was the simplest explanation of the observed results.

FIG XXIII

ENTHALPY~COMPOSITION CHART FOR THE CARBON HYDROGEN SYSTEM AT 1.0 BAR

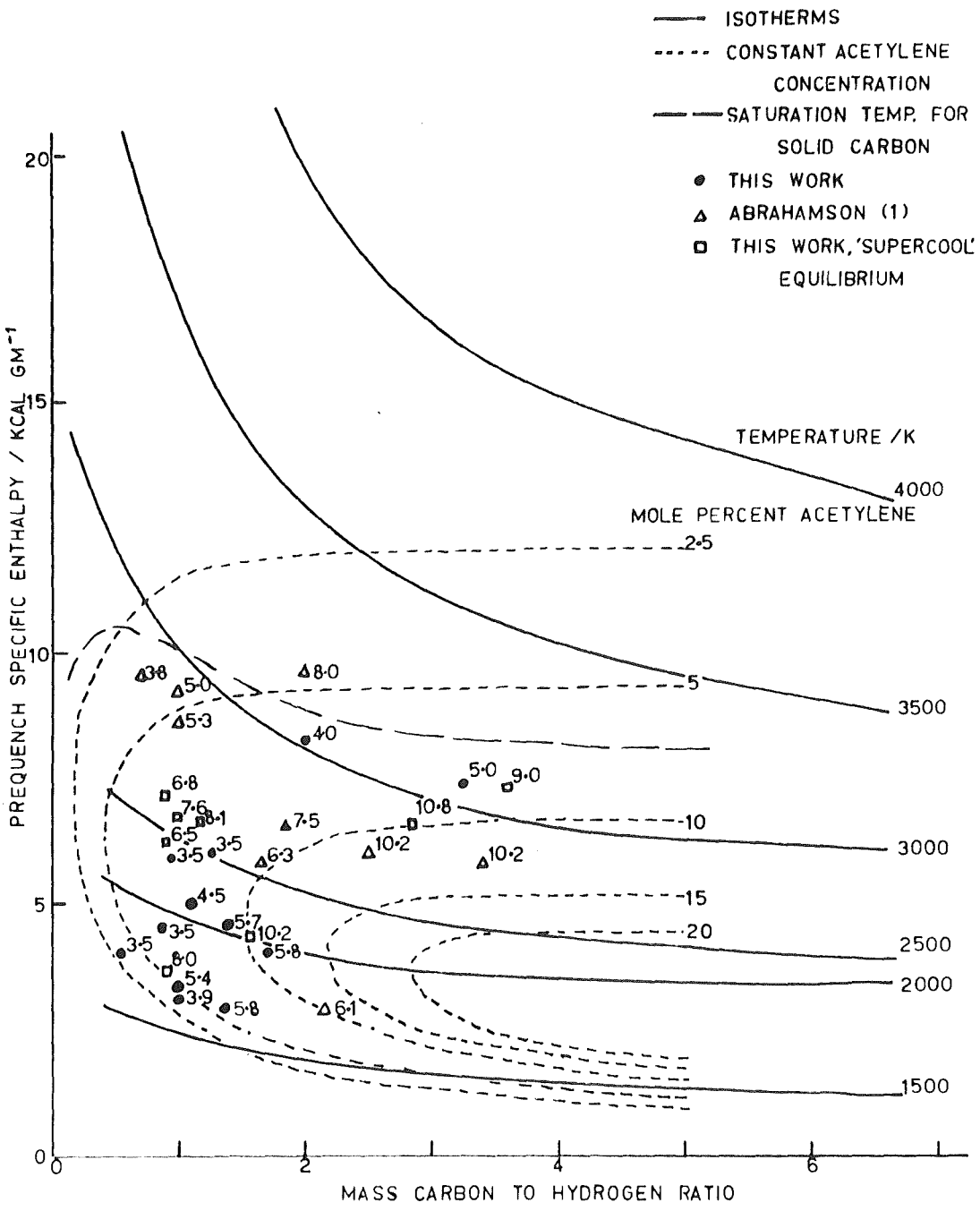

The results obtained in this work for steady-state operation show a maximum acetylene concentration of about 6%, thus suggesting the attainment of full equilibrium, contrary to what would be expected from the application of Abrahamson's theory. It is suggested that these results are not, however, inconsistent with the stated theory.

Considerable uncertainty is associated with the points in fig. XXIII from this work, both with respect to specific enthalpy and carbon to hydrogen ratio. The carbon to hydrogen ratios were calculated on the basis of the reagent feeds to the reactor. Whilst this will give accurate figures for the hydrogen side deposition of carbon in the reaction chamber and on the walls of the quench tube reduces the flow of carbon in the reacting gas mixture, the amount of carbon thus deposited ranged up to 40% of the total carbon fed (see chapter 4) so that the carbon to hydrogen ratios used to plot the points in fig. XXIII may be overestimated by up to 40%. It is impossible to be more specific than this because of the impossibility of measuring instantaneous carbon deposition rates. Similarly it is impossible to base carbon to hydrogen ratios on product analyses because of the uncertainty of the amount of carbon monoxide present and the possibility of carbon deposition subsequent to the pre-quench position through decomposition of acetylene. This error overshadows the ± 6% uncertainty in the reagent feed calibrations.

The mass flow rates used in determining the pre-quench specific enthalpies were based on a product stream assumed to consist only of acetylene and hydrogen with an acetylene concentration given by the spectrophotometric analysis. As was shown in chapter 5, significant amounts of other compounds, particularly carbon monoxide and methane, can be expected in the product stream. The presence of these compounds has a significant effect on the mass flow, analysis of the data in table VII showing that the error in mass flow arising out of the simplifying assumption mentioned above can underestimate the mass flow by up to 30%. This indicates that the specific enthalpy could be overestimated by up to 30%.

Even allowing for a possible overestimate of up to 40% in the carbon to hydrogen ratio and a possible overestimate of up to 30% in the pre-quench specifi enthalpy, the results from this work still seem to show significant departures from those shown by Abrahamson and from what would be predicted by his theory. The reason for this can be found in a consideration of the quench process. Abrahamson's theory depends upon a very high rate of quench in order to preserve the state of "supercooled" equilibrium. In order to prevent decomposition of the product acetylene to carbon, the product gas must be cooled to below about 800 K, the temperature below which decomposition rates are insignificant (119), in a time small compared with the time taken for significant decomposition of acetylene. Using the data of Palmer and Dormish (120), the time required for a 10% decomposition of acetylene in a 10 mol percent acetylene in hydrogen stream would be 5×10^{-5} sec at 2000 K and 3×10^{-3} sec at 1500 K. This indicates that the product stream must be cooled to about 800 K within about 10^{-4} secs. The extent to which this is attained will depend to a very large extent on the temperature of the gas pre-quench. At the start of a run, a greater percentage of the energy input to the arc will be lost to the initially cold reactor walls than will be at subsequent times in the run when the reaction chamber walls will have heated up. Using Finkelnberg's (89) result that 72% of the energy input to a carbon arc is dissipated by radiation and calculating the amount reradiated by the walls, assuming an emissivity for graphite of 0.81 (121), the nett heat loss to the reaction chamber walls at various wall temperatures was calculated. For the initially cold walls at 300 K, the nett heat loss of energy to the walls from the arc was about 70% of the input energy, but this fell to about 10% for a wall temperature of 1500 K, corresponding to an increase in specific enthalpy of the pre-quench reagents of up to three times. A computer program was written to estimate the temperature profile down the quench tube for various pre-quench enthalpies (see Appendix III). The profiles obtained show that as the pre-quench enthalpy rises the length of quench tube required to reduce the gas temperature to below 800 K increases.

During the time required for 10% decomposition of a 10 mol percent acetylene stream (10^{-4} secs), a gas with a pre-quench enthalpy of 10 kcal gm^{-1} travels about 1 cm into the quench tube. The temperature profiles show that at the end of this distance the temperature is still about 2000 K. This means that decomposition of the product is inevitable. During the same time a stream with a pre-quench enthalpy of about 5 kcal gm^{-1} (corresponding to the start of a run) is cooled to about 600 K and this explains why acetylene yields in accordance with Abrahamson's theory were found at the beginning of a run but showed a gradual departure from those predicted as the run continued.

Development of a Reactor Model

A physical model for the operation of the reactor can be developed by considering in summarised form the various phenomena discussed in the previous chapters and with reference to the motion of carbon within the reacting system. As discussed in Appendix II, the anode is ablated, in a strict relationship with the current, to form an anode flame containing small charged carbon particl entrained in molecular carbon (predominantly C_3) and, except for very close to the anode face, hydrogen. The arc proper was very short, no greater than 0.5 cm in length, and moved continually over the anode surface, this being reflected in the small fluctuations in arc voltage and current for a constant power input. The cathode tip would thus be expected to have come into close contact with the anode flame where no forces existed to sweep the latter away from the cathode. Under these conditions, the charged carbon particles were trapped in the cathode fall region and deposited on the cathode. However, when hydrogen was introduced into the arc along the axis of the cathode, the anode flame with its carbon was blown away from the cathode and no deposit of carbon occurred on it. The forces and heat transfer involved in this process are outlined in Appendix II. The lack of carbon close to the cathode was highlighted by the fact that the cathode jet which issued from the cathode spot was red in colour, this being an indication that hydrogen was the sole

species present in the jet. These two states are shown in fig. XXIV. In the latter case, the carbon-rich anode flame, because of the reaction chamber geometry, was blown close to the wall of the chamber opposite the cathode and this explains why the principal deposits of carbon on the chamber walls were found in this position. It is considered that the preference of the majority of this deposit to be below the plane of the cathode is due to the setting up of eddies and stagnant regions in this area of the reaction chamber. The design of the exit tube guarded against this happening in the upper regions of the reaction chamber. Thus the vapour stream leaving the arc chamber consisted of a mixture of molecular carbon and hydrogen species. It is proposed that this gaseous mixture attained an equilibrium based on the gas phase only, in line with the theory of "supercooled" equilibrium, and that it was in this state that the reagents entered the quench tube.

Although Abrahamson's theory of "supercooled" equilibrium cannot be supported with any certainty, there is reason to suppose that the results obtained in this work are at least consistent with it. The initial acetylene concentrations show values in excess of the maximum two-phase equilibrium values and show reasonable agreement with the single-phase equilibrium as shown in fig. XXIII and in line with the theory of "supercooled" equilibrium. However, these concentrations fall off with time to steady-state values which are considerably lower than those predicted and it is considered that this is the result of an inadequate quench system as discussed at the beginning of this chapter. Thus the "supercooled" equilibrium theory is supported, provided sufficiently rapid quench rates are obtained in the quench process otherwise the acetylene concentrations obtained will tend towards the two-phase equilibrium values.

To conclude this chapter, there are two other, unconnected, phenomena which require consideration: erosion of the cathode and the massive deposit of carbon on the cathode encountered in a two-cathode system.

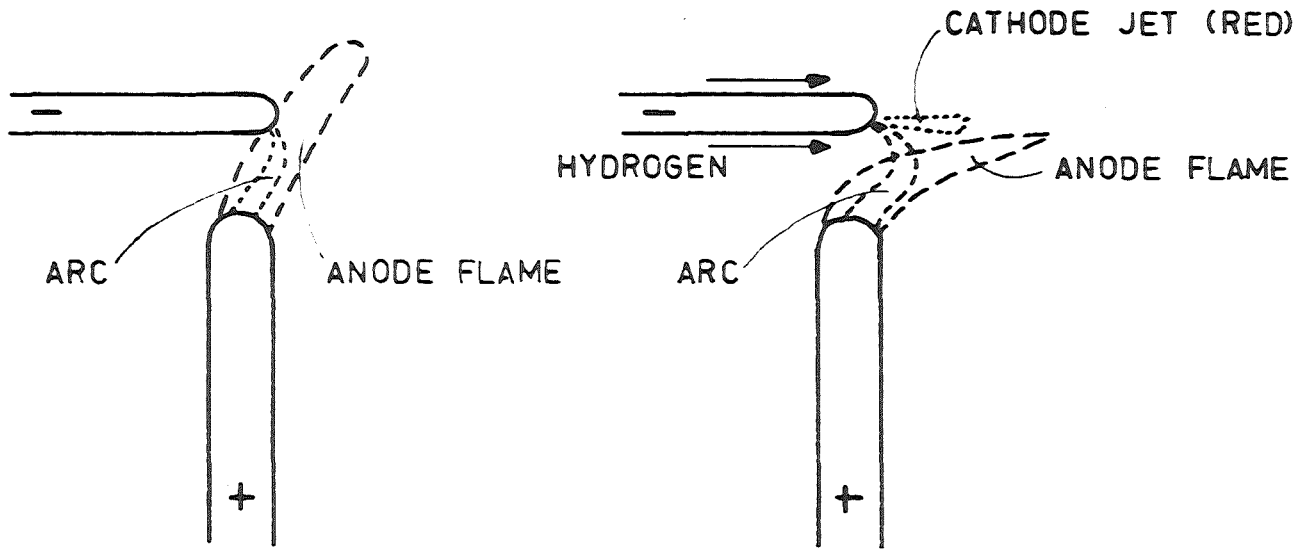

ARC WITH NO CATHODE HYDROGEN FLOW
ANODE FLAME
CONTACTS CATHODE

ARC WITH CATHODE HYDROGEN
ANODE FLAME
SWEPT WIDE OF CATHODE

FIG XXIV

Evaporation of the Cathode:

Evaporation of the cathode occurred in two quite distinct modes; at low power levels the surface of the cathode showed a tendency to pit for up to 2 cm back from the cathode tip following long periods of operation, whereas for high power levels, of the order of 10 kW, the cathode rapidly vaporised from the point of arc attachment. It is considered that two different mechanisms were involved for these two phenomena. As outlined in chapter 5, gases are evolved from graphite on heating and it is considered that during evolution from within the graphite matrix these gases exploded small particles of carbon from the graphite surface thus resulting in the observed pitted appearance. At high power levels, however, erosion of the cathode was rapid and took place only from the point of arc contact. Guillery (124) found that at a certain critical current, corresponding to a current density of about 5000 A cm^{-2}, cathode erosion suddenly increased and concluded that this corresponded to reaching the sublimation point of graphite. Guillery also noted that this effect varied with variation in the type of carbon used and that the critical current for a "hard" carbon was 400 A for an 8 mm diameter cathode. Kratsch et al (125) studied the ablation of graphites in relation to their structure and concluded that the initial process in ablation of graphite was the evaporation of the carbonised pitch used to bind the graphite together. This resulted in most of the material being eroded from the graphite being in the form of small carbon particles. It is suggested that at currents of 300 A enough heat was imparted to the low density binder (density 0.8 gm cm^{-3}, c.f. 2.2 gm cm^{-3} for the particles) in the vicinity of the cathode spot to cause its evaporation and subsequent disintegration of the cathode at this point and that this is consistent with the findings of Guillery who used a carbon with considerably less binder.

Two-cathode System:

The runs performed with a system involving two cathodes showed a very much increased tendency towards massive and rapid build-up of carbon on the cathodes under conditions for each cathode which would keep a single cathode system free of deposit. It is considered that this is consistent with the mechanisms outlined above for a single cathode system if one considers the position of the anode flame. In the case of a single cathode, the anode flame, containing the majority of the ablated carbon, is blown away from the cathode by the cathode-hydrogen flow and to a certain extent by the cathode jet. However, with two cathodes, these forces which keep the single cathode clean are in opposition with the result that the anode flame is not directed away from the cathodes and, because of the very small inter electrode gaps, the cathode tips are very close, if not within, the anode flame, thus allowing carbon to deposit rapidly on them.

CHAPTER 7

SCALE-UP AND ECONOMIC CONSIDERATIONS

When considering the economic viability of a process such as the one described in this work, the most important parameters for discussion are the yield of product, the conversion of feedstock to product and lastly, but most importantly, the energy required to produce a unit of product. A knowledge of the effect of scale of plant on these parameters is necessary for the prediction of the performance of large-scale plant, a precursor to the economic evaluation of the process. Allowing for some assumptions, significant comparisons can be drawn between the results of this work and those obtained by Abrahamson (1). An indication of the relative scale of the two plants can be gained by considering the power inputs and reagent flow rates used. Abrahamson used power inputs of up to 3 kW and reagent throughputs of up to 70 gm hr^{-1} compared with 15 kW and 400 gm hr^{-1} respectively for this work, i.e. the plant described in this work is about five times as large as that used by Abrahamson. The first point evident when comparing the two works is the apparent diminution in effectiveness of the quench process with increase in scale under steady-state conditions. Abrahamson had no trouble in obtaining the rapid quench rates required for the preservation of "supercooled" equilibrium, whereas in this work these rates seemed impossible except at the very start of a run. This is reflected in the gradual decline in the performance of the reactor with time as discussed in the previous chapter. Thus the steady-state yield of acetylene of about 6% compares with an initial value of up to 11.8%, carbon conversion to acetylene falls from approaching 100% to about 50% and minimum energy consumptions rise from 45 kWh kg^{-1} acetylene to 80 kWh kg^{-1} acetylene. In order to enable meaningful comparisons between this work and that of Abrahamson to be made, a condition of "supercooled" equilibrium will be assumed and the results obtained at the

beginning of runs in this work, although not steady state, will be used in comparisons. However, in practice, the quench operation is of the utmost importance and it will be considered in more detail first.

The Quench Process

At first sight it would appear that one effect of scale is a diminution in the effectiveness of a water-cooled tube as a quench method and hence a diminution in the efficiency of the reactor in that as the power level is increased to increase the carbon feed rate the pre-quench enthalpy increases and the quench rate required for "supercooled" equilibrium is unable to be obtained. However, this is not necessarily the problem it appears at first sight. If the theory of "supercooled" equilibrium is assumed to hold, then fig. XXIII shows that the maximum yield will be obtained at pre-quench enthalpies of about 3.5 kcal gm^{-1} for mass carbon to hydrogen ratios greater than about 2.5. Using the current ablation curve of fig. XVI and assuming a typical arc voltage of 50 V, the energy required to vaporise 500 gm hr^{-1} of carbon would be 9460 kcal hr^{-1}. If a mass carbon to hydrogen ratio of 2.5 is assumed and taking a nett radiation loss to the surroundings of 10% of the energy input, then the pre-quench enthalpy becomes 12.2 kcal gm^{-1}, well above the optimum value. Under these conditions, the quench tube will not be capable of effecting the desired quench time and "supercooled" equilibrium will not be obtained as outlined in the previous chapter. Thus the problem can be seen to be one of obtaining the desired pre-quench enthalpy rather than that of an increasingly inefficient quench system as the scale of plant increases. Solutions to this problem will be discussed in a subsequent section. The fact that Abrahamson did not have this problem to such a degree with the small-scale reactor may be traced to the greater heat losses through the walls of the reaction chamber, calculated to be of the order of 60% of the total heat input compared with 10% at steady state in this work.

Cathode Erosion

One other feature which is evident when comparing the small-scale apparatus of Abrahamson with the larger one described in this work is the phenomenon of cathode erosion. The use of carbon as a cathode material appears to have significant advantages over the tungsten used by Abrahamson. Carbon is cheaper and easier to fabricate, it does not introduce any additional elements into the reacting system and does not have the disadvantage of forming tungsten carbide on the tip of the cathode at high currents (see chapter 4). However, experiments in this work showed that as the current increased beyond about 300 A, vaporisation of the cathode occurred, according to the mechanism outlined in chapter 6, such that operation at higher currents would be impossible. There are two possible ways of overcoming this problem: spreading the current loads over additional cathodes or using a consumable cathode. The use of more than one cathode has been described in this work and been shown to be unsuccessful in that it seemed unduly susceptible to the formation of large carbon deposits on the cathode tip. As a result, the recommended solution is the use of a consumable cathode. Such a system would obviate the necessity for elaborate cathode geometries to prevent carbon deposit on the cathode tip as these would be consumed by cathode evaporation. Tight control of the arc would also be possible by adjusting the cathode feed rate to keep the arc voltage constant for constant power input. This latter feature would be eminently suitable for automatic control.

Efficiency of Energy Usage

If the "supercooled" equilibrium results of Abrahamson (1) are compared with those obtained in this work, it can be seen that an increase in scale by a factor of five (see page 69 for details) gives a reduction in the minimum energy requirement from 130 kWh kg^{-1} acetylene (1) to 45 kWh kg^{-1} acetylene (see page 69), in both cases at a mass carbon to hydrogen ratio of 2.5 (see fig. XIX for the optimum carbon to hydrogen ratio for this work). It is

considered that this decrease is due to a more efficient use of energy in the reaction chamber. The liberation of energy within the reaction chamber can be considered as two terms, anode ablation and radiation losses from the arc to the reaction chamber walls.

Fig. XXIII shows the desirable pre-quench enthalpy of the product to be 3.5 kcal gm^{-1} at a mass carbon to hydrogen ratio of 2.5. Consider two typical experimental carbon ablation rates from this work, 108 gm hr^{-1} at 150 A and 327 gm hr^{-1} at 200 A (see fig. XVI). The energy dissipated in a small region at the face of the anode is given by (79)

$$E = I(V_a + \phi) \qquad ---(1)$$

where I is the arc current, V_a is the anode voltage drop, and ϕ is the work function for graphite (4.6 V). The anode voltage drop is shown by Finkelnberg (89) to be about 30 V for currents greater than about 90 A. The enthalpy difference between graphite at room temperature and graphite at the sublimation temperature 4100 K) is given by the JANAF tables (107) as 21.168 kcal mol^{-1} and the heat of vaporisation of graphite at 4100 K is 66.9 kcal mol^{-1} from consideration of the equilibrium calculations of the carbon/hydrogen system discussed in the previous chapter. This results in the following table.

Current, A		150	200
Carbon ablation,	gm hr^{-1}	108	327
Energy dissipated at anode,	kcal hr^{-1}	4450	5950
Energy to heat carbon to 4100 K,	kcal hr^{-1}	191	576
Energy for vaporisation,	kcal hr^{-1}	602	1835
Total energy to vaporise carbon,	kcal hr^{-1}	793	2411

TABLE XI

For these two cases and for a carbon to hydrogen ratio of 2.5, the mass flows of hydrogen are 43.2 and 131 gm hr^{-1} respectively. Thus the total mass flows of reagents are 151.2 and 458 gm hr^{-1} and the energy input required to raise

these reagent flows to the desired pre-quench enthalpies are 530 and 1600 kcal hr^{-1} respectively. This shows that the heat which must be transmitted to the reagents is less than that transferred at the anode. This means that the use of the heat dissipated in the arc is unimportant for the system being considered in this work and the effect of scale can be considered by looking at the anode alone. The main aim must be to maximise the amount of heat liberated at the anode which is used to vaporise graphite.

The figures given in table XI show that at 150 A and 200 A the portion of the energy dissipated at the anode used to vaporise graphite is 18% and 41% respectively. The increase in vaporisation efficiency with increase in current for a constant anode diameter can be explained by considering a heat balance over a typical anode. Visual observations during operation of the arc showed that the bright tip of the anode extended back down the anode by up to one anode diameter and did not appear to vary significantly with arc current. Heat can be lost from the anode tip by three mechanisms other than useful vaporisation of graphite. These are radiation from the hot tip, convecti from this tip to the anode hydrogen flow and back conduction down the cathode. Spalding (126), using Reynolds flow method, estimated, using enthalpy as a potential for heat transfer, that the convective heat transfer to hydrogen from the side of the anode was of the same order as the loss by radiation. Assuming a temperature of 3800 K for the hot tip, an emissivity of 0.8 and assuming the fourth power of the surroundings temperature to be negligible compared with the fourth power of the tip temperature, the energy loss by radiation is 1600 kcal hr^{-1}.

From the above, the convection losses will also be 1600 kcal hr^{-1}. These these two mechanisms account for nearly all the heat losses from the anode. The remainder, 300-400 kcal hr^{-1}, can be accounted for as back conduction down the anode. Radiation from the anode face has not been included because it is considered that this will be negligible as reradiation

from the crystallites, suspended just above the anode surface, will be large. Now it can be seen for a constant anode diameter these losses will be constant being independent of current and so, as the current is increased, a greater proportion of the heat liberated at the anode is used to vaporise graphite assuming it has a constant work function, thus explaining the observed results. This suggests the desirability of maximising the current for a given power input which, in turn, implies a short arc gap if the power level is to be held constant. As has been discussed in chapter 4 and appendix II, a short arc gap is undesirable from the point of view of carbon deposition on the cathode. This would limit the amount by which the current could be increased for a constant power input in the reactor described in this work. Adoption of a consumable cathode (see page 71) could possibly remove this limitation.

The data of Abrahamson (1) enables a consideration of the effect of increase of anode diameter on energy utilisation to be made. There is no overlap in the ablation range used by Abrahamson and that used in this work. It is felt, however, that this is not important and that a more valid comparison can be made by considering data at the same ablation rate to anode cross-sectional area ratio, i.e. equal ablation rate per unit cross-section of anode. The following table shows such a comparison. These figures show the greater efficiency obtained with a larger anode diameter. This phenomenon can also be explained in light of a heat balance over the anode. For a given linear feed of anode, the amount of carbon ablated is proportional to the square of the diameter of the anode, whereas the heat losses from the anode are proportional to the first power of the diameter of the anode. If the efficiency of energy usage at the anode is defined as follows:

$$\text{Efficiency} = \frac{\text{Energy used to vaporise carbon}}{\text{Energy used to vaporise carbon + Radiation and Convection losse}}$$

then

$$\text{Efficiency} = \frac{KD^2}{KD^2 + K'D}$$

where D is the anode diameter and K and K' are constants.

	Abrahamson	This work
Current, A	50	200
Carbon ablation rate, gm hr^{-1}	53	327
Anode diameter, cm	.3175	.793
Ablation rate, unit cross Section anode, gm hr^{-1} cm^{2}	1485	5940
Energy dissipation at anode, kcal hr^{-1}	395	2465
Energy to vaporise carbon, kcal hr^{-1}		
% Energy used to vaporise carbon	26.5	41.5

TABLE XII

K contains terms such as enthalpy of vaporisation and heat required to raise graphite to its sublimation temperature and K' contains such terms as the temperature and emissivity of the side of the anode. In addition, K contains the ablation rate per unit cross-section of anode. For situations where this latter term is constant, both K and K' will be reasonably constant, independent of the anode diameter. Using the data presented in table XII, values of K and K' of 4920 kcal hr^{-1} cm^{-2} and 3990 kcal hr^{-1} cm^{-1} are obtained for an ablation rate per unit cross-section of anode of 665 gm cm^{-2} hr^{-1}. Substitution of the anode diameters used gives energy usage efficiencies of 28% and 49.5% respectively. It is considered that this is a reasonable agreement with the experimental values. This enables an energy usage efficiency prediction to be made for larger diameter anodes, e.g. increasing the diameter to 1.5 cm would result in an energy usage efficiency of 65%.

As mentioned on page 73, the energy liberated at the anode is sufficient to raise the reactants to the desired pre-quench enthalpy. This means that the energy liberated in the arc itself, as radiation, is surplus and must be disposed of by radiation to the hot reaction chamber walls. This may explain why other workers in this field have always opted for cold walls in the

reaction chamber as this minimises reradiation of energy to the reactants. Hot walls may be turned to an advantage, particularly since the discovery of large deposits of natural gas in New Zealand (see chapter 1) by introducing an additional gaseous reagent stream following the arc. Cold methane, introduced thus, would soak up the additional energy and could be fed in amounts calculated to give the desired pre-quench enthalpy. This would then turn the hot reaction chamber walls to an advantage as energy losses through the walls would be minimised and the maximum possible use would be made of the electrical energy. Methane has the added advantage of having a mass carbon to hydrogen ratio of 3.0 which is very close to the apparent desired optimum in the pre-quench reactants and so no adjustment in the carbon and hydrogen flows to the reactor would be necessary for changes in methane flow. However, the addition of methane may not be quite as advantageous as appears at first sight as the probability of forming C_2 from the condensation of methane may be low in these circumstances (128).

Consider a 1.5 cm diameter anode for which an efficiency of energy usage at the anode of 65% has been predicted for an ablation rate per unit cross-section of anode of 665 gm cm^{-2} hr^{-1}. Consider a current of 450 A (that required to give an ablation rate per unit cross-section of anode of 665 gm cm^{-2} hr^{-1}) and an arc voltage of 60 V. The energy used to vaporise carbon is then given by equation 1 as 8.7×10^3 kcal hr^{-1}. This vaporises 1185 gm hr^{-1} of carbon, a linear anode feed rate of 0.9 cm sec^{-1} which is similar to that achieved in this work. Assuming the optimum carbon to hydrogen ratio of 2.5, the mass flow of reagent is 1660 gm hr^{-1}. The optimum pre-quench enthalpy of 3.5 kcal gm^{-1} requires 5800 kcal hr^{-1}. The energy input to the arc is 23,200 kcal hr^{-1}, i.e. an overall energy usage of only 25% is required. Assuming a 90% conversion of carbon to acetylene, the acetylene yield is 1155 gm hr^{-1} acetylene which results in an energy requirement of 23.4 kWh kg^{-1} acetylene.

If, however, more of the energy input to the arc could be utilised, this figure would be lowered considerably. For example, if a further 50% of the energy input could be used to react methane rather than being wasted, an additional 11,600 kcal hr^{-1} would be used. This amount of heat could raise about 3300 gm hr^{-1} of methane to the desired pre-quench enthalpy. This would result in a total carbon feed of 4485 gm hr^{-1} and, once again allowing for a 90% conversion of carbon to acetylene, this results in an acetylene production of 4370 gm hr^{-1} acetylene and an energy requirement of 6.18 kWh kg^{-1} acetylene. This figure, which is competitive with the best obtained by all other workers, shows the real advantage of using methane as an additional feedstock. As the above figure is also below those reliably quoted for methane-only plasmatrons (see chapter 2), the potential of the dual system is evident.

Comparison with Plasmatron Devices

An interesting comparison can be drawn between this modified process and those processes which use a plasmatron device for the reaction of solid reagents, particularly coal. In this latter group of processes, the solid reagent particles are fed into a plasma typically of argon or hydrogen, and must be vaporised before leaving the hot zone. The experience of various workers in this field (69-79) is that large amounts of unreacted solids are found in the product and this suggests that the rate of heat transfer within the hot zone is not great enough. This has resulted in very high energy requirements, the minimum so far reported being about 140 kWh kg^{-1} acetylene (72). The rate of temperature rise in a particle within a hot gas is given by

$$\frac{dT}{dt} = \frac{3h\Delta T}{RC_p\rho}$$

where h is the heat transfer coefficient between the gas and the particle, ΔT is the temperature difference between the gas and the particle, and R is the radius of the particle of specific heat C_p and density ρ. Using this expression for a coal particle of 100×10^{-4} cm diameter, the minimum time for the particle to reach 1000 K has been shown to be of the order of 10^{-3} sec (127).

Under these conditions, it is virtually impossible to vaporise completely the solid particle and thus it appears that this type of process is unlikely to become economic. The expression above shows that the rate of temperature increase is inversely proportional to the radius of the particle so that decreasing the radius of the solid particle should increase the efficiency of the device. This has been found to be the case (75,67) and taking this to its logical conclusion the most efficient operation of this type of device would be when the solid particles reached atomic proportions, i.e. the situation obtained in the arc device described in this work. Thus it can be concluded that solid feed plasmatrons are inherently inferior to consumable electrode devices from a heat transfer point of view.

Gas plasmatron processes can be compared usefully with this device on an energy utilisation basis. Those processes which are based on an inert gas plasmatron must have inherently lower energy utilisation efficiencies as the electrical energy is converted to thermal energy with efficiencies of typically 60% (27) before being transferred in turn to the reagents with further inefficiencies. It is obviously preferable to transfer the electrical energy directly to the reagents as occurs in this work. The same applies to a limited extent in hydrogen plasmatrons typically using methane as a reactant as, since the mass carbon to hydrogen ratio in methane is 3.0, the large amounts of hydrogen from the plasmatron will dilute the reacting mixture to well below the optimum mass carbon to hydrogen ratio of 2.5 and in terms of "supercooled" equilibrium only low acetylene yields can result (see fig. XXIII).

In conclusion, it can be noted that all processes which have become economic have used direct heating of the reagents and have used an additional reagent feed following the arc chamber (sometimes incorporating this as the quench process).

Summary

In the aforegoing, the conditions for high yields, up to 20%, and conversions, up to 90%, and low energy requirements, down to 7 kWh kg^{-1}, have been predicted. It has been shown that the process as it stands at present is unlikely to ever be an economic proposition because of the low efficiency of heat transfer to the reactants under optimum operating conditions. This situation is shown in fig. XXV. It has been shown that this situation can be rectified by the use of an additional reagent feed consisting of methane which has the potential of raising the energy usage efficiency and reducing the energy consumption to below 7 kWh kg^{-1} acetylene, thus making the modified process superior to some other types, e.g. plasmatrons, and highly competitive with the remainder. It is thus concluded that this work should be continued in this modified direction. Criteria for scaling up the process have been discussed in the light of the results of this work and those of Abrahamson (1) and predictions made for the performance of larger plants.

Process	Energy Consumption kWh kg^{-1}	Reference
Abrahamson	130	1
This work	45	page 72
Huls Arc	6.9	7
Predicted by this work using additional methane	7.0	page 77

ENERGY CONSUMPTION* PER UNIT OF ACETYLENE COMPARING THIS WORK WITH OTHER PROCESSES

*Exclusive of the energy used in separation of acetylene from the product stream, reported to be 2.9 kWh kg^{-1} acetylene (7).

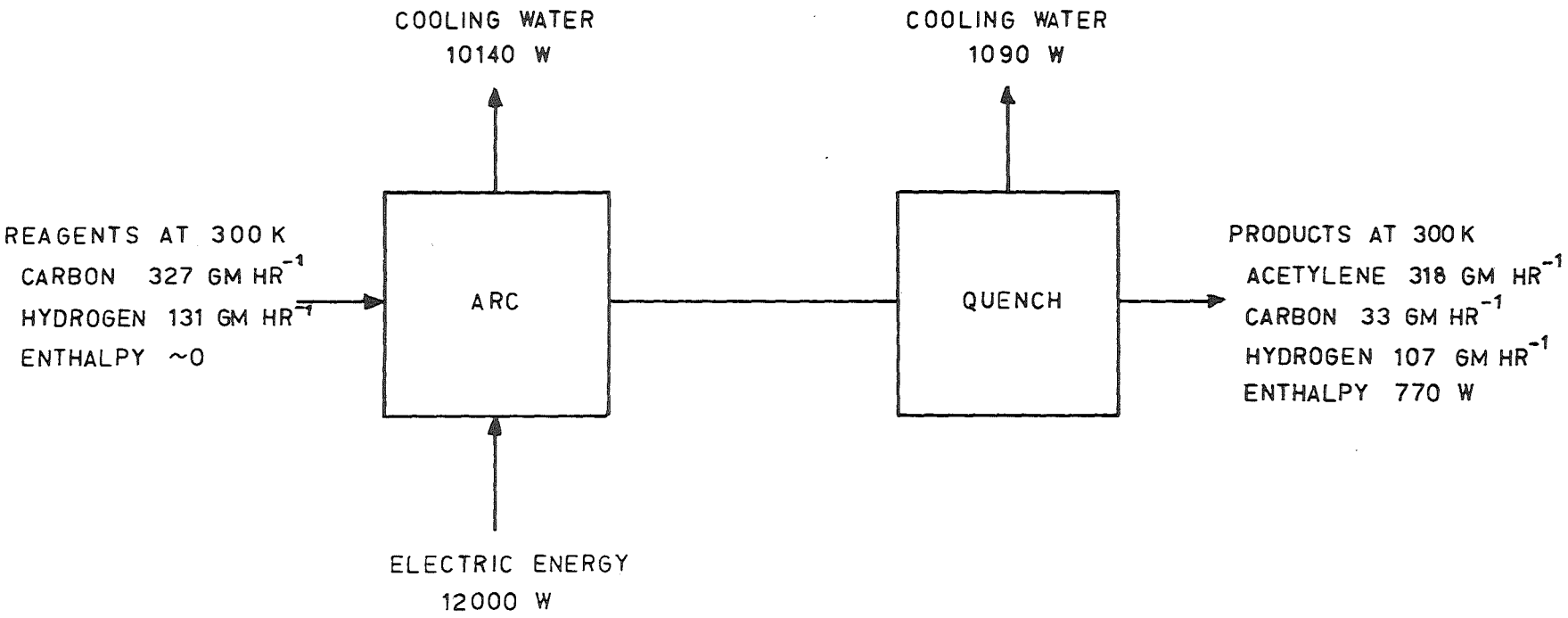

FIG XXV

HEAT AND MASS FLOWS UNDER OPTIMUM OPERATING CONDITIONS

APPENDIX I

DETERMINATION OF THE CARBON:HYDROGEN RATIO AND THE RATE OF CARBON FLOW FROM THE REACTOR BY THE METHOD OF HALDANE

From an analysis of a sample of the combusted gas from the burner

Volume of sample = V cm^3

Volume of carbon dioxide = x cm^3

Volume of oxygen = y cm^3

If the sample is assumed to contain only oxygen, nitrogen and carbon dioxide, then:

	Carbon dioxide	Oxygen	Nitrogen
Volume, cm^3	x	y	V-(x+y)
Volume fraction	x/V	y/V	1-(x+y)/V

If the gas is treated as an ideal gas, then the mole fractions of the components will be the same as the volume fractions. Considering one mole of the gas sample and assuming that all the nitrogen present originated in the excess air burnt with the reactor gas, then:

Moles of air used to burn the reactor gas contained in the sample = $(1 - \frac{x+y}{V})/.78$

Moles of oxygen in this air = $.21 \times (1 - \frac{x+y}{V})/.78$

= $.269 \times (1-\frac{x+y}{V})$

Moles of oxygen in gas sample = $(x+y)/V$

Hence the moles of oxygen used to form water from the hydrogen in the reactor gas = $.269 (1 - \frac{x+y}{V}) - (x+y)/V$

= $.269 - 1.269(x+y)/V$

Moles of water produced by combustion = $2(.269 - 1.269(x+y)/V)$

= $.54 - 2.54(x+y)/V$

= moles of hydrogen in the reactor gas

Assuming all the carbon in the reactor gas is converted to carbon dioxide,

the moles carbon in the reactor gas $= x/V$

Hence molar carbon:hydrogen $= \dfrac{x/V}{.54 - 2.54(x+y)/V}$

$= \dfrac{x}{.54V - 2.54(x+y)}$

From this expression, the mass carbon:hydrogen ratio can be found and, if the hydrogen flow through the reactor is known, the carbon flow can also be found.

APPENDIX II

THE EXISTENCE OF CARBON PARTICLES IN THE HIGH INTENSITY CARBON ARC, AN ANALYSIS OF THEIR MOTION AND AN ESTIMATE OF HEAT TRANSFER TO THEM IN THE VICINITY OF THE ARC

The existence of carbon particles in a high-intensity carbon arc was first postulated by Finkelnberg (89) who invoked them to explain the discrepancy between the measured amount of carbon deposited on the cathode of a carbon arc and the amount of this resulting from the commonest ion C_2^+ which was only 4% of the total. Finkelnberg postulated that the remaining 96% of the deposited carbon was transported to the cathode in the form of small carbon particles split off the anode during ablation. Pfender and Boffa (90) used a 25 kW plasmatron to generate an aerosol of carbon particles in argon at 1 bar. Electron microscope studies showed these particles to lie in the size range .01 to 1.0 microns. Similar size distributions were found by Whittaker and Kintner (91) who observed, by means of the Tyndall effect, the emission of carbon particles from graphite being sublimed in vacuum at 3000 K. These particles were collected on silicon grease and studies under an electron microscope. Abrahamson (92) estimated that a carbon particle of 0.05 microns diameter could carry up to 100 electronic charges and that this charge would fall to 3 electronic charges of 10^{-3} microns.

Palmer and Shelef (96) summarised the literature on the vaporisation of carbon and concluded that the distribution of C_n species leaving the anode crater of an arc approximated an equilibrium relationship and that by far the most predominant species was C_3 with a mole fraction of about .85 at 4000 K. Thus the space immediately in front of an ablating carbon anode can be considered to contain carbon particles of about 0.1 micron diameter carrying about 100 electronic charges entrained in a vapour stream of C_3 molecules.

An estimate of the relative amount of particulate carbon can be obtained from Finkelnberg's observation that 40% of the ablated carbon deposited on the cathode and an assumption that this is due, in the main, to unvaporised carbon particles.

Forces Acting on the Carbon Particles

To estimate the relative magnitudes of the forces acting on the carbon particles described above, it is necessary to decide on a temperature for the short carbon arc. Finkelnberg and Maecker (97) give temperature profiles for a 200 A carbon arc with an inter-electrode spacing of about 4 cm. These show a central core temperature of 10,000 K but this falls of to about 4000 K at a radius, about the centre line of the arc, of about 1 cm, i.e. the temperature of the arc is very dependent on radial position. For this analysis, a compromise temperature of 6000 K was assumed.

Although it has been stated that the carbon particles, resulting from ablation of the anode, are entrained in a vapour stream of C_3 molecules, this will, in fact, only be true very near the anode. The true atmosphere through which the particles move on their path to the cathode will be a mixture of C_3 molecules and partially dissociated hydrogen. Abrahamson (92) estimates that the carbon vapour is significantly mixed with the surrounding gas within 0.2 mm of the anode. An analysis based on this mixed atmosphere would be extremely complex and to simplify the problem the worst possible case, either hydrogen or C_3 molecule atmosphere will be considered here.

The forces considered to have the greatest effect on the motion of the carbon particles are the electric field, concentration gradients and expansion of the carbon stream due to ablation.

Electric Field

According to Thomson and Thomson (93), the electric field of an arc imparts a drift velocity to a particle in the arc given by

$$v_d = KE$$

where E is the electric field gradient (V cm^{-1} and K, the mobility of the particles, is given by

$$K = e(1 + 3\lambda)/2R_a)/6\pi\mu_B R_a$$

where e is the particle charge (coulomb), R_a is the radius of the particle (cm), μ_B is the gas viscosity (gm cm^{-1} sec^{-1}), and λ, the mean free path of the particle through the gas is given by

$$\lambda = (\sqrt{2}\pi n_B (R_a + R_B)^2)^{-1}$$

where n_B is the gas molecular density (molecules cm^{-3}) and R_B is the radius of the gas molecule (cm). The drift velocity will be greatest for motion through a hydrogen atmosphere. The gas molecular density, n_B, of hydrogen at 6000 K is 1.2×10^{18} molecules cm^{-3}, the radius of the gas molecule, R_B, can be estimated from the Leonard-Jones parameters for hydrogen (95) at 2.5×10^{-8} cm and, using a particle radius, R_a, of 1×10^{-5} cm, the mean free path of the particle through the gas, λ, is 5.4×10^{-10} cm. The viscosity of hydrogen at 6000 K lies in the range 4×10^{-4} to 8×10^{-4} gm cm^{-1} sec^{-1} (94,101) and, assuming a charge on the particle of 100 electronic charges, the mobility of the particle, K, is 1.4×10^{-10} A sec^2 gm^{-1}. Taking a value of 15 V cm^{-1} (89) for the electric field gradient, this results in a drift velocity for the particle of 2.2×10^{-2} cm sec^{-1} which is very low.

Expansion:

Finkelnberg (89) observed that, when the cathode diameter was large compared with the anode, the deposits formed on the cathode had a diameter the same as the anode. If it is assumed that the carbon transport to the cathode occurs in plug flow with a diameter the same as that of the anode, this gives a plug diameter of 0.8 cm for this work. Using the assumption that the vapour stream consists of C_3 molecules and is 60% of the carbon ablated, then for a carbon feed rate of 1.72 gm min^{-1} the vapour stream with its entrained carbon particles would have a velocity of about 500 cm sec^{-1} as a result of expansion of the material stream on ablation.

Diffusion

Bird, Stewart and Lightfoot (95) give the following equation for the diffusion path length, δ, of a particle in a vapour stream

$$\delta = (4\mathscr{D}_{AB}t)^{\frac{1}{2}}$$

where t is the specific time (i.e. the time required to move unit distance) of the vapour stream (sec), and the diffusivity of the particle A in gas B is given by

$$\mathscr{D}_{AB} = kT/4\pi R_a \mu_B$$

where k is the Boltzmann constant and T is the absolute temperature (K). For an arc gap of 0.5 cm and using the vapour stream velocity calculated above, the specific time, t, is 2×10^{-3} sec. Substitution in the above equations gives a diffusion path length of 2.6×10^{-4} cm for the carbon particles in the time taken to reach the cathode.

Comparison of these figures shows that the predominant contribution to the motion of the carbon particles is the velocity imparted to them by expansion of the carbon stream on ablation of the anode.

Heat Transfer to Carbon Particles

Although the aforegoing sections have dealt with the existence of carbon particles at the face of the anode and their subsequent motion along the path of the arc, it is instructive to consider the heat transfer to the particles in the anode flame, that expanse of hot gas in front of the anode, through which the arc may pass on its way to the cathode but which occupies a much larger area and is generally of lower temperature than the arc itself. Any particles not attracted to the cathode or blown away from the latter by hydrogen streams will pass into the anode flame and the degree to which they are vaporised in this area is worthy of consideration. Heat transfer to the particle in this region takes place through a number of mechanisms, radiation from the hot gas and energy transfer due to the collison of the particles with molecules and electrons in the gas.

Consider a typical particle of diameter 1×10^{-5} cm moving through an atmosphere of C_3 molecules with a velocity of 500 cm sec^{-1}.

Heat Transfer by Radiation

For particles at around 4000 K, the assumed temperature of the anode flame close to the anode, the wavelengths of importance from an energy transfer point of view are greater than 400×10^{-7} cm (102). For particles where the particle diameter is small compared with the wavelength, as in this case, complete opacity is not obtained and all the particle is subjected to heating from the incident radiation. For such a situation, an absorption cross-section σ_{abs} has been defined for a small particle, radius R_a, which is related to the wavelength, λ, by the expression

$$\sigma_{abs} / \pi R_a^2 = p_\lambda R_a$$

where p_λ is the "Rayleigh factor" estimated by Main and Bauer (103) to be 9×10^4 cm^{-1} for small graphite particles. For $R_a = 5 \times 10^{-6}$ cm, the absorption efficiency is thus .45, i.e. 45% of the radiation incident on the particle is actually absorbed. For a black body at 4000 K, the radiated power is 3.54×10^2 cal sec^{-1} cm^{-2} so that the energy absorbed by a particle due to radiation is (assuming Kirchoff's law) 1.25×10^{-8} cal sec^{-1}.

Energy Transfer by Gas Molecule - Particle Collision

Because the particle diameter, 1×10^{-5} cm, is much smaller than the mean free path of the surrounding gas, 70 μm for C_3 molecules at 4000 K, kinetic gas theory may be used. The hard sphere collision number of B particles with an A particle is given, according to kinetic gas theory, by (104)

$$z_{BA} = (R_a + R_B)^2 n_B (8\pi kT(1/M_a + 1/M_B))^{\frac{1}{2}}$$

where M_a and M_B are the weight per molecule of A and B respectively. Consider B as a C_3 molecule with radius $R_B = 0.5 \times 10^{-7}$ cm, molecular density $n_B = 2 \times 10^{18}$ molecules cm^{-3} and weight per molecule $M_B = 6 \times 10^{-23}$ gm $molecule^{-1}$ and A as a carbon particle with radius $R_a = 5 \times 10^{-6}$ cm, and

weight per "molecule" $M_a = 2.75 \times 10^{-16}$ gm molecule^{-1}. For a temperature of 4000 K, this results in a number of collisions, $z_{BA} = 6.13 \times 10^{12}$ collisions per second.

Only inelastic collisions need be considered here. When a small particle collides with a much larger and slower one, energy and momentum conservation requires that the kinetic energy of the small particle transferred to potential energy of the larger one be limited to a value just less than the kinetic energy of the small particle (105). Thus a gas molecule striking a carbon particle will initially dissipate $\frac{1}{2} mv^2 = 3/2\ kT_g$ energy, assuming contact is long enough to enable the molecule and particle to come to thermal equilibrium, when the molecule then leaves the particle surface it will do so with energy $3/2\ kT_p$ where T_g and T_p are the temperatures of the gas and particle respectively. The condensation coefficients of C_1 and C_3 on graphite at 2300 K have been measured as 0.4 and 0.1 respectively (106). Thus, taking a value of 0.1 for the fraction of collisions which are inelastic should allow a conservative estimate of the energy transferred by molecule-particle collisions. For a gas temperature of 4000 K, the number of collisions is 6.13×10^{12} sec^{-1}, thus the energy transferred is $9.2 \times 10^{11}\ k(T_g - T_p)$ cal sec^{-1}. An estimate of the particle temperature, T_p, is difficult; a conservative value can be obtained by considering the particle to be at the sublimation temperature for solid graphite at 1 bar and a typical carbon to hydrogen ratio, say 1.2. This results in a particle temperature of 2850 K. Thus the energy transferred by molecule-particle collision is 3.5×10^{-9} cal sec^{-1}.

Energy Transferred by Electron-Particle Collision

This mode of energy transfer is of importance only within the arc proper where electron concentrations are significant. Because this analysis is concerned with the more general area of the anode flame region where low electron densities exist, this mode of energy transfer can be neglected compared with that due to molecule collisions.

This analysis shows that the majority of the energy transferred to carbon particles in the anode flame is ~~through the molecule-particle collision mechanism~~ by radiation and that the rate of transfer is of the order of 1.6×10^{-8} cal sec^{-1}.

APPENDIX III

ESTIMATION OF QUENCH TUBE TEMPERATURE PROFILES

Gas Stream Properties

To prevent unnecessary complications in estimating the gas stream properties the gas stream was assumed to consist of hydrogen alone. For the purposes of computer calculations, the specific heat and thermal conductivity of hydrogen were obtained from the following polynomials (129,130) respectively.

$$C_p = 3.589 - 5.551 \times 10^{-4} T + 6.942 \times 10^{-7} T^2 - 1.452 \times 10^{-10} T^3 \quad \text{cal gm}^{-1} \text{K}^{-}$$

$$k = 2.250 \times 10^{-4} + 7.560 \times 10^{-7} T + 3.458 \times 10^{-11} T^2 \quad \text{cal cm}^{-1} \text{sec}^{-1} \text{K}^{-1}$$

The viscosity of hydrogen was obtained from the data of Vanderslice et al (94).

Values of the above three properties were estimated for a typical "real" product stream of 4 mole percent acetylene, 4 mole percent carbon monoxide and 92 mole percent hydrogen. Over the range 400 K to 2400 K, the values of the three properties for pure hydrogen were within 12% for the specific heat, 8% for the thermal conductivity and 15% for the viscosity of the values for the "real" product stream, showing the validity of the "pure hydrogen" assumption as a first approximation.

Heat Transfer Coefficients

The following correlations were used to calculate the various heat transfer coefficients.

Water side:

Jakob (131) gives the following equation for the heat transfer from the outer surface of the inner tube of an annulus for $200 \ll Re \ll 2000$.

$$h_o D_e/k = 1.02(vD_e\rho/\mu)^{.45}(\mu C_p/k)^{.5}(D_e/L)^{.4}(D_2/D_1)^{.8}(\rho^2 \beta g \Delta t D_e^{\ 3}/\mu^2)^{.05}$$

where D_e = equivalent diameter of annulus, cm

D_1 = inner diameter of annulus, cm

D_2 = outer diameter of annulus, cm

h_o = water-side heat transfer coefficient, cal cm^{-2} sec^{-1} K^{-1}

k = thermal conductivity of water, cal cm^{-1} sec^{-1} K^{-1}

μ = viscosity of water, gm cm^{-1} sec^{-1}

ρ = density of water, gm cm^{-3}

C_p = specific heat of water, cal gm^{-1} K^{-1}

v = water velocity, cm sec^{-1}

L = length of annulus, cm

β = coefficient of thermal expansion of water, K^{-1}

Wall coefficient:

This is given by

$$h_{wall} = k_{wall}/x_w$$

where k_{wall} = thermal conductivity of wall, cal cm^{-1} sec^{-1} K^{-1}

x_w = thickness of wall, cm

h_{wall} = wall heat transfer coefficient, cal cm^{-2} sec^{-1} K^{-1}

Gas-side coefficient:

Two correlations were used for this coefficient, one for the high-temperature entrance region due to Skrivan and Jaskowsky (13) and one for the sub-plasma temperature region (less than 1000 C) due to Kays (122).

Skrivan and Jaskowsky

$$h_i D_i/k_h = 9.5 \times 10^{-3} (Re)^{1.25} (x/D_i)^{-1.67} (k_h/k_w)^{.4}$$

Kays

$$h_i D_i/k_h = 3.66 + \frac{.104(x/D_i)/Re\ Pr)^{-1}}{1 + .016(x/D_i)/Re\ Pr)^{-.8}}$$

where h_i = gas-side heat transfer coefficient, cal cm^{-2} sec^{-1} K^{-1}

D_i = inside diameter of tube, cm

k_h = thermal conductivity of hydrogen at bulk temperature, cal cm^{-1} sec^{-1}

k_w = thermal conductivity of hydrogen at wall temperature, cal cm^{-1} sec^{-1}

x = distance from tube entrance, cm

Re = Reynolds number of hydrogen

Pr = Prandtl number of hydrogen

Calculation of Temperature Profile

The temperature profile down the quench tube was established by dividing the length of the tube into 1 cm long segments and performing a heat balance over each segment to establish the segment temperature. Using an initial estimate of the temperature of the section (based on the end temperature of the previous section) and the wall temperature, the gas-side heat transfer coefficient was calculated using the relevant equation. With this coefficient, the heat flow, q, from the hot gas to the tube wall was calculated from

$$q = h_i A_i (T_g - T_w)$$

where A_i = wall area of section, cm^2

T_g = gas temperature, K

T_w = wall temperature, K

Using this heat flow, the wall and water-side heat transfer coefficients and assuming a water temperature of 300 K, a revised wall temperature was calculated using the following equation.

$$T_w = q/U_i A_i + 300$$

where U_i is an overall heat transfer coefficient based on the inside diameter of the tube.

$$U_i = (D_i x_w / \bar{D}_l / k_{wall} + D_i / D_o h_o)^{-1}$$

where $\bar{D}_l = D_o / D_i (\ln D_o / D_i)^{-1}$

D_o = outside diameter of tube.

This value of the wall temperature was then used to repeat the procedure until the recalculated wall temperature agreed with the previous estimate. When this condition was reached, the temperature drop over the section was calculated from

$$\Delta T_g = q/mC_p$$

where ΔT_g = temperature drop over the section K

m = mass flow rate of gas, gm sec^{-1}

From this, the temperature of the downstream end of the section and the average section temperature were estimated. The average section temperature was then

used to repeat the calculation until successive iterations agreed to within 5 K. This procedure was then repeated for successive sections down the length of the quench tube to give the temperature profile.

This procedure is shown in block diagram form in fig. XXVIII.

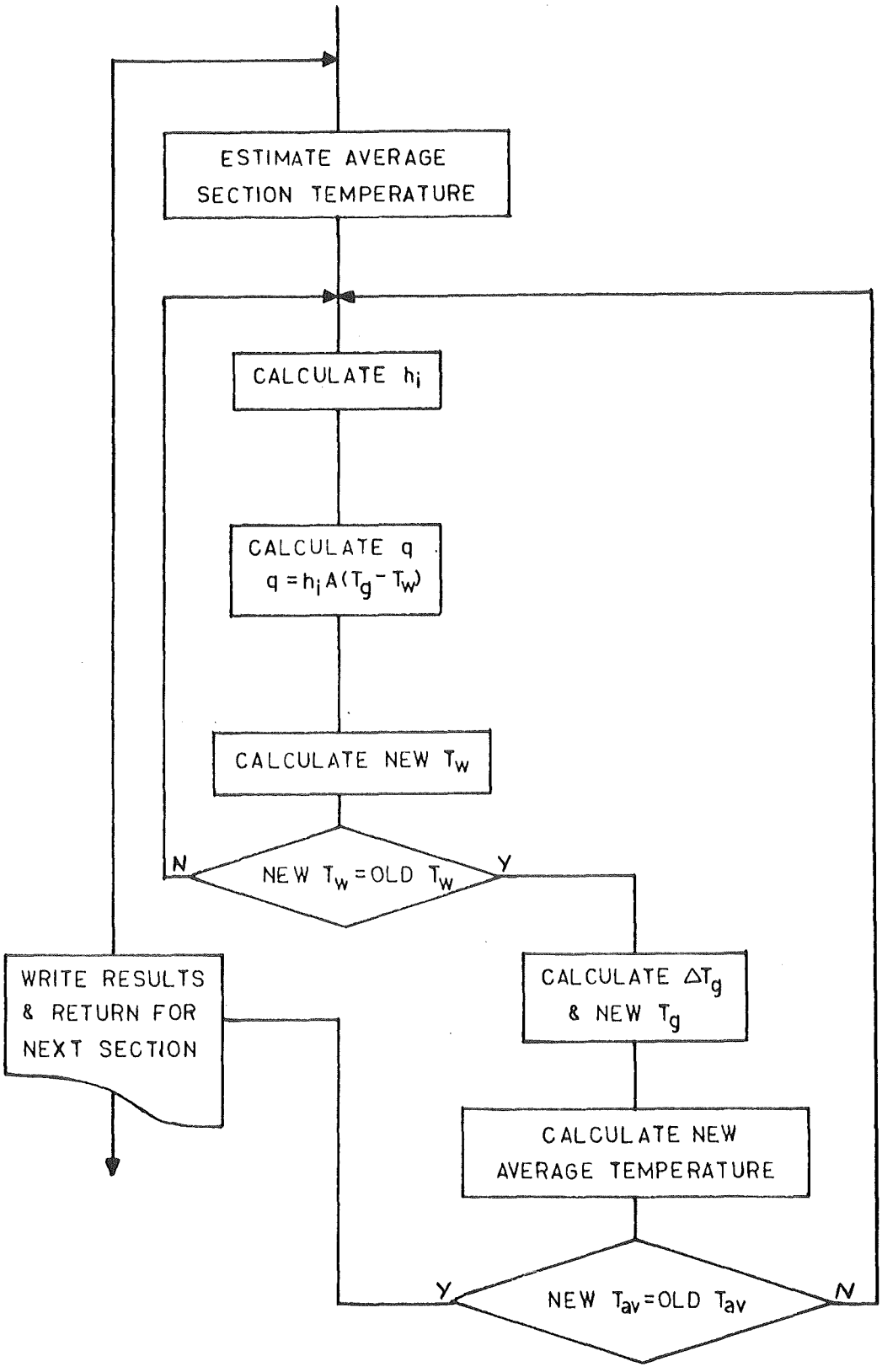

FIG XXVIII BLOCK DIAGRAM FOR TEMPERATURE PROFILE PROGRAM

REFERENCES

1. Abrahamson J. "The Reactions of Coal in a High Intensity Arc", Ph.D. Dissertation, University of Canterbury (1971)
2. Abrahamson J. and Stott J.B. "N.Z. PVC Production Proposals", N.Z. Engineering, 25(9) 241 (1970)
3. Miller S.A. "Acetylene, its Properties and Uses", Vol I, p394, Ernest Benn Ltd (1965)
4. Weaver T. "What Acetylene Costs", Petroleum Refiner, 32 (5) 151 (1953)
5. Patton J.L., Grubb G.C. and Stephenson K.F. Petroleum Refiner, 37 (11) 180 (1958)
6. Barry M.J. et al "Acetylene/Ethylene from Naphtha", Chem. Eng. Prog., 56 (1) 39 (1960)
7. Anon. "Acetylene (Electric Arc) - Chemische Werke Huls", Hydrocarbon Processing, 44 (11) 161 (1965)
8. Iberson V.J. "Plasma Chemical Reactions", High Temperatures - High Pressures, 1 243 (1969)
9. Freeman M.P. "Chemical Research in Streaming Thermal Plasmas", Advances in High Temperature Chemistry (L. Eyring, Ed.) Vol 2 p151 (1969)
10. Parsons R.J. "Progress Review No. 61 - The use of Plasmas in Chemical Synthesis", J. Inst. Fuel, 43 (359) 524 (1970)
11. Gerdeman D.A. and Hecht N.L. Arc Plasma Technology in Materials Science, p7 Springer-Verlag (1972)
12. Sundstrom D.W. and De Michiell R.L. "Quenching Processes for High Temperature Chemical Reactions", Ind. Eng. Chem., Proc. Des. Develop., 10 (1) 114 (1971)
13. Skrivan J.F. and Von Jaskowsky W. "Heat Transfer from Plasmas to Water Cooled Tubes", Ind. Eng. Chem., Proc. Des. Develop., 4 (4) 371 (1965)
14. Goldberger W.M. and Oxley J.H. "Quenching the Plasma Reaction by Means of the Fluidised Bed", AIChemE Journal, 9 (6) 778 (1963)
15. Schallus E. and Gotz A. "Endothermic Reactions in the Electric Arc". Ger.P. 1,012,899 (1957), also US Pat. 2,916,534 (1959) and Brit.Pat. 831,522 (1960

16. Sennewald K., Schallus E. and Pohl F. "The Production of Acetylene by the Thermal Cracking of Hydrocarbons by means of Very High Temperature Hydrogen", Chem-Ing-Tech., 35 (1) 1 (1963)

17. Sennewald K. et al "Cracking of Hydrocarbons to Acetylene, Ethylene, Methane and Hydrogen with Hydrogen Heated in an Electric Arc", Ger. Pat. 1,468,159 (1970)

18. Anon. Chem.Engineering, 78 (17) 56B (1971)

19. Gehrmann K. and Schmidt H. "Pyrolysis of Hydrocarbons using a Hydrogen Plasma", Proc. Eighth World Petroleum Congress (Moscow), vol 4 p379 (1971)

20. Gladisch H. "Acetylene Production in Electric Arcs", Chem-Ing-Tech., 41 (4) 204 (1969)

21. Polak L. "Kinetics and Thermodynamics of Chemical Reactions in Low Temperature Plasma" (1965) Nauka Moscow

22. Polak L.S. in "Proc. of the VII World Petroleum Congress", p283

23. Gulyaev G.V. "The Conversion of Methane to Acetylene in a Plasma Jet", Int. Chem. Eng. 3 (4) 531 (1963)

24. Minc S., Szymanski A. and Waryka A. "Synthesis of Acetylene in Plasma Jet", Int. Chem. Eng., 7 (2) 228 (1967)

25. Valibekov Yu.V. and Bolotov G.N. "An Investigation of the Process for Producing Acetylene, its Homologs and Technical Hydrogen from Natural Gas by the Plasma Jet Synthesis Method", Int. Chem. Eng., 9 (4) 683 (1969)

26. Valibekov Yu.V. and Bolotov G.N. "Formation of Acetylene from Natural Gas from the Komsomol'skoe Deposit in an Argon Plasma Jet", Izv. Akad. Nauk Tadzh. SSR Otd. Fiz-mat geol-khim Nauk, (3) 53 (1970)

27. Kozlov G.I., Khudyakov G.N., Kobzev Yu.N. and Platonova A.I. "Investigation of Acetylene Formation from Methane in a Hydrogen Plasma Jet", Int. Chem. Eng., 8 (2) 289 (1968)

28. Kobzev Yu.N., Kozlov G.I. and Khudyakov G.N. "Preparation of Acetylene in a Plasma Jet", Electron Orab. Mater., (1) 22 (1968)

29. Kobzev Yu.N., Kozlov G.I. and Khudyakov G.N. "Formation of Acetylene and its Homologs in a Plasma Jet of Natural Gas", Khim. Vys. Energ., 4 (6) 519 (1970)

30. Polak L.S. et al "Production of Acetylene and Olefins by Pyrolysis of Gasoline in a Hydrogen Plasma", Generatory Nizkotemp Plazmy, 516-22 (1969)

31. Volodin N.L. et al "Plasma Chemical Pyrolysis of Gas Oil", Khim Vys. Energ., 5 (3) 280 (1971)

32. Khudyakov G.N., Kobzev Yu.N. and Kozlov G.I. "Acetylene from Methane", Brit. Pat. 1,146,090 (1969)

33. Sidorov V.I., I'lin E.T. and Polak L.S. "Preparation of Acetylene from Hydrocarbons by Electric Arc Process", Khim. Prom., 44 (4) 276 (1968)

34. Anon. "Plasma Acetylene Process Developed", Chem. and Eng. News, 42 (3) 42 (1964)

35. Diamond Alkali Co. "Electric Arc Reactor", Brit. Pat. 1,137,029 (1968)

36. Anon. "Linde Co. Arc Process", Chem. Week, 83 (24) 27 (1958)

37. Anderson J.E. and Case L.K. "An Analytical Approach to Plasma Torch Chemistry", Ind. Eng. Chem., Proc. Des. Develop., 1 (3) 161 (1962)

38. Leutner H.W. and Stokes C.S. "Producing Acetylene in a Plasma Jet", Ind. Eng. Chem., 53 (5) 341 (1961)

39. Gladisch H. "How Huls make Acetylene by DC Arc", Hydrocarbon Processing, 41 (6) 159 (1962)

40. Anon. "New Technology might Lower Acetylene Cost", Chem. and Eng. News, 41 (29) 54 (1963)

41. Cichelli M.T. and Schotte W. "Acetylene", Brit. Pat. 938,823 (1963)

42. Schulze R.A. "Du Pont Arc Acetylene Process", Chem. and Ind. 45 1539 (1968)

43. Anon. Chem. Eng., 75 (11) 71 (1968)

44. Anon. Chem. Trade Journal, 153 896 (1963)

45. Anon. "The Production of Acetylene and Ethylene by Hydrocarbon Cracking", Brit. Pat. 895,386 (1962)

46. Anon. "Czech. Acetylene Process claims Highest Yields", Chem. Eng., 67 62 March 7 (1960)

47. Anon. "Two-stage Process Boosts Acetylene Yields", Chem. Eng., 67 120 Nov 14 (1960)

48. Cagas F., Staud M. and Lazarev A. "AC Arc Cuts Acetylene Costs", Hydrocarbon Processing, 41 (3) 161 (1962)

49. Westinghouse Electric Corp. "Arc Heater for the Production of Acetylene", Brit. Pat. 1,125,241 (1968)

50. Maniero D.A., Kienast P.F. and Hirayama C. "Electrical Arc Heaters for High Temperature Chemical Processing", Westinghouse Engineer, 26 (3) 66 (1966)

51. Hirayama C., Fey M.G. and Camp F.E. "Pressure Effects on Product Selectivities in the Pyrolysis of Methane in an Arc Plasma Heater", Chem. Eng. Prog. Sympos. Ser., 67 (112) 117 (1971)

52. Hougen O.A. and Watson K.M. Chemical Process Principles, Pt III, p832, Wiley NY (1947)

53. Krukonis V.J. and Schoenberg T. "Formation of Acetylene from Coal Reacted in a High Intensity Arc", 7th Int. Conf. on Coal Science, Prague 1968

54. Bond R.L., Galbraith I.F., Ladner W.R. and McConnell G.I.T. "Production of Acetylene from Coal using a Plasma Jet", Nature, 200 1313 (1963)

55. Bond R.L., Ladner W.R. and McConnell G.I.T. "Reactions of Coal under Conditions of High Energy Input and High Temperatures", Am. Chem. Soc. Adv. in Chem. Series, No. 55, Coal Science, p650 (1966)

56. Bond R.L., Ladner W.R. and McConnell G.I.T. "Reactions of Coal in a Plasma Jet", Fuel, 45 (5) 381 (1966)

57. I'lin D.T. and Eremin E.N. "Pyrolysis of Gasoline Vapour to Acetylene and Olefins in a Water Vapour Plasma", Int. Chem. Eng., 3 (2) 229 (1963)

58. Kawana Y., Makino M. and Kimura T. "Formation of Acetylene from Coal by Argon Plasma", Int. Chem. Eng., 7 (2) 359 (1967)

59. Kawana Y. and Makino M. "Formation of Acetylene from Coal by Argon-Hydrogen and Hydrogen Plasmas", Kogyo Kagaku Zasshi, 70 (10) 1657 (1967)

60. Kawana Y. "Manufacture of Acetylene from Hydrocarbons by Plasma Jet", Chem. Economy and Eng. Review, 4 (1) 13 (1972)

61. Graves R.D., Kawa W. and Kitechue R.W. "Reactions of Coal in a Plasma Jet", Ind. Eng. Chem., Proc. Des. Develop., 5 (1) 59 (1966)

62. Kawa W., Graves R.D. and Hiteshue R.W. "Reactions of Coal in Argon and Argon-Hydrogen Plasmas", U.S. Bureau of Mines Rept RI-6829 (1966)

63. McDonald E.G. "Plasma Reactions with Powdered Coal", Ph.D. Dissertation, University of Utah (1966)

64. Anderson L.L., Hill G.R., McDonald E.G. and McIntosh M.J. "Flash Heating and Plasma Pyrolysis of Coal", Chem. Eng. Prog. Symp. Series, 64 (85) 81 (1968)

65. Newman J.O.H. et al "Hydrogen Plasma Pyrolysis of Coal and Coal Tar Fractions", 7th Int. Conf. on Coal Science, Prague (1968)

66. Baddour R.F. and Iwasyk J. "Reactions between Elemental Carbon and Hydrogen at Temperatures above 2800 K", Ind. Eng. Chem., Proc. Des. Develop., 1 (3) 169 (1962)

67. Baddour R.F. and Blanchet J.L. "Reactions of Carbon Vapour with Hydrogen and Methane in a High Intensity Arc", Ind. Eng. Chem., Proc. Des. Develop., 3 (3) 258 (1964)

68. Blanchet J.L. and Parent J.R. "Vapour Phase Reactions of Graphite with Light Hydrocarbons", Can.J.Chem. Eng., 45 (6) 361 (1967)

69. Cholette A., Courtois P.A. and Parent J.R. "Reactions of Carbon Vapour with a Mixture of Argon-Propane in a High Intensity Arc", Can. J. Chem. Eng., 47 392 (1969)

70. Lafond R., Meubus P., Kaliaguine S. and Parent J.R. "Reactions of Carbon Vapour with Methane in a High Intensity Arc", 19th Can. Chem. Eng. Conf., Edmonton, 1969, High Temperature Technology

71. Ammann P.R., Baddour R.F., Mix T.W. and Timmins R.S. "Coal Conversion in an Electric Arc", Chem. Eng. Prog., 60 (6) 52 (1964)

72. Plooster M.N. and Reed T.B. "Carbon-Hydrogen-Acetylene Equilibrium at High Temperatures", J. Chem. Phys., 31 (1) 66 (1959)

73. Krukonis V.J., Gannon R.E. and Schoenberg T. "Conversion of Coal to Acetylene in a Magnetically Rotated Arc Reactor", 19th Can. Chem. Eng. Conf., Edmonton, 1969, High Temperature Technology

74. Anon. "Acetylene from Coal Soon", Chem. Eng., 76 76 March 24 (1969)

75. Gannon R.E., Krukonis V.J. and Schoenberg T. "Conversion of Coal to Acetylene in Arc Heated Hydrogen", Ind. Eng. Chem., Prod. Res. Develop., 9 (3) 343 (1970)

76. Anon. "New Techniques Brighten Outlook for Plasmas", Chem. Eng. News, 48 (23) 56 June 1 (1970)

77. Mosse A.L. et al "Reactor Installation Schemes Applied to the Pyrolysis of Petroleum in a Plasma Jet", Zh. Inzh. Fiz., 20 (3) 462 (1971)

78. Ammann P.R. and Baddour R.F. "Coal Conversion in an Electric Arc", Chem. Eng. Prog. 60 (6) 52 (1964)

79. Finkelnberg W. "The High Current Carbon Arc and its Mechanism", J. Appl. Physics, 20 468 (1949)

80. Dushman S. "Thermionic Emission", Rev. Mod. Phys., 2 (4) 38 (1930)

81. Cobine J.D. Gaseous Conductors, Dover Publications (1958)

82. Marquis M.A. et al "Energy Transfer in the High Intensity Arc. I A Steady State Treatment of Endothermic Processes Near the Anode Surface" in Arcs in Inert Atmospheres and Vacuum (W.E. Kuhn, Ed.), p152, Wiley NY (1956)

83. Williamson A.G. Private Communication

84. Haldane J.S. and Graham J.I. "Methods of Air Analysis", p8, Charles Griffin (1935)

85. Dechavatanapaisan S. "Carbon Anodes for Plasma Acetylene Generator", B.E. Project Report, Dept Chem. Eng., Univ. Canterbury (1970)

86. Glass D.M. "Carbon Anodes for Plasma Acetylene Generator", B.E. Project Report, Dept Chem. Eng., Univ. Canterbury (1971)

87. Patel N. "Carbon Anodes for Plasma Acetylene Generator", B.E. Project Report, Dept Chem. Eng., Univ. Canterbury (1972)

88. Lau P. "Carbon Anodes for Plasma Acetylene Generator", B.E. Project Report, Dept Chem. Eng., Univ. Canterbury (1973)

89. Finkelnberg W. "The High Current Carbon Arc", FIAT Final Report 1052 (1947)

90. Pfender E. and Boffa C.V. "Generation of Ultrafine Aerosols with a Transpiration Cooled Anode in a High Intensity Arc", Rev. Sci. Instrs., 41 (5) 655 (1970)

91. Whittaker A.G. and Kintner P. "Particle Emission during Sublimation of Graphite", Carbon, 7 414 (1969)

92. Abrahamson J. "Graphite Sublimation Temperatures, Carbon Arcs and Crystallite Erosion" to be published in Carbon

93. Thomson J.J. and Thomson G.P. "Conduction of Electricity through Gases", vol 1, p188, Dover Publications (1969)

94. Vanderslice J.T., Weissman S., Mason E.A. and Fallon R.J. "High Temperature Transport Properties of Dissociating Hydrogen", Phys. Fluids, 5 (2) 155 (1962)

95. Bird R.B., Stewart W.E. and Lightfoot E.N. "Transport Phenomena", p744, Wiley NY (1960)

96. Palmer H.B. and Shelef M. "Vaporisation of Carbon" in Chemistry and Physics of Carbon (P.L. Walker, Ed.) vol 4, p85, Marcel Dekker NY (1968)

97. Finkelnberg W. and Maecker H. "Elektrische Bogen und thermisches Plasma" in Handbuch der Physik (S. Flugge, Ed.) vol 22, p282, Springer-

Verlag, Berlin (1956)

98. Colton J.W. "Process for Making Acetylene using a Plasma Furnace", U.S. Pat. 3,256,358 (1966)

99. Doukas G. et al "Electric Arc Furnace for Acetylene Production", Ger. Pat. 1,293,152 (1969)

100. Bokros J.C. "Properties of Pyrolytic Graphite" in Chemistry and Physics of Carbon (P.L. Walker, Ed.) vol 5 p57, Marcel Dekker NY (1969)

101. Brezing D. "Transport Properties of Hydrogen", Rept AD 609 345, Nat. Tech. Inform. Ser., U.S. Dept of Commerce (1964)

102. Siegel R. and Howell J.R. "Thermal Radiation Heat Transfer", p22, McGraw-Hill (1972)

103. Main R.P. and Bauer E. J. Quant. Spectro. Radiat. Transfer, 6 1 (1966)

104. Glasstone S. "Textbook of Physical Chemistry", p276, 2nd Ed., Macmillan (1948)

105. Papoular R. "Electrical Phenomena in Gases", Iliffe, London (1965)

106. Chupka W.A., Berkowitz J., Meschi D.J. and Tasman H.A. in Advances in Mass Spectroscopy (R.M. Eliot, Ed.) vol 2 p99, Pergamon NY (1963)

107. JANAF Thermochemical Tables, 2nd Ed., NSRDS = NBS 37 Nat. Bur. Stand., Washington (1970)

108. Nicholson D.S. "Utilisation of Coal in New Zealand 1920-1955", N.Z. Dept Scientific Indust. Research, Inform. Ser. No 19 (1958)

109. Zinder International Ltd "Second Report on Utilisation of Kapuni Natural Gas", N.Z. Govt Printer (1965)

110. N.Z. Minister of Energy Resources "Development of the Maui Gas Field", Statement by the Hon. W.W. Freer, N.Z. Govt Printer (1973)

111. Duff R.E. and Bauer S.H. "The Equilibrium Composition of the C/H System at Elevated Temperatures", Los Alamos Scientific Lab. Report LA-2556 (1961)

112. Lieberman M.L. and Mark J.L. "Chemical Vapor Deposition of Carbon: Thermochemical Calculations of Equilibrium Gas Compositions", Nat. Tech. Inform. Ser., SC-DR-72 0775 U.S. Dept of Commerce (1972)

113. Anderson R.B. and Emmett P.H. "Surface Complexes on Carbon Blacks. I. High Temperature Evacuation Studies", J. Phys. Chem., 56 (6) 753 (1952)

114. Redmond J.P. and Walker P.L. "Gas Content of Graphites", Nature, 186 (4718) 72 (1960

115. Ashton B.W., Labaton V.Y. and Smith A. "Desorption Studies on Nuclear Graphite", Third Conf. on Industrial Carbons and Graphite, London, p329 (1970)

116. Lang F.M. and Magnier P. "Action of Oxygen and Carbon Dioxide above 100 millibars on 'Pure' Carbon", in Chemistry and Physics of Carbon (P.L. Walker, Ed.), vol 3 p121, Marcel Dekker NY (1968)

117. Ma Y.H. and Shipman C.W. "On the Computation of Complex Equilibria", A.I.Chem.E. Journal, 18 (2) 299 (1972)

118. Duff R.E. and Bauer S.H. "Equilibrium Composition of the C/H System at Elevated Temperatures", J. Chem. Phys., 36 (7) 1754 (1962)

119. Munson M.S.B. and Anderson R.C. "Vinylacetylene as an Intermediate in the Formation of Acetylenic Carbon", Carbon, 1 (1) 51 (1963)

120. Palmer H.B. and Dormish F.L. "The Kinetics of Decomposition of Acetylene in the 1500 K Region", J. Phys. Chem., 68 (6) 1553 (1964)

121. Handbook of Chemistry and Physics (Weast R.C., Ed.) 49th Ed., Chemical Rubber Co., 1968-1969

122. Kays W.M. in "Fluid Dynamics and Heat Transfer" (Knudsen J.G. and Katz D.L., Eds) p376, McGraw-Hill NY (1958)

123. Johnson J.R., Choksi N.M. and Eubank P.T. "Entrance Heat Transfer from a Plasma Stream in a Circular Tube", Ind. Eng. Chem., Proc. Des. and Develop., 7 (1) 34 (1968)

124. Guillery P. "Properties of Negative Crater, Mechanism and Prevention of Winding", unpublished report (1942) (Quoted in Finkelnberg W. FIAT Final Rept 1052 (1947)).

125. Kratsch K.M., Martinez M.R., Clayton R.I., Greene R.B. and Wuerer J.E. "Graphite Ablation in High Pressure Environments", Paper presented AIAA Entry Vehicle Systems and Technology Conf., Williamsburg, Virginia (1968). McDonnell Douglas Astronautics Co. Western Div., Santa Monica, California

126. Spalding D.B. "Convective Mass Transfer", Arnold (1963)

127. Stott J.B. Private Communications

128. Dixon-Lewis G., Private Communication

129. Anon. The TPRC Data Series (Y.S. Touloukian, Ed.) Vol. 6, "Specific Heat", p 28, IFI/Plenum, N.Y. (1970)

130. Anon. The TPRC Data Series (Y.S. Touloukian, Ed.) Vol. 3, "Thermal Conductivity of Non Metallic Liquids and Gases", p 41, IFI/Plenum, N.Y. (1970)

131. Jakob M. "Heat Transfer", Vol. 1, p 551, Wiley, N.Y. (1957)